

EMSA 2012

**9th European Magnetic Sensors & Actuators
Conference**

Book of Abstracts

Prague, Czech Republic

July 1-4, 2012

EMSA 2012

9th European Magnetic Sensors & Actuators Conference Book of Abstracts

Volume editors: Radek Sedláček
Antonín Platil
Pavel Ripka

Contact: Czech Technical University in Prague,
Faculty of Electrical Engineering,
Technická 2, 166 27 Prague 6
Phone: (+420) 224 353 954, e-mail: platil@fel.cvut.cz

Printed by: Česká technika - nakladatelství ČVUT
Žitkova 4, 166 36 Praha 6
163 pages, 1st issue

Czech Technical University in Prague, Faculty of Electrical Engineering
Prague, June 2012
125 copies

ISBN 978-80-01-05078-1

Table of Contents

International Committee	IV
Technical Programme Committee	IV
Local Organizing Committee	IV
Foreword.....	V
Main Topics.....	VI
Date/Conference venue.....	VI
Programme at Glance	VII
EMSA2012 Conference Programme in Detail	VIII
List of abstracts	20 - 157
Author's index	159 -162

International Committee

Barandiaran, Jose M. (Spain)
Chiriac, Horia (Romania)
Derebasi, Naim (Turkey)
Hristoforou, Evangelos (Greece) - Chairman
Meydan, Turgut (UK)
Nikitin, Petr (Russia)
Popovic, Radivoje S. (Switzerland)
Reininger, Thomas (Festo, Germany)
Robbes, Didier (France)
Vazquez, Manuel (Spain)

Technical Programme Committee

Manuel Barandiaran	Massimo Pasquale
Christophe Dolabdjian	Antonin Platil
Alan Edelstein	Pavel Ripka
Paolo Freitas	Rudolf Schaefer
Vit Hlinovsky	Slawomir Tumanski
Evangelos Hristoforou	Manuel Vazquez
Petr Kaspar	Ondřej Životský
Olga Kazakova	Karel Závěta
Pavel Kejik	Ivan Zemánek
Ludek Kraus	Rysuoke Hasegawa
Anthony Moses	Václav Havlíček
Eugene Paperno	

Local Organizing Committee

Antonín Platil	Petr Nováček
Petr Kašpar	Aleš Zikmund
Pavel Ripka	Mattia Butta
Radek Sedláček	Vojtěch Petrucha
Michal Janošek	Michal Vopalenský
Pavel Mlejnek	

Foreword

It is my pleasure to welcome you to the 9th European Magnetic Sensors and Actuators Conference, hosted from July 1st to 4th on Czech Technical University in Prague.

The European Magnetic Sensors and Actuators Conference (EMSA) is already a well known European forum that serves to assess the status, recent progress, and development in the field of magnetic sensor technology and magnetic actuators.

It was first held in 1996 in Iasi-Romania and since then has continued every two years in Sheffield-UK, Dresden-Germany, Athens-Greece, Cardiff-UK, Bilbao-Spain, Caen-France, and Bodrum-Turkey, and now Prague - Czech republic.

The aim of the conference is to generate an overview of research in magnetic sensors and actuators, to recognize their relevance in modern industry and to identify potential future collaborations.

EMSA 2012 provides an excellent opportunity to bring together scientists and engineers from universities, research institutes and industry to present and discuss their most recent results covering both fundamental and applied aspects of magnetic sensors and actuators.

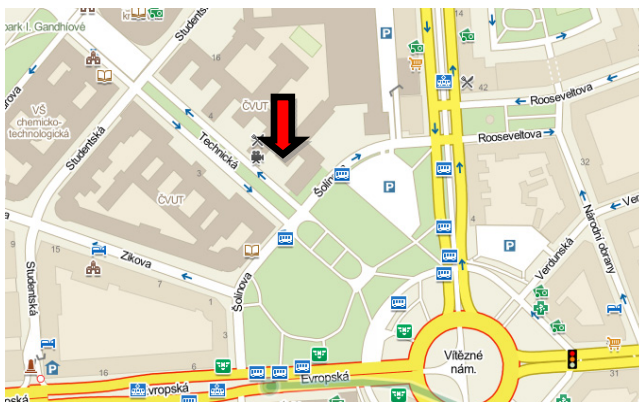
Antonín Platil,
on behalf of the Local organizing committee.

Main Topics

- Materials
- Physical phenomena
- Modelling and simulation
- Magnetic sensors - concepts, design and applications
- Magnetic actuators - concepts, design and applications
- Magnetic MEMS
- Nanotechnology and Miniaturisation
- Integration
- Applications
- Metrology

Date/Conference venue

July 1 - 4, 2012 (Sunday - Wednesday)
Czech Technical University in Prague
Technická 2
166 27 Prague 6
Czech Republic



Programme at a Glance

Sunday, 1st July	
17:00	Registration
17:00	Welcome Party
Monday, 2nd July	
09:00	Conference opening
09:15-11:00	Hall effect 1
11:00-11:30	Coffee break
11:30-12:45	Hall effect 2
12:45-14:00	Lunch
14:00-15:15	GMI
15:15	Coffee break
15:30-17:00	Poster session MP1-MP44
Tuesday, 3rd July	
09:00-10:45	Fluxgate, induction, scalar magnetometers
10:45-11:15	Coffee break
11:15-12:15	Magnetolectricity, AMR
12:15-13:45	Lunch
13:45-15:15	Magnetic microwires
15:15	Coffee break
15:30-17:00	Poster session TP1-TP45
19:00	Conference Banquet in Rudolph's foundry, Restaurant Vikarka (Vikářská 39 - Prague Castle)
Wednesday, 4th July	
09:00-10:15	Nanoparticles, permanent magnets
10:15-10:45	Coffee break
10:45-12:00	NDE, SQUID, MAGNETOELASTIC, CALIBRATION
12:00-13:30	Lunch
13:30-15:00	Metrology
15:00	Closing session

EMSA2012 Conference Programme in Detail

Sunday, July 1, 2012

17:00 Registration

17:00 Welcome party

Monday, July 2, 2012

09:00 - 09:15 CONFERENCE OPENNING

09:15 - 11:00 HALL EFFECT 1 - ORAL SESSION

09:15 MO10 Invited: **High Volume Production of Magnetic Sensors for the Automotive Market**
Schott Ch., Blyzniuk M.

10:00 MO11 **Epitaxial Graphene Sensors for Detection of Small Magnetic Moments**
Kazakova O., Panchal V.

10:15 MO12 **Suppressing the DC offset and LF noise in QWHS Hall based microsystems using the spinning current modulation technique**
Mosser V.

10:30 MO13 **Study of asymmetric cross shape planar Hall effect sensor**
Mansour M., Coillot Ch., Nguuyen Van Dau F., Roux A.

10:45 MO14 **Magnetic mapping using Hall Effect sensors**
Seron D., Zaragoza V., Mosser V., Haddab Y.

11:30 - 12:45 HALL EFFECT 2 - ORAL SESSION

11:30 MO20 Keynote: **Layout and Architecture Issues in Hall based CMOS microsystems**
Kejik P., Bourdelle P. F., Reymond S., Salvi F., Farine P. A.

12:00 MO21 **Novel measurement setup optimize the sensitivity of a planar Hall resistance biosensor**
Tran Q. H., Kim K., Sunjong O., Dehbaoui M., Kamara S., Dumas R., Charar S., CheolGi K., Terki F.

12:15 MO22 **3-D Magnetic Vector Field Camera Using Integrated Hall and MR Sensor Arrays**
Lee J., Kim J., Jun J., Cho Ch.

Monday, July 2, 2012

12:30 MO23 **Transmission line type thin film sensor and measurement of MCG**
Yabukami S., Nakano H., Ozawa T., Kato K., Kobayashi N., Arai K.I.

14:00 - 15:15 GMI - ORAL SESSION

14:00 MO30 Keynote: **Development of a high sensitivity Giant Magneto-Impedance magnetometer: comparison with a commercial Flux-Gate**

Dufay B., Saez S., Dolabdjian C., Yelon A., Menard D.

14:30 MO31 **GMI in nanostructured FeNi/Ti multilayers with different thicknesses of the magnetic layers**

Fernández E., Svalov A. V., Kurlyandskaya G. V., García-Arribas A.

14:45 MO32 **Noise and sensitivity of GMI sensing elements**

Menard D., Yelon A., Dufay B., Saez S., Dolabdjian C.

15:00 MO33 **Dynamic sensing of magnetic nanoparticles in microchannel using GMI technology**

Fodil K., Denoual M., Dolabdjian C., Harnois M., Senez V.

15:30 - 17:00 POSTER SESSION MP01 - MP44

MP01 **3D model of coherent rotation of magnetization in magnetoresistive elements**
Vopálenský M.

MP02 **Low frequency noise of anisotropic magnetoresistors in ac-excited magnetometers**

Vyhnánek J., Janošek M., Ripka P.

MP03 **Super-paramagnetic nanoparticle bio-marking and hyperthermia based tumor treatment**

Hristoforou E.

MP04 **Wireless radiofrequency sensors for the characterization of dielectric properties of biological tissues**

Masilamany G., Joubert P. Y., Serfaty S., Diraison Y. L., Griesmar P.

MP05 **Biosensors Based on Magnetic Nanoparticles**

Nikitin P.I., Khodakova J.A., Nikitin M.P., Orlov A.V.

- MP06 **Neel Effect toroidal current sensor**
Vourch E., Wang Y., Joubert P. Y., Couderette A., Cima L.
- MP07 **Effective Power Signal Filtering using LC Filters with Air Core Coils**
Somolinos J. A., Morales R., Morón C., Garcia A.
- MP08 **Experimental Analysis of Magnetic Losses in a Three Phase Embedded Electrical Transformer**
Aissaoui M., Moussaoui D., Oudina A.
- MP09 **Impulse Current Transformer with Nanocrystalline Core**
Prochazka R., Hlavacek J., Draxler K., Fryml K.
- MP10 **Comparison of functional characteristics of miniature, double axis fluxgate sensors in Vacquier and Foerster configurations**
Frydrych P., Szewczyk R., Salach J., Trzcinka K.
- MP11 **Optimization of driving current parameters for two axis fluxgate sensor**
Frydrych P., Szewczyk R., Salach J., Trzcinka K.
- MP12 **Noise Characteristics of Ferroprobe and Magnetic Microwire Four Channel Magnetometers of VEMA Series**
Hudák J., Čverha A., Lipovský P., Sabol R., Blažek J., Praslička D., Moucha V.
- MP13 **An offset temperature dependence of a fluxgate magnetometer and its compensation**
Petrucha V.
- MP14 **Current measurement with a GMI sensor**
Asfour A., Yonnet J. P., Zidi M.
- MP15 **Prediction of Giant Magneto Impedance on Co-Complex Coated Fe-Based Amorphous Wires Using Neural Network**
Caylak O., Derebasi N.
- MP16 **High Performance Current Sensor Utilising Giant Magnetoimpedance (GMI) in Co-based Amorphous Wires**
Fisher B., Panina L., Fry N., Mapps D.
- MP17 **Differential magnetic permeability: A tool for coiled giant magneto-impedance design**
Moutoussamy J., Coillot Ch., Chanteur G.

- MP18 **AC characterization of magneto-impedance microsensors for eddy current non-destructive testing**
Peng T., Moulin J. , Alves F., Le-Bihan Y.
- MP19 **FeNi-based Thin Film Meander Sensitive Elements for GMI Detectors**
Volchkov S.O., Yuvchenko A.A., Lepalovskiy V.N., Vas'kovskiy V.O., Safronov A.P., Kurlyandskaya G.V.
- MP20 **The prospects of using film structures based on In-containing semiconductor materials in magnetic field sensors for thermonuclear reactor magnetic diagnostic systems**
Bolshakova I., Viererbl I., Đuran I., Kovalyova N., Kovarik K., Kost Y., Makido O., Sentkerestiová J., Shtabalyuk A., Shurygin F.
- MP21 **Spin accumulation from the spin Hall effect and the anisotropic effect studied using the effective mean-free-path model**
Chen S. P., Chang Ch. R.
- MP22 **Improved Quantum Well Hall Sensors for Micromagnetometry**
Mosser V., Seron D., Konczykowski M., Bansropun S.
- MP23 **Shiftable Attenuation of Low Magnetic Fields Using a Magnetically Soft Layer on an Integrated Hall Sensor**
Peters V., Beran P., Hohe H. P.
- MP24 **Original induction sensors: orthogonal and cubic configuration**
Coillot Ch., Boda M., Moutoussamy J.
- MP25 **Metal detector signal imprints of detected objects**
Nováček P., Ripka P., Roháč J.
- MP26 **Step Response Identification of Metallic Targets by Numerical Simulation**
Polik Z.
- MP29 **Improving the Magnetolectric Response of Laminates Containing High Temperature Piezopolymers**
Gutiérrez J., Lasheras A., Barandiaran J. M., Vilas J. L., San S. M., León L. M.
- MP30 **Investigation of the near-carrier noise for a strain-driven ME laminates by using cross-correlation techniques**
Zhuang X., Lam Chok Sing M., Dolabdjian C.
- MP31 **Magneto-Elastic Sensors for the Detection of Pulse Waves**
Hlenschi C., Corodeanu S., Chiriac H.

- MP32 **Inductive Stress Sensor based on Magnetic Bistability of FeSiBP amorphous microwires**
Olivera J., Varga R., Hernández M., Badini-Confalonieri G.A., Vázquez M.
- MP33 **Magnetoelastic Characteristics of FeNi-based Amorphous Ring-shaped Cores under Uniform Compressive and Tensile Stresses**
Salach J., Szewczyk R., Bieńkowski A., Jackiewicz D.
- MP34 **Calibration of the 3D coil system's orthogonalities**
Zikmund A., Ripka P.
- MP35 **Investigation of Magnetic Nanoparticles for Biomedical Applications**
Nikitina I.L., Yuriev M.V., Vetoshko P.M., Nikitin P.I.
- MP36 **Magneto-optical Sensitive Elements for Single Magnetic Nanoparticle Detection**
Skidanov V., Vetoshko P., Stempkovskiy A.
- MP37 **A Magnetic Based Displacement-to-Frequency Transducer**
García A., Morón C., Tremps E., López M. J., Ramirez P.
- MP38 **Wireless magnetic position sensing system composed of multi channels digitizer for realtime monitoring**
Hashi S., Kuboki T., Ishiyama K., Yabukami S., Ozawa T., Takashima K., Kitamura Y., Itoh Y., Kanetaka H.
- MP39 **Position detection using magnetoimpedance sensor array for designing in situ reconfigurable sensor networks**
Ipatov M., Zhukova V., Gonzalez J., Zhukov A.
- MP40 **Consideration of planar coil inductance for thin type displacement sensor**
Wakiwaka H., Hattori Y., Ito D., Tashiro K., Yajima H., Hosaka T., Kanazawa T., Fujiwara N.
- MP41 **Optimization of a SQUID gradientmeter for use in unshielded environment**
Baltaq O., Rau M.C.
- MP42 **A New Calibration Method for a 2nd order SQUID Gradiometer System**
Baltaq O., Rau M.

Monday, July 2, 2012

- MP43 **Bias-voltage controlled tunneling resistance in a magnetic tunneling junction with an inserted thin metallic layer**
Chen S. P.
- MP44 **Behavior of DC tolerant current transformers in wide frequency range**
Mlejnek P., Kašpar P.

Tuesday, July 3, 2012

09:00 - 10:45 FLUXGATE, INDUCTION, SCALAR MEGNETOMETERS - ORAL SESSION

- 09:00 TO10 **Invited: Recent developments in space magnetometry**
Magnes W.
- 09:45 TO11 **Beat interferences in fundamental mode orthogonal fluxgates**
Sasada I., Han F., Harada S.
- 10:00 TO12 **Orthogonal fluxgate with annealed wire-core**
Butta M., Sasada I.
- 10:15 TO13 **Noise and drive field amplitude in RQ-tape-wound toroidal fluxgate sensors**
Butvin P., Janošek M., Butvinová B., Ripka P., Chromčíková M., Švec P.
- 10:30 TO14 **Measurement of DC currents in the power grid by current transformer**
Ripka P., Draxler K., Styblíková R.,

11:15 - 12:15 MAGNETOELECTRICITY, AMR - ORAL SESSION

- 11:15 TO20 **Induction magnetometer using a low noise ASIC from sensor to ADC: design, performances and limitation**
Rhouni A., Sou G., Coillot Ch., Leroy P.
- 11:30 TO21 **Temperature characteristics of resonance magnetoelectric interaction in PZT/Ni disk resonators**
Chashin D.V., Burdin D.A., Ekonomov N.A., Fetisov Y.K.
- 11:45 TO22 **New magnetoelectric composite structures for magnetic field sensors**
Fetisov L.Y., Perov N.S., Medvedev A.V., Srinivasan G., Srinivasulu G.
- 12:00 TO23 **Investigation of the role of crystallographic texture on the sensitivity of AMR thin film sensors**
Bartok A., Daniel L., Baudin T., Razek A.

Tuesday, July 3, 2012

13:45 - 15:15 MAGNETIC MICROWIRES - ORAL SESSION

- 13:45 TO30** Invited: **Amorphous and nanocrystalline microwires**
Chiriac H.
- 14:30 TO31 **Micromagnetic modelling on high frequency response of amorphous microwires**
Torrejón J., Thiaville A., Adenot-Engelvin A. L, Vazquez M.
- 14:45 TO32 **Tailoring the switching field dependence on external parameters in magnetic microwires**
Varga R., Gamcova P., Klein P., Zhukov A., Vazquez M.
- 15:00 TO33 **Effects of annealing treatment on microwave properties of amorphous FeSiB-base microwires**
El Kammaoui R., Badini-Confalonieri G.A., Vázquez M.

15:30 - 17:00 POSTER SESSION TP01 - TP45

- TP01 **Performance Comparison of Two Different Tubular Linear Actuators for the Active Accelerator Pedal Application**
Kim Y. K., Lee J. J., Jung I. S.
- TP02 **Magnetically actuated rotary walking of superparamagnetic particle chains on a solid surface**
Lee Ch. P., Tsai S. Y., Wei Z. H., Lai M.F.
- TP03 **Cogging Torque Reduction of Surface Permanent Magnet Motor with Asymmetric Stator Slots**
Lee J. J., Rhyu S. H., Kim Y. K., Jung I.S.
- TP04 **Comparison Between The Performances of The Conventional and The Augmented Railgun**
Abdallah M., Lahrech H., Mohellebi H.
- TP05 **Electronic control of the switched reluctance motors**
Morón C., Tremps E., Ramirez P., Garcia A., Somolinos J.A.
- TP06 **Design Analysis and Experimental Validation of a Double Rotor Synchronous PM Machine Used for HEV**
Pišek P., Štumberger B., Marčíč T., Vrtič P.

- TP07 **Design Consideration for High Power Density and Fast Response Permanent Magnet Brushless DC Actuator**
Tang Y., Xu Y., Zou J.
- TP08 **Magnetic and magnetostrictive measurements of RE doped cobalt ferrite bulks and thin films**
Dascalu G., Stratulat M. S., Caltun O. F., Focsa C.
- TP09 **Improved magnetostrictive properties of manganese substituted cobalt ferrite for automobile torque sensor applications**
Dascalu G., Caltun O. F., Rao G. S. N., Rao B. P., Rao K. H.
- TP10 **Deposition and Etch Technologies for High Volume Manufacturing of Magnetic Sensors**
Devasahayam A. J., Cerio F., Rook K.
- TP11 **Mean field model for ferromagnetic nanowire arrays**
Dobrotă C. I., Stancu A.
- TP12 **Metamaterials sensor for electromagnetic nondestructive evaluation**
Savin A., Faktorová D., Steigmann R., Grimberg R.
- TP13 **Anisotropy Field in Ni Nanostripe Arrays**
Flores A. G., Raposo V., Iñiguez J., Zazo M., Redondo C., Navas D.
- TP14 **Dependence of Ferromagnetic Resonance Field with Diameter Sample in Permalloy Nanodot Arrays**
Flores A. G., Raposo V., Iñiguez J., Zazo M., Redondo C., Navas D.
- TP15 **Fabrication and Properties of CoFe₂O₄-PZT Magnetolectric Thin Films**
Giouroudi I., Alnassar M., Grössinger R., Kosel J.
- TP16 **Structural studies, low field magnetic properties and application of amorphous FeCoMoCuB alloys**
Hasiak M., Miglierini M., Łukiewski M., Kaleta J.
- TP17 **Microstructure and magnetic properties of amorphous FeCo-based alloys with different Fe/Co ratio**
Hasiak M., Miglierini M., Łukiewski M., Zbrozczyk J., Kaleta J.
- TP18 **Polycrystalline Fe-Ga Melt-Spun Ribbons for Energy Harvesting Devices**
Lupu N., Škorvánek I., Grigoras M., Tibu M., Marcin J., Chiriac H.

- TP20 **Optical and Magneto-Optical Properties of Ion Implanted (YBiCa)₃(FeGeSi)₅O₁₂ Garnet Films**
Kalandadze L.
- TP21 **Magnetic and magneto-volume properties of Co-doped off-stoichiometric Ni₂MnGa**
Kaštil J., Fabbrici S., Kamarád J., Albertini F., Arnold Z.
- TP22 **Temperature dependence of the switching field in Fe_{67.5}Si_{7.5}B₁₅Cr₁₀ microwire**
Klein P., Richter K., Varga R., Vázquez M.
- TP23 **Effect of strontium ferrite on physical-mechanical and magnetic properties of rubber composites**
Kruželák J., Dosoudil R., Hudec I., Bellušová D.
- TP24 **Synthesis and characterization of Co based ferrite nanocomposites**
Nica V., Gherca D., Brinza F., Pui A.
- TP25 **Core losses and permeability of the compacted NiFe and NiFeMo alloys in ac and dc magnetic fields**
Olekšáková D., Kollár D., Füzér J., Roth S.
- TP26 **The Laws of Bulk Elasticity in Physical Processes of Effect of Parameters (T-H-P) in Metals, Semiconductors, Magnetodielectrics**
Polyakov P. I.
- TP27 **Particulate Fe-Al Thin Films Oxidized Selectively for GHz Frequency Applications**
Jang P., Shin S.
- TP28 **Magnetopolymer composites with magnetic soft ferrite filler**
Rekošová J., Dosoudil R., Ušáková M., Hudec I.
- TP29 **The magnetocaloric effect of Heusler microwires in low and high magnetic fields**
Ryba T., Varga R., Vargova Z., Zhukova V., Zhukov A.
- TP30 **Properties of Fe-Al Cores Made of Fe-Al Powders Annealed in Damp Hydrogen Atmosphere**
Shin S., Jang P.
- TP31 **Alternative route for obtaining NiFe₂O₄ thin films for sensor by pulsed laser deposition**
Stratulat S., Ursu C., Caltun O. F.

- TP32 **Local Flux Density and Barkhausen Noise Distribution for Grain-Oriented Electrical Steels**
Turner S., Hall J.P., Moses A.J., Jenkins K.
- TP33 **Sensor of mechanical Barkhausen noise signal**
Maciakowski P., Augustyniak B., Chmielewski M.
- TP34 **Possibilities of measuring stress and health monitoring in materials using contact-less sensor based on magnetic microwires**
Praslicka D., Blažek J., Smelko M., Hudak J., Mikita I., Varga R., Zhukov A.
- TP35 **Modelling the influence of stress on magnetic characteristics of construction steels**
Jackiewicz D., Szewczyk R., Salach J.
- TP36 **Non destructive evaluation of loose assemblies using eddy currents and artificial neural networks**
Joubert P. Y., Vourch E., Gac G. L., Larzabal P.
- TP37 **Identification of Plastic Deformation in Steel Samples Using Two-Axial Transducer with Rotational Excitation Field**
Psuj G.
- TP38 **A Formal Presentation of Differential Sensactors Pairs With Common and Crossed Feedback**
Robbes D., Allegre G., Flament S.
- TP39 **Minimalistic devices and sensors for micromagnetic materials characterization**
Szielasko K., Mironenko I., Altpeter I., Herrmann H. G., Boller Ch.
- TP40 **Determination of the Magnetic Losses in Laminated Cores under PWM Voltage Supply**
Vidal N., Gandarias K., Almandoz G., Poza J.
- TP41 **New RF EMAT for complex fluid characterization**
Wang Y., Wilkie-Chancellor N., Serfaty S., Martinez L., Roucaries B., Le Huérou J. Y.
- TP42 **Sensor of Magnetic Flux Density Waveform Distortion**
Zemánek I., Havlíček V., Havránek A.
- TP43 **Dynamic Hysteresis Loops Modelling by Means of Extended Hyperbolic Model**
Nová I., Havlíček V., Zemánek I.

Tuesday, July 3, 2012

- TP44 **Anisotropic Magneto-Resistance in Ni80Fe20 Antidot Arrays Prepared by Bottom-up and Top-down Nanolithography**
Coisson M., Barrera G., Boaritano L., Celegato F., Enrico E. (Pasquale M.)
- TP45 **Temperature drift of offset and sensitivity in full-bridge magnetoresistive sensors**
Vopálenký M., Platil A.

Wednesday, July 4, 2012

09:00 - 10:15 NANOPARTICLES, PERMANENT MAGNETS - ORAL SESSION

- 09:00 **WO10** Keynote: **Magnetic nanoparticles for therapy and diagnostic**
Pollert E., Kašpar P., Závěta K., Herynek V., Burian M., Jendelová P.
- 09:30 **WO11** **Magnetic and crystalline structure in ordered arrays of Co nanopillars**
Vivas L.G., Trabada D.G., Ivanov Y., Chubykalo-Fesenko O., Del Real R.P., Vázquez M.
- 09:45 **WO12** **Sensors magnetizations technique overview**
Tizianel S.
- 10:00 **WO13** **Analytical Calculation of Magnet Systems for Sensor and Actuator Applications**
Yonnet J. P., Allag H.

10:45 - 12:00 NDE, SQUID, MAGNETOELASTIC, CALIBRATION - ORAL SESSION

- 10:45 **WO21** **Resonance parameters of a magnetoelastic viscosity sensor and their dependence with temperature**
Bravo-Imaz I., García-Arribas A., Gorritxategi E., Arnaiz A., Barandiaran J. M.
- 11:00 **WO22** **Non-destructive measurement of permeability and magnetostriction in ribbons and wires**
Ktena A., Hristoforou E.
- 11:15 **WO23** **Separability of multiple deep crack defects with a NDE Eddy Current System**
Hamia R., Cordier C., Dolabdjian C.

Wednesday, July 4, 2012

11:30 WO24 **Nanosensors based on superconducting quantum interference device for nanomagnetism**

Granata C., Esposito E., Ruggiero B., Russo R., Russo M., Silvestrini P., Vettoliere A.

11:45 WO25 **Digital magnetometers calibration method with 3D coils**

Mohamadabadi K., Jeandet A., Hillion M., Coillot Ch.

13:30 - 15:00 METROLOGY - ORAL SESSION

13:30 WO30 Keynote: **Towards wafer scale inductive determination of magnetostatic and dynamic parameters of MTJ stacks**

Serrano-Guisan S., Liebing N., Sievers S., Nass P., Rott K., Reiss G. Pasquale M., Langer J., Ocker B., Schumacher H.W.

14:00 WO31 **Modeling and characterization of graphene Hall sensors**

Manzin A., Rajkumar R.K., Kazakova O., Cox D.C., Silva S.R.P., Tzalenchuk A.

14:15 WO32 **Triaxial magnetic compensation system for well-defined metrological calibrations of magnetometers**

Janošek M., Ulvr M., Petrucha V., Kupec J.

14:30 WO33 **Magnetization Dynamics of Nanostructured Antidot Arrays**

Pasquale M., Kuepferling M., Ambra A., Celegato F., Boariano L., Deleo N., Coisson M., Magni A., Schumacher H.W.

14:45 WO34 **Magnetic Environment and Measurement Systems with Improved Field Stability using the Single Volume Approach**

Turner S., Hall M.J., Harmon S.A.C.

15:00 CLOSING SESSION

Note: Posters MP27, MP28 and TP19 withdrawn.

Poster TP12 rescheduled to Monday poster session.

Monday, July 2

ORAL SESSION

HALL EFFECT 1

High Volume Production of Magnetic Sensors for the Automotive Market

SCHOTT Christian¹ and BLYZNIUK Mykola²

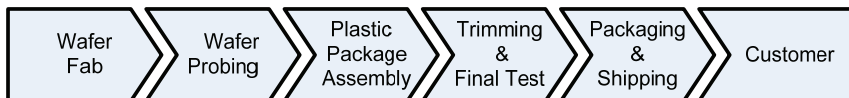
¹Melexis Technologies SA, CH-2022 Bevaix, Switzerland

²Melexis Ukraine, Kyiv, Ukraine

Integrated magnetic sensors are today extensively used in modern automobiles for contactless measurement of linear/angular position and electrical current. The applications are manifold from Windshield wiper position over Gas/Clutch/Brake pedal position to Gearshift, Transmission, Throttle Valve Position and Steering Sensors.

A car manufacturer typically uses one sensor solution for a whole model series or model platform. Sensor manufacturing volumes for single applications are typically some hundred thousand to 1 million/year. Standard products used for various applications (like generic angle position sensors) can reach volumes as high as several tens of millions per year.

This makes it a challenge to manufacture, test and finally deliver such devices on time. Silicon wafers must first be processed in the silicon foundry. Then a first test by probing on the wafer is run on the devices. After this step only the good parts are assembled into plastic packages. Then those plastic parts are run through the final trimming and test procedure to guarantee a product which is conformal to each individual item of its specification. At the end the parts are packaged and shipped to the customer for integration into the final application.



The real challenge however consists in making the sensors work without failure inside the automobile under extreme environmental conditions for a period of typically 15 years.

And this is the point where the automotive quality system plays a vital role [1].

First of all the sensor has to demonstrate after its development that it is capable to survive the harsh environmental conditions. This is proven during the device and package qualification procedure where the sensor is submitted to various kinds of temperature shocks and electrical stressing. Then the sensor has to demonstrate that there is no risk of serious functional degradation before the planned life span is reached. Since real time investigations are not possible, so-called accelerated life-time tests are carried out. Those tests simulate, in an accelerated manner over several weeks, the accumulated degradation stress of 15 years under real conditions in the car. Additionally to those sample tests, which only set the frame for the product robustness, each individual manufactured part must run through so-called reliability screening tests. By means of statistical process control, controlled over-clocking and over-voltage tests exactly those parts are filtered out, which do not fail now, but which have some kind of untypical weakness, indicating a strongly increased risk for failure during their life inside the car.

The above supply chain and quality system is illustrated by the example of a standard angular position sensor.

References

[1] Automotive Electronics Council AEC Q100 Rev. G Base Document.

Epitaxial Graphene Sensors for Detection of Small Magnetic Moments

Olga Kazakova¹ and Vishal Panchal¹

¹National Physical Laboratory, Teddington, UK

Semiconductor submicron Hall sensors are widely accepted for detection of superparamagnetic nanobeads in biomedical applications. Epitaxial graphene on 4H-SiC (0001) substrate presents an alternative route for development of ultra-sensitive Hall detectors. The material allows for improved coupling due to the reduced vertical distance between the active channel and magnetic nanoobject. Recent advances in graphene science allow incorporating tuneable photoactive material as a top gate [1, 2] and/or incorporation of side electrodes providing a control of the carrier density and improved magnetosensitivity. Graphene Hall sensors with the channel width of 0.5-20.0 μm were studied at room temperature using magnetotransport and noise spectral measurements. For a typical device at room temperature, the Hall coefficient is $R_H \approx 800 \Omega/\text{T}$, carrier density $n_e \approx 8 \times 10^{11} \text{ cm}^{-2}$ and mobility of $\sim 3000 \text{ cm}^2/\text{Vs}$, yielding to $B_{\text{min}} \approx 1 \mu\text{T}/\sqrt{\text{Hz}}$.

In order to take into account such variables, as local properties of the substrate, defects, environmental factors and geometry, we performed microscopic scale mapping of the surface potential and work function distribution in graphene Hall sensors (Fig. 1 left). Further improvement of the device performance has been achieved by incorporating of lateral gates and modification the active channel, allowing for decrease of the carrier density and minimum detectable field.

Finally, we have performed detection of a single superparamagnetic Dynal bead with diameter of 1 μm and a magnetic moment $\sim 10^8 \mu_B$ using micro-sized graphene Hall sensors. For magnetic moment detection, a combined AC-DC measurement method was used, where only the in-phase component of the AC signal (V_x) was used for the detection [3,4]. The results of applying three pulses of DC field are shown in Fig. 1 right. The cross with the bead shows a clear step-wise change in the in-phase component, $V_x \sim 7 \mu\text{V}$, whereas no notable change of the signal was detected for control crosses 2 and 3.

Thus, we demonstrated epitaxial graphene magnetometers can outperform modern state-of-the-art semiconductor devices. Such devices are readily available and very attractive for chemical and bio sensing as well as for magnetic storage applications.

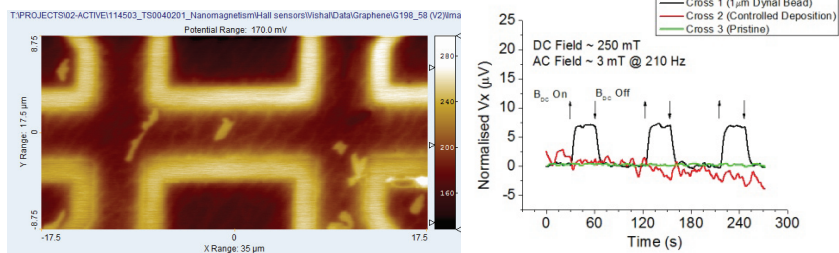


Fig. 1. Left: Surface potential mapping of the side-gated Hall sensor. Right: Bead detection experiment.

- [1] A. Tzalenchuk et al., Nature Nanotechnology 5, (2010), 186.
- [2] S. Lara-Avila et al., Advanced Materials 23, (2011), 878.
- [3] L. Di Michele et al., J. Appl. Phys. 108, (2010), 103918.
- [4] L. Di Michele et al., J. Appl. Phys. 110, (2011), 063916.

Suppressing the DC offset and LF noise in QWHS Hall based microsystems using the spinning current modulation technique

V. Mosser, vincent.mosser@itron.com

ITRON France, Issy Technology Center,
52 rue Camille Desmoulins 92448 Issy-les-Moulineaux, France

The spinning current technique, in principle, suppresses both the DC offset and low-frequency (LF) noise of Hall sensors [1], and should allow these sensors to achieve their full potential at low frequencies compatible with precision measurements [2].

However, it turns out that its practical implementation is tricky: the residual sensor noise is almost always well above (tens of dB) the theoretical thermal noise limit, especially in silicon based Hall sensors. In contrary to silicon based Hall sensors [3], III-V based Quantum Well Hall Sensors (QWHS) don't show a significant piezoresistance effect. Therefore, in this type of sensors, the spinning current implementation should be more simple to implement.

We built a microcontroller based circuit including a firmware allowing to change the spinning frequency and modulation scheme. The microsystem is directly interfaced with a PC that is used for programming the firmware as well as for the collection and visualization of data. The full-scale of the microsystem can be adapted to various measurement requirements by changing the preamplifier gain. The spinning frequency can be changed in the 20Hz–14 kHz range, i.e. well above the intrinsic corner frequency of the Hall sensor.

A systematic analysis permitted us to determine optimized conditions for implementing a 4-phase spinning current modulation scheme, taking into account limitations due to the parasitic elements in the switching circuitry i.e. capacitance and switch resistance.

Under these conditions, the microsystem is able to truly suppress most of the LF noise and DC offset from both the GaAs based QWHS Hall cross and preamplifier. The parasitic induced e.m.f. when measuring AC signals is eliminated as well.

We achieve a noise floor 2-3 dB above the theoretical thermal noise limit, i.e. typically 30 nT/ $\sqrt{\text{Hz}}$. For a Hall microsystem with a +/-50mT range, the residual DC offset that remains after the dynamic offset cancellation performed by the spinning current modulation, *i.e. without any compensation*, is at most in the 100 nanotesla range, i.e a fraction of a percent of the earth magnetic field. It might be further reduced using standard compensation techniques.

This absolute determination of zero-field conditions, of the same order than that of AMR compasses [4], is believed to be the best performance ever reported for Hall sensors without concentrator.

References

- [1] Zeno Stoessel and Markus Resch, "Flicker noise and offset suppression in symmetric Hall plates", *Sensors and Actuators* **A37-38**, 449-452 (1993)
- [2] A. Kerlain and V. Mosser, "Dynamic low-frequency noise cancellation in quantum well Hall sensors (QWHS)", *Sensors & Actuators A* **142**, 528-532 (2008)
- [3] Pavel Ripka and Michal Janošek, "Advances in Magnetic Field Sensors", *IEEE Sensors Journal* **10**, 1108-1116 (2010)
- [4] J. Včelák, P. Ripka, A. Platil, J. Kubík, and P. Kašpar, "Errors of AMR compass and methods of their compensation", *Sens. Actuators A* **129**, pp. 53-57, 2006.

Study of asymmetric cross shape planar Hall effect sensor

Malik MANSOUR^{1,2}, Christophe COILLOT¹, Frederic NGUYEN VAN DAU² and Alain ROUX¹

¹LPP Laboratory of Plasmas Physics, CNRS - Ecole Polytechnique, Palaiseau, France

²Thales Research and Technology, 1 Avenue Augustin Fresnel, Palaiseau, France

Magneto-resistive sensors are promising candidates for space applications due to their low size and weight. Among them, sensors based on planar Hall effect (PHE) have received particular interest for low frequency magnetic measurements since they offer several advantages like a low offset drift [1]. However PHE sensors detectivity, about few nT/sqrt(Hz) at 10 Hz, is smaller by, at least, one order of magnitude than the required detectivity for geophysic or space science applications, for which fluxgate magnetometers are generally used.

Many studies have been devoted to PHE sensors detectivity improvement by increasing their resistivity thanks to an appropriate shape [2], or by reducing their magnetic anisotropy [3]. Despite their assets, none of these solutions allows to improve significantly sensors detectivity at very low frequency (from 10 mHz to 1 Hz) where the $1/f$ noise component become dominant.

In this work we investigate the noise behavior of an exchange-biased asymmetric cross shape PHE sensor by the help of a homemade ultra low noise conditioning electronic having a voltage noise about $0.4 \text{ nV}/\sqrt{\text{Hz}}$ at 100 mHz.

Thanks to this asymmetric geometry, we investigate the different noise contributions of the polarisation and measurement sensor leads. As a result we show that it is possible to take benefit from the cross shape assymetry to improve sensor performance, both at frequencies where the thermal noise is dominant, as well as at very low frequencies.

References

- [1] A. Schul, F. Nguyen Van Dau and J.R. Childress: Low-field magnetic sensors based on the planar Hall effect. *Appl. Phys. Lett.* 66, 2751 (1995).
- [2] A. Persson, R.S. Bejhed, H. Nguyen, K. Gunnarsson, B.T. Dalslet, F.W. Østerberg, M.F. Hansen and P. Svedlindh: Low frequency noise in planar Hall effect bridge sensors. *Sensors and Actuators A.* 171 (2011).
- [3] V. Mor, M. Schultz, O. Sinwani, A. Grosz, E. Paperno, and L. Klein: Planar Hall effect sensors with shape-induced effective single domain behavior. *J. Appl. Phys.* 111, 07E519 (2012).

Magnetic mapping using Hall Effect sensors

SERON David¹, Zaragoza Vincent, Mosser Vincent, Haddab Youcef

¹ITRON-ITC, 52 rue Camille Desmoulins, Issy-les-Moulineaux, 92130 FRANCE

We present an application of magnetic Hall Effect sensors, whose objective is to map the magnetic field density around the gap of magnetic C-circuits intended to integrate electricity meters. This experimental study provides several important results, such as the qualification of different magnetic soft materials in terms of saturation induction or the extension of the field homogeneity in the gap, which could lead to a reduction in size of the C-circuit. It also gives an order of magnitude of the fringing field area around the gap of the C-circuit. To quantify the fringing field extent, we use the concept of effective surface S^* defined as: $B_g \cdot S^* = B \cdot S$, where B_g is the field density in the gap, B the field density into the material and S the C-circuit section. S^* has to be known to compute the C-circuit gain from measurements of rings from the same materials. Up to now, we used an S^* value derived from Finite Element Modeling (FEM) simulations [1] and this study will validate our previous results.

The magnetic Hall Effect sensors are the sensors of choice for this study. Our proprietary sensor is made from AsGa/AlGaAs/InAs 2-D quantum wells. They offer a large dynamic range and a high linearity, in full agreement with the field density to be measured. Their sensitivity allows measuring very low field density values far from the gap and their small size yields the possibility to map the field density with very small steps, in our case of the order of 10 microns.

We first describe the experimental setup built in order to implement this study. Before using the sensor to map the field, we proceed to a calibration of the Hall voltage (V_H) versus the magnetic field density on a dedicated test bench in our laboratory. The magnetic sensor is then welded on a PCB clamped on a motorized system that is remote-controlled in the 3-dimensions and with an accuracy lower than 1-micron. We developed specific algorithms to define a 2D-path for mapping and to search the field density maximum for materials qualification. We proceeded to differential measurements of the Hall voltage with a Lock-in amplifier technique that we will describe.

From the mapping results, it is then easy to extract the effective magnetic surface S^* from integration of the flux density. Our results are in very good agreement with the FEM simulations with a discrepancy lower than 10%. As anticipated from FEM simulations, S^* can be large as 8 times the section of the C-circuit. We also compare different magnetic materials in terms of saturation induction using the same test setup. Such results will help getting the best adapted material for metering purpose, but also the minimum size of the C-circuit that maintains an optimal metering accuracy.

References:

[1] A Kerlain, V. Mosser, Y. Haddab, H. Van Wick: *Large air gap magnetic core for high dynamic, high linearity, open loop current sensor*. Proceedings of the 19th Soft Magnetic Materials Conference, M3-08, (2009).

Monday, July 2

ORAL SESSION

HALL EFFECT 2

Layout and Architecture Issues in Hall based CMOS microsystems

KEJIK Pavel¹, BOURDELLE Pierre-François², REYMOND Serge², SALVI Fabrice³,
FARINE Pierre-André¹

¹Institute of Microelectronics, EPFL, 1015, Lausanne, Switzerland

²Sensima technology SA, 1196, Gland, Switzerland

³LEM SA, 1228, Plan-les-Ouates, Switzerland

The Hall cells intended for industrial applications are mainly produced in silicon integrated circuit technology. Recently, the increased use of other technologies, such as GaAs, InAs and InSb, have been reported [1]. However, a single chip solution comprising the Hall cell and the accompanying electronics has only been realized in silicon technology. A poor mobility of the silicon compare to others III-V high mobility materials makes the sensitivity of a Hall device integrated in a traditional CMOS process low and therefore offset susceptible.

Typical offset level of a Hall plate device is in the range of 10 mT, or 500 μ V if converted with a typical voltage related sensitivity of 0.05 V/VT and a bias voltage of 1 V. The most efficient method to suppress the offset of the Hall device itself is the spinning current technique [2]. Its efficiency depends on the Hall device bias conditions and the suppression factor is in the range of 50 to 500. It means that the front-end electronics has to treat the signals in the sub-micro volt range.

Usually, in publications related to the offset suppression in Hall magnetic sensors [3,4], this problem is treated either at the device physics level, as a problem of the Hall device alone, without taking into account limitations of the associated electronic circuits, or as a problem of the sensor electronic circuit with a Hall device represented merely by a very primitive and, therefore, non-adequate model. This distinction prevents a complete analysis of the offset problem and as a consequence the origin of offset in Hall based magnetic systems remains obscure.

Our contribution deals with the root cause of an incomplete offset cancellation in a real Hall based microsystem. We demonstrated that the major source of offset and offset drift is the signal treatment electronics. In order to identify the different offset sources in the system and quantify their contributions to the overall offset behaviour, we realized for this purpose a Hall microsystem test chip in 0.35 μ m CMOS standard process. Based on the results we established the design and layout methodologies, to find out a good trade-off between offset reduction, bandwidth, and current consumption for a given system architecture.

References

- [1] I. Shibusak et al., "Properties and Applications of InSb Single Crystal Thin Film Hall Elements", Technical Digest of the 18th Sensor Symposium, pp. 233-238, 2001.
- [2] P. Munter, "A low -offset spinning-current Hall plate", Sensors and Actuators A: Physical, 21-23 (1990) 743-446
- [3] P. Dimitropoulos, et al.: Horizontal Hall Devices: A Lumped-Circuit Model for EDA Simulators, proceedings of Transducers 2007, pp. 1677-1680, 10-14 June 2007
- [4] A. Bilotti, G. Monreal, R. Vig: Monolithic Magnetic Hall Sensor ICs Using Dynamic Quadrature Offset Cancellation. IEEE Journal of Solid-State Circuits, Vol. 32, No. 6, June 1997

Novel measurement setup optimize the sensitivity of a planar Hall resistance biosensor

TRAN QUANG HUNG¹, Kim Kunwoo², Sunjong Oh², Mourad Dehbaoui¹, Souleymane Kamara¹, Dumas Richard¹, Salam Charar¹, CheolGi Kim² and Ferial Terki¹

¹Laboratoire Charles Coulomb UMR 5221 CNRS-UM2, Montpellier, France

²Center for NanoBioEngineering and Spintronics, Chungnam National University, Daejeon 305-764, Republic of Korea

Efforts on healthcare everywhere have led magnetoresistive biosensors to a fascinating field. One of its precious advantages is the creation of a cheap handheld point-of-care tool which in a few minutes can easily perform multiplexed diagnose the life-threatening diseases or monitoring chronically ill patients. In this biosensor, the magnetic nanoparticles are coated with chemical groups that will bind to the biomolecules, and then could be detected by magnetic sensor. The nanoparticle–biomolecule complexes react with ‘probe’ molecules that are immobilized onto the surface of the magnetoresistive sensors. Finally, the presence of the magnetic nanoparticles on the sensor surface produces a signal change of the magnetoresistive sensor by applying an external magnetic field [1]. Consequently, both the high magnetic moment nanoparticles such as α -Fe, CoFe, α -Fe@Fe₃O₄ nanoparticles, and high field-sensitivity magnetoresistive sensors are never-ending desired for enhancement of the biosensor resolution in detecting the bioanalytes.

Among various magnetoresistive biosensors, planar Hall effect (PHE) sensor has received vast interest since it meets the needs for high sensing biosensor technology such as: high resolution owing to its small noise, small offset and linear response. To enhance the sensitivity of a PHE sensor, we have optimized both the sensor materials, and the sensor designs. In continuity development of the sensor sensitivity, we report here, the improved measurement configuration to enhance the sensitivity of a PHE sensor. The voltage change of the sensor causing by paramagnetic particles is calculated for a wide range of applied field. Thus, the critical field for maximum change of the voltage is deduced. In addition, the sensitivity of the sensor has been investigated as a function of the external magnetic field direction. By optimizing the measurement setup, the sensitivity of the sensor could be enhanced by one order in magnitude. The experimental setup for a hybrid alternative and continuous field is introduced for enhancing the sensitivity of the sensor. This optimizing method could be a paradigm easily adapted for enhancement of the sensitivity of other magnetoresistive biosensors.

References

[1] Adarsh Sandhu: New probes offer much faster results. *Nature Nanotechnology*, **2**, (2007) 746.

3-D Magnetic Vector Field Camera Using Integrated Hall and MR Sensor Arrays

Jinyi Lee^{1,2}, Jungmin Kim², Jongwoo Jun^{2*}, and Changhyun Cho^{1,2}

¹Department of Control and Measuring Robot Engineering, Chosun University, Gwangju, Korea

²Reserach Center for Real Time NDT, Chosun University, Gwangju, Korea
Corresponding author: jwjun@chosun.ac.kr

Qualitative determination of the distribution of magnetic field (MF) vectors is important to evaluate and improve the quality of magnets, magnetic assemblies, electronic motors, and voice coils. The distribution of MF vectors is also a basis for nondestructive methods such as magnetic flux leakage testing and eddy current testing. Currently, there are three ways of determining the MF vector distribution: (1) 2-D scanning using a mono-axial or tri-axial magnetic sensor [1], (2) 1-D scanning using linearly integrated magnetic sensor arrays [2], and (3) 2-D measuring using matrix-type solid-state arrayed magnetic sensors [3-5].

The first two types of devices offer a high spatial resolution, but their structure is complicated, owing to the presence of scanning equipment, and they require a longer time than matrix-type arrayed magnetic sensors for measuring MF vectors. Therefore, it is difficult to measure a time-dependent MF, i.e., an alternating MF, using these devices. The third type of device was proposed by Benitez [3], Koen [4] and Lee [5, 6], respectively. Although the spatial resolution of the cameras developed by Lee and Koen is higher than that of Benitez's device, these cameras can measure only one directional component of MF vectors. On the other hand, the use of tri-axial sensors enables the measurement of all three directional components using Benitez's device, although this also limits its spatial resolution.

On the other hand, Lee suggested a method, which integrated 2-D giant magnetoresistive (GMR) sensor arrays and 2-D Hall sensor arrays using Lee's arraying method to measure all components of the MF vectors and visualize them on a 2-D plane with a high spatial resolution [7]. However, GMR sensor is sensitive to magnetic fields in x- or y-direction. Therefore, only 2-directional magnetic field could be obtained at the same time

In this study, we integrated 2-D magnetoresistive (MR) sensor arrays and 2-D Hall sensor arrays to measure all components of the MF vectors and visualize them on a 2-D plane with a high spatial resolution. The first layer, i.e., the 2-D MR sensor array, and the second layer, i.e., the 2-D Hall sensor array, are sensitive in the x-direction (or y-direction) and z-direction, respectively.

The arrangement of arrays and wires used to integrate each MR and Hall sensor was similar to that used in Lee et al.'s camera, as shown in Fig.1 [5, 6]. The gap between each layer of MR sensors and Hall sensors was 1.5mm. By using a proto-type sensor array, the Hall and MR sensors were represented by four equivalent resistors, as shown in Fig.1. If the switching circuits SW_x and SW_y are turn-on and turn-off, respectively, Fig.1(b) is same with Fig.1(a). Also, in the inverse case, Fig.1(b) is same with them of 90 degree's rotation of Fig.1(a). Therefore, by using SW_x and SW_y, we can measure the x- and y-direction magnetic field, respectively. Fig. 2 shows the vector distribution on the artificial cracks of a magnetized ferromagnetic specimen. The cracks have 4 mm diameter, and 5 and 15 mm depth. The lift-off is 1.2 mm.

Further details about the principle, circuits, and measurements will be presented at the EMSA'2012 and IEEE Transaction of Magnetics.

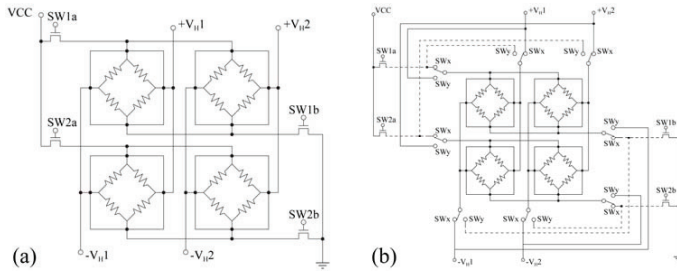


Fig.1 Representation of matrix-type Hall and MR sensors with four equivalent resistors; (a) Hall sensor arrays, (b) MR sensor arrays

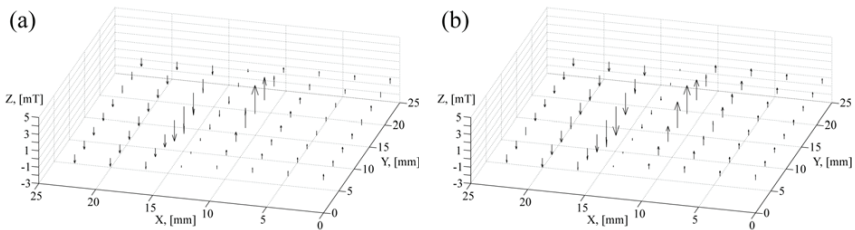


Fig.2 A sample of 3-D magnetic field on cracks with different depths; (a) 5mm, (b) 15mm

Acknowledgment

This work was supported by the National Research Foundation of Korea (NRF) grant funded by the Korea government (MEST) (No. 2011-0030110), and the MKE (The Ministry of Knowledge Economy) under the ITRC (Information Technology Research Centre) support program supervised by the NIPA (National IT Industry Promotion Agency) (NIPA-2012-H0301-12-2008).

References

- [1] T. Nishio, Q. Chen, W. Gillijns, K. D. Keyser, K. Vervaeke, V. V. Moshchalkov: Scanning Hall probe microscopy of vortex patterns in a superconducting microsquare. *Physical Review B* 77, (2008), 2-5.
- [2] C. H. Smith, R. W. Schneider, T. Dogaru, S. T. Smith: Eddy-Current Testing with GMR Magnetic Sensor Arrays. *Review of Progress in Quantitative Nondestructive Evaluation* 23/23, (2003), 406-413.
- [3] D. Benitez, P. Gaydecki, S. Quek, V. Torres: Development of a solid-state multi-sensor array camera for real time imaging of magnetic fields. *Journal of Physics: Conference Series* 76, (2007), 1-7.
- [4] K. Vervaeke: Inspection of magnetization vector and magnetic field distribution of uniaxial and multipole sensor magnets using fast high resolution MagCam magnetic field mapping and analysis. *Sensor Proceedings*, (2011), 762-767.
- [5] J. Jun, J. Kim, J. Lee, Y. Park: A hand-held magnetic camera system for real time crack inspection. *Sensors Applications Symposium*, (2011), 298-301.
- [6] J. Lee, J. Jun, J. Hwang: Magnetic sensor array and apparatus for detecting defect using the magnetic sensor array. *PCT WO2008/054056/A1*.
- [7] J. Kim, J. Lee, J. Jun, M. Le, C. Cho: Integration of Hall and Giant Magnetoresistive Sensor Arrays for Real-Time 2-D Visualization of Magnetic Field Vectors. *Intermage 2012, ET-10*, (2012), submitted for publication.

Transmission line type thin film sensor and measurement of MCG

S. Yabukami¹, H. Nakano¹, T. Ozawa¹, K. Kato¹, N. Kobayashi², K.I. Arai²,

¹Tohoku-Gakuin University, 985-8537, Tagajo, Japan

²Research Institute for Electric and Magnetic materials, 982-0807, Sendai, Japan

A highly sensitive magnetic field sensor operating at room temperature shows promise for biomagnetic measurement. High frequency carrier type sensors [1] have potential for high-sensitivity applications similar to SQUID (Superconducting Quantum Interference Devices). In the present study we developed a transmission line type thin film sensor for biomagnetic application. The sensor element consists of coplanar pattern of Cu, ceramic substrate ($\epsilon_r=115$) and amorphous CoNbZr film. The carrier current flows in the Cu conductor, not in the magnetic thin film, so the sensor is different from conventional GMI sensors with respect to this. Small magnetic field changes permeability and shifts the phase of carrier in the transmission line because of skin effect and ferromagnetic resonance. The films were deposited by RF sputtering, and anisotropy was driven by annealing. The impedance and phase difference of the sensor were measured using the S-parameter of a network analyzer (HP8752A). A small AC magnetic field was applied to the sensor element and a very small phase change was detected using a Dual Mixer Time Difference method [1]. The experiments were carried out in a magnetically shielded room (Attenuation: 34 dB at 1 Hz). The resolution of magnetic field detection was about 13 pT when a small magnetic field of 1 kHz was applied. The human body lay on a bed made of SUS304. The sensor was placed several mm from the body. The sampling rate was 5 kHz. Fig. 1 shows a measured magnetocardiogram (MCG) signal and electrocardiogram (ECG). We marked the peaks of the R wave, and averaged the MCG signal 200 times, resulting in improvement of the signal-to-noise ratio. In MCG, rapid changes of the R wave and slow change of the T wave were roughly observed. MCG signals including R wave and T wave were synchronized with ECG signals (Lead I). The reasonable R wave around 100 pT was obtained.

Reference

[1]S. Yabukami, K. Kato, Y. Ohtomo, T. Ozawa, K.I. Arai, *Journal of Magnetism and Magnetic Materials*, vol.321, pp.675-678 (2009).

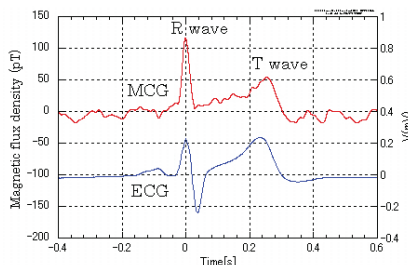


Fig. 1 Measured MCG and ECG.

Monday, July 2

ORAL SESSION

GMI

Development of a high sensitivity Giant Magneto-Impedance magnetometer: comparison with a commercial Flux-Gate

B. Dufay^{1,2}, S. Saez¹, C. Dolabdjian¹, A. Yelon², D. Ménard²

¹Université de Caen Basse-Normandie,

ENSICAEN and CNRS, UMR6072 GREYC, F-14032 Caen, France

²Ecole Polytechnique de Montréal, Département de Génie Physique & Regroupement Québécois des Matériaux de Pointe, Montréal, Québec, Canada H3C3A7

The Giant Magneto-Impedance (GMI) effect has attracted considerable attention mainly due to its potential for magnetic sensing. An important characteristic for such applications is the equivalent magnetic noise level, since it ultimately determines the lowest measurable magnetic field. However, only a relatively small number of studies have treated the use of GMI sensors in a real magnetometer configuration and addressed noise performance.

Here, a fully operational GMI-based magnetometer is presented. The excitation current amplitude is set at the optimal value, determined by the physical properties of the sensing wire [1]. The sensing element consists of a detection coil, strongly coupled to the wire, in a two-port configuration. Its optimization is based on the surface impedance tensor of the sensing element [2, 3], in which we include parasitic capacitance and geometric parameters of the coil. Conditions for optimizing the electronic noise level are deduced from the model presented in [4]. The analysis leads to an overall understanding of the system and allows us to identify the main limiting parameters for noise reduction.

The optimized sensor and its conditioning electronics have been operated in a field-locked loop, yielding a fully operational magnetometer, capable of measuring field in an unshielded environment. Experimental noise performance correlates well with that expected from the sensitivity and noise models. Characteristics of the GMI-magnetometer are comparable to those of a commercial Flux-Gate magnetometer, as shown in Table I.

	Sensitivity	Bandwidth	Noise level at 1 Hz	White noise level	Maximum excursion	Sensing element size
	kV/T	Hz	pT/ $\sqrt{\text{Hz}}$		μT	$l \times \varnothing$ in mm
GMI	100	DC to 90kHz	35	1.5	± 100	20×0.4
Flux-Gate	143	DC to 3kHz	<6	<6	± 70	18×4

Table I: Measured characteristics of the GMI-based magnetometers, compared to a commercial Flux-Gate Bartington MAG-03IEL70 (low noise).

References

- [1] B. Dufay, S. Saez, C. Dolabdjian, A. Yelon and D. Ménard: *Physical properties and giant magnetoimpedance sensitivity of rapidly solidified magnetic microwires*, Journal of Magnetism and Magnetic Materials 324 (2012), pp. 2091-2099.
- [2] D. Ménard and A. Yelon: *Theory of longitudinal magnetoimpedance in wires*, Journal of Applied Physics, vol.88 (2000), p.379.
- [3] S. Sandacci, D. Makhnovskiy, L. Panina, K. Mohri and Y. Honkura, *Off-diagonal impedance in amorphous wires and its application to linear magnetic sensors*, IEEE Transactions on Magnetics, vol.40, no.6 (2004), pp.3505-3511.
- [4] B. Dufay, S. Saez, C. Dolabdjian, A. Yelon and D. Ménard: *Impact of electronic conditioning on the noise performance of a two-port network giant magnetoimpedance magnetometer*, IEEE Sensors Journal, vol.11, no.6 (2011), pp.1317-1324.

GMI in nanostructured FeNi/Ti multilayers with different thicknesses of the magnetic layers

E. FERNÁNDEZ¹, A. V. Svalov¹, G. V. Kurlyandskaya¹, A. García-Arribas¹

¹Departamentento de Electricidad y Electrónica, Universidad del País Vasco UPV/EHU, Bilbao, Spain

The GMI (Giant Magneto-Impedance) effect is the great change of the electrical impedance that certain soft ferromagnetic materials exhibit when an external magnetic field is applied. This effect is basically a consequence of the reduction of the effective cross section of the sample when an AC current flows, due to the skin effect. For sensor applications compatible with miniaturization and electronic integration, thin film GMI materials with low coercivity, very high magnetic permeability, high saturation magnetization and a well-defined magnetic anisotropy are required. One of the most suitable materials for this purpose is the Fe₁₉Ni₈₁ permalloy. For good GMI response the magnetic film has to be rather thick (about 1 μm). Previous studies have demonstrated that, once the thickness reaches 200 nm, an out of plane component of the magnetization appears, leading to an increase of the coercivity and ruining the magnetic softness [1]. The insertion of 6 nm thick titanium layers between successive permalloy layers, interrupts the developing of the out of plane component of the magnetization, allowing to obtain about one micron thick films without deteriorating the magnetic softness [2]. It is still to be elucidated whether a strategy with few thick FeNi layers is advantageous over stacking a relatively large number of thinner magnetic layers. For this purpose, we have prepared a series of samples with different number and thickness of the magnetic layers separated by thin Ti separators: [FeNi(100nm)/Ti(6nm)]₃/FeNi(100nm), [FeNi(50nm)/Ti(6nm)]₇/FeNi(50nm), and [FeNi(25nm)/Ti(6nm)]₁₅/FeNi(25nm) structures were deposited by magnetron sputtering onto glass substrates. The overall thickness of magnetic material is 0.4 μm for all of them. The samples have been cut in rectangles 10 mm long and 2 mm wide. A transverse magnetic anisotropy was produced during deposition under a constant magnetic field of 250 Oe.

Magnetic and GMI measurements, as well as domain observations have been performed in the samples, and the results will be comparatively discussed in the paper. One important point to consider in the analysis of the magnetic behavior of the samples is the prevalence of Bloch or Neel domain walls in each magnetic layer, depending on the thickness of the magnetic layers [3] This, together with their possible interaction between layers conditions the magnetic and GMI response of the FeNi/Ti multilayered samples.

References

- [1] A. V. Svalov, I. R. Aseguinolaza, A. García-Arribas, I.Orue ,J .M. Barandiaran, J. Alonso, M. L. Fdez-Gubieda, G.V. Kurlyandskaya, "Structure and Magnetic Properties of Thin Permalloy Films Near the Transcritical State", IEEE Trans. Magn. 46, (2010) 333.
- [2] G. V. Kurlyandskaya, A. V. Svalov, E. Fernandez, A. Garcia-Arribas, and J. M. Barandiaran, "FeNi-based magnetic layered nanostructures: Magnetic properties and giant magnetoimpedance", J. Appl. Phys. 107, (2010) 09C502-3.
- [3] S. Middelhoek, "Domain Walls in Thin Ni-Fe Films", J. Appl. Phys. 34 (1963) 1040.

Noise and sensitivity of GMI sensing elements

D. Menard¹, A. Yelon¹, Basile Dufay², S. Saez², C. Dolabdjian²,

¹Ecole Polytechnique de Montréal, Département de Génie Physique & Regroupement Québécois des Matériaux de Pointe, Montréal, Québec, Canada H3C3A7

²Université de Caen Basse-Normandie,
ENSICAEN and CNRS, UMR6072 GREYC, F-14032 Caen, France

Increasing the intrinsic sensitivity of magnetic sensing elements requires theoretical models of their electromagnetic response as a function of relevant parameters, such as bias and excitation fields, material properties and geometry. These models are particularly useful when they yield simple expressions for the sensitivity (V/T) and noise spectral density (V/ $\sqrt{\text{Hz}}$), two critical metrics directly related to the development of highly sensitive magnetometers. While we have developed such models for the noise [1] and the sensitivity [2] of giant magnetoimpedance (GMI) microwires and started to test their experimental validity [3], further work is needed in order to fully explore the interrelations between the design parameters and to extract and validate some useful design rules.

Here, we review and refine our initial models of noise and sensitivity and systematically explore the consequences of these models on the design of GMI sensing elements. Specifically, we review the effect of excitation fields, material properties and geometric parameters and highlight the trade-off involved on various performance metrics of the sensors. Special emphasis is placed on the difficulties related to the experimental determination of the relevant physical properties of soft magnetic microwires. We propose an experimental procedure for addressing some of these difficulties. Finally we analyze different avenues of improving the performance of GMI sensors, distinguishing between the causes related to ideally perfect wires and those related to defects and imperfections of real wires. Our most recent set of data lead us to believe that there is still significant room for improving the equivalent magnetic noise density and that reducing the material imperfections is currently one of the main challenges for achieving this goal.

References

- [1] L.G.C. Melo, D. Ménard, A. Yelon, L. Ding, S. Saez, C. Dolabdjian: *Optimization of the magnetic noise and sensitivity of giant magnetoimpedance sensors*. J. Appl. Phys. 103, (2008), 033903 1–6.
- [2] D. Menard, D. Seddaoui, L.G.C. Melo, A. Yelon, B. Dufay, S. Saez, C. Dolabdjian: *Perspectives in giant magnetoimpedance magnetometry*, Sensor Lett., 7, (2009), 439-442.
- [3] B. Dufay, S. Saez, C. Dolabdjian, A. Yelon and D. Ménard: *Physical properties and giant magnetoimpedance sensitivity of rapidly solidified magnetic microwires*, J. Magn. Mater. 324, (2012), 2091-2099.

Dynamic sensing of magnetic nanoparticles in microchannel using GMI technology

K.Fodil¹, M. Denoual¹, C. Dolabdjian¹, M. Harnois² and V. Senez²

¹Université de Caen Basse-Normandie, GREYC, Caen, FRANCE

²Université de Lille Nord de France, IEMN, Lille, FRANCE

This paper presents the detection of magnetic nanoparticles flowing into a microchannel using Giant Magnetic Impedance (GMI) wire sensor [1]. Magnetic labeling with nanoparticles is intensively studied since it can be operated in opaque media and do not suffer from bleaching like fluorescent labeling. SQUID magnetic sensor is not well adapted for room temperature systems. Giant Magneto-Impedance (GMI) materials are rising since their sensitivity and noise properties are better than those of GMR (Giant Magneto-Resistance) sensors [2]. The novelty of this work is to explore the use of GMI microwires for detection of magnetic nanoparticles flowing in a microtube channel (140 μm radius). The magnetization of the liquid sample induces a magnetic induction at a point P of the space which maximum can be expressed by $\vec{B}_{np}(P) = \frac{\mu_0 \chi H_{magn} V}{4\pi d^3} (2 \cos(\theta) \cdot \vec{r} + \sin(\theta) \cdot \vec{\theta}) [T]$, where χ is the susceptibility of the magnetic liquid, V is the volume of the magnetic liquid, θ is an angle depending on P position, d is the distance between the point P and the magnetic liquid. By magnetizing the magnetic nanoparticles in the liquid perpendicularly to sensitive axis of the Giant Magneto-Impedance microwire sensor, we have observed magneto-impedance signal variations induced by the magnetic field from the magnetic nanoparticles. The microfluidic device is placed between two sets of Helmholtz coils (Fig. 1). The first set of Helmholtz coils is parallel to the sensitive axis of the GMI microwire to define a proper working point for the GMI microwire sensors with a DC bias field, H_{bias} . The second set is perpendicular to the sensitive axis of GMI microwire generates the AC field, H_{magn} . It magnetizes the magnetic liquid in the channel. A video camera and an acquisition card record the displacement of the liquid and the data at the same time (Fig. 2), respectively.

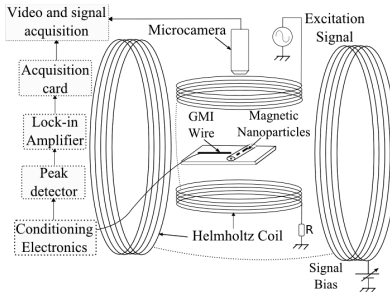


Fig. 1: Schematic view of the general set-up.

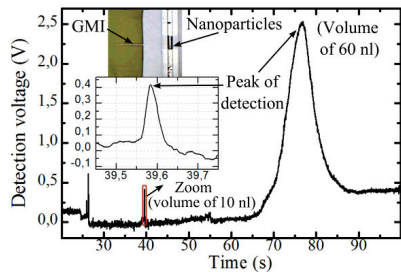


Fig. 2: Measured signal during the transit of volumes of the ferrofluid in the microtube.

The figure 2 show transits of the ferrofluid with different speed and volume. The picture is extracted from video recording. We can note that the smallest volume of nanoparticles fluid detected was 10 nl. Taking into account the SNR of our set-up, we expect to detect volumes down to 100 pl.

References:

- [1] A. García-arribas, F. Martínez, A. Fernández, I. Ozaeta, & G. V. Kurylanskaya: GMI detection of magnetic-particle concentration. *Sensors and Actuators A: Physical* 172(1), 103-108. Elsevier B.V. (2011).
- [2] D. L. Graham, H. A. Ferreira & P. P. Freitas: Magnetoresistive-based biosensors and biochips. *Trends in biotechnology*, 22(9). (2004).

Monday, July 2

POSTER SESSION MP1 - MP44

3D model of coherent rotation of magnetization in magnetoresistive elements

MICHAL VOPÁLENSKÝ

¹Department of Electrical Engineering and Informatics, College of Polytechnics Jihlava, Jihlava, Czech Republic

All through the available literature, the rotation of magnetization in narrow and thin magnetoresistive stripes is always described in a plane of the stripe only, i.e., a 2D model is used [1-3]. This approach is well justified in most of applications. However, a question can arise: does a magnetic field applied orthogonally to the plane of the magnetoresistive stripe (in the z-axis) have *any* significant influence on the rotation of magnetization and hence on the sensor response?

To be able to assess the effects the orthogonal field (z-axis) can invoke in the magnetoresistive stripe, the 2D model must be extended to 3D. To be able to make this step, demagnetizing factors along all the three stripe axes must be known. Although a single-number demagnetizing factors can be defined for ellipsoids only [4], there are models available describing the demagnetizing factors in non-ellipsoidal bodies [5, 6].

This paper deals with a mathematical conception of a 3D model of magnetization orientation in narrow magnetoresistive stripes. Using the approximate demagnetization factors, formulas are built that enable a numerical solution for the magnetization angle when considering the demagnetization in all the three sample axes. The resistivity tensor [1] or the vector equation [7] can then be used to calculate the resistivity the material imposes in the direction of the electrical current flowing through. Using the model, one can evaluate the influence of the out-of-the-plane field components on the sensor behavior.

References

- [1] S. Tumanski: Thin film magnetoresistive sensors. Institute of Physics Publishing, 2001, ISBN 0 7503 0702 1
- [2] J. P. J. Groenland, C. J. M. Eijkkel, J. H. J. Fluitman, R. M. de Ridder: Permalloy thin-film magnetic sensors. *Sensor and Actuators A*, Vol. 30 (1992), Iss. 1–2, 89–100
- [3] U. Dibbern: Magnetic field sensors using the magnetoresistive effect. *Sensors and Actuators A*, Vol. 10 (1986), 127–140
- [4] J. A. Osborn: Demagnetizing factors of a general ellipsoid. *Physical Review*, Vol. 67 (1945), No. 11–12, 351–357
- [5] A. Aharoni: Demagnetizing factors for rectangular ferromagnetic prisms. *Journal of Applied Physics*, Vol. 83 (1998), No. 6, 3432–3434
- [6] A. Aharoni: L. Pust, M. Kief: Comparing theoretical demagnetizing factors with the observed saturation process in rectangular shields. *Journal of Applied Physics*, Vol. 87 (2000), No. 9, 6564–6566
- [7] T. R. McGuire, R. I. Potter: Anisotropic magnetoresistance in ferromagnetic 3d alloys. *IEEE Transactions on Magnetics*, Vol. Mag-11 (1975), No. 4, 1018–1038

Low frequency noise of anisotropic magnetoresistors in ac-excited magnetometers

Jan Vyhnaněk¹, Michal Janošek¹, Pavel Ripka¹

¹Czech Technical University in Prague, Faculty of Electrical Engineering, Dept. of Measurement, Technická 2, 166 27 Prague, Czech Republic

Magnetoresistors can replace induction sensors in applications like nondestructive testing [1] and metal detection [2], where high spatial resolution or low frequency response is required. Although GMR sensors have higher measuring range and sensitivity compared with AMR, they show also higher hysteresis and noise especially at low frequencies. Therefore AMR sensors are chosen to be evaluated in low noise measurements with combined processing of DC and excitation field with respect to the arrangement of processing electronics.

When an AMR is working in an external excitation field, it can measure the eddy current response to detect the presence of a metal or defects in applications for NDT. Because its measuring range is small and because of the large common-mode from the excitation and Earth's field, the sensor should be nulled by a compensation field or the excitation field has to be positioned perpendicularly to the sensor sensitive axis. The sensitive magnetic layer of an AMR can be remagnetized by strong magnetic field pulses ("flipping") which erase the history of the sensor, so the hysteresis is improved and sensitivity restored even if a strong external field was applied [3]. Periodical flipping can also be used to shift the signal spectrum by the modulated output to a low noise region of signal amplifiers avoiding their offsets and low-frequency noise.

However flipping pulses are power demanding and limit the maximum flipping frequency by the allowed power losses and recovery time of the sensor output. Therefore the flipping frequency is preferred to be low, but then it can be difficult to filter out and compensate the excitation frequency, which is close to the flipping frequency. The least power consuming option is to remagnetize the AMR once in long time intervals and perform the measuring within them. The $1/f$ noise and offset of the amplifiers are however not avoided in this case and are added to the sensor noise. A low noise instrumentation amplifier AD8429 with $1 \text{ nV}/\sqrt{\text{Hz}}$ white noise is connected to the AMR sensor HMC1001. The noise resulted in $150 \text{ pT}/\sqrt{\text{Hz}}$ at 1 Hz with flipping. Without flipping, the combined noise including the $1/f$ noise of the amplifier resulted in $220 \text{ pT}/\sqrt{\text{Hz}}$.

When the flipping frequency is lower and the excitation frequency high enough to be separated by filters, both the DC and excitation frequency is processed in low noise region of amplifiers. If the flipping frequency and the excitation frequency are the same, the excitation waveform is rectified and can be simply processed by a low pass filter; the $1/f$ noise of the amplifiers has to be taken into account for in this case. However, problems with amplifier noise can be solved by using AC bridge excitation.

[1] A. Jander, C. Smith, R. Schneider: Magnetoresistive Sensors for Nondestructive Evaluation. Proc. SPIE vol. 5770, (2005), 1-13.

[2] R.J. Wold, C.A. Nordman, E.M. Lavelly, M. Tondra, E. Lange, M. Prouty: Development of a handheld mine detection system using a magnetoresistive sensor array, Proc. SPIE vol. 3710, (1999), 113-123.

[3] H. Hauser, P.L. Fulmek, P. Haumer, M. Vopálenský, P. Ripka: Flipping Field and Stability in Anisotropic Magnetoresistive Sensors, Sensors and Actuators vol. 106, no. 1-3, (2003), 121-125.

Super-paramagnetic nanoparticle bio-marking and hyperthermia-based tumor treatment

Evangelos Hristoforou

School of Mining and Metallurgical Engineering, National Technical University of Athens,
Athens, Greece

The aim of this paper is the development of a reliable diagnosis and staging method for breast and prostate malignancies with simultaneous destroying of the cancer cells applying inductive heating techniques. The method is based on the attachment of super-paramagnetic nanoparticles (SPAN) onto the cancer cell surface through the binding of specific protein molecules (with overexpressed receptors on the cancer cell membrane). Given that a breast or prostate cancer cell disposes two orders of magnitude more receptors than a healthy cell (1:100 ratio), the blood circulation and the nano-dimensions of the complex allow initially their extravasation through the existing pores of the incompletely developed blood vessels which feed cancer tumors and their attachment to the cancer cells by binding of the attached on their surface ligands (protein molecules) to the overexpressed protein receptors on cancer cell surface, in a time interval of clearly less than an hour. An innovative magnetic method, subject of PCT pending patent, promises the measurement of the spatial distribution of super-paramagnetic nanoparticles. The sensitivity of the method could possibly touch the limits of monocytic measurement under given conditions (sensitive magnetometers), which is very important for micro-metastases diagnosis. Possible cancer cells found on breast epithelium or prostate can be killed applying increased inductive heating. The increase of temperature to healthy cells is minimum ($\Delta T < 2^{\circ}\text{C}$) due to the small amount of the mounted nanoparticles to them. On the contrary, the cancer cells are killed due to the huge increase of temperature to them ($\Delta T > 50^{\circ}\text{C}$). The released nanoparticles are eliminated from the body following the same process as the attached on their surface protein-ligand.

Wireless radiofrequency sensors for the characterization of dielectric properties of biological tissues

Gayathri Masilamany^{1,2}, Pierre-Yves Joubert¹, Stéphane Serfaty²
Yohan Le Diraison², Pascal Griesmar²

¹IEF, Université de Paris-Sud, CNRS, 91 405 Orsay, France

²SATIE, ENS Cachan and Université de Cergy-Pontoise, CNRS, 94 230 Cachan, France

The accurate knowledge of the dielectric properties of biological tissues is a major issue for human health. Indeed, these properties are related to the physiological or pathological state of tissues, and may be used as relevant indicators, especially in the radiofrequencies (RF) and microwave bandwidths, either to monitor or detect pathologies [1]. It has been shown that some tissue pathologies are characterized by variations of both the electrical conductivity σ and the dielectric permittivity ε [2]. Considering the values of these parameters in the RF bandwidth (typically $\sigma \approx 0.2$ S/m and $\varepsilon \approx 40$ at 100 MHz for human skin [1]), RF techniques appear to be particularly relevant for sensing both parameters with equal sensitivity, conversely to microwaves techniques which are more sensitive to permittivity changes [3]. Measurement techniques using open-ended coaxial probes have been proposed and implemented in the RF bandwidth [Che 04]. However these contact probes are highly sensitive to the calibration process, and cannot be used for *in vivo* measurements. In this paper, the authors investigate the relevance of a contactless RF technique with either *in vivo*, *ex vivo* or *in vitro* characterizations in view. The proposed method is based on the use of radiating RF resonators featuring a high quality factor, used as transmit and receive sensors and implemented in a wireless scheme. The resonators are constituted of micro-strip patterns deposited on low loss dielectric substrate [4] so as to reach a high sensitivity to the dielectric properties of the investigated tissue. Placed either around, at the surface or inside the tissue, the resonators are sensitive to the modification of the induced magnetic field due to the local changes of the complex dielectric properties of the investigated media. These modifications are sensed through the impedance changes of the resonator, by the means of an external RF probe, electromagnetically coupled to the resonator. In this study, two RF resonators operating around 300 MHz are considered: a bracelet resonator designed for volume characterization, and a multi-turn surface coil resonator. These resonators are implemented for the characterization of tissue phantoms made of saline agarose gels, exhibiting various dielectric properties representative of physiological or pathological tissues. The sensitivities to the σ and ε parameters obtained in the case of volume, surface or embedded characterizations are evaluated compared and discussed. The ability to evaluate the complex dielectric parameters starting from the impedance variations measurement is also discussed for the three considered measurement configurations.

References

- [1] Gabriel C., "Dielectric Properties of Biological Materials", Taylor & Francis, 2006.
- [2] Haemmerich D, Staelin ST, Tsai JZ, Tungjitkusolmun S, Mahvi DM, Webster JG, In vivo electrical conductivity of hepatic tumours, *Physiol Meas.* 2003 May; 24(2):251-60.
- [3] X. Li, S. Hagness, B. D. Van Deen, D. van den Weide, "Experimental investigation of Microwave Imaging via Space-Time Beamforming for Breast Cancer Detection", in *Proc. of the IEEE International Microwave Symposium*, vol. 1, pp 379-382, 2003.
- [4] L.F. Chen et al *Microwave Electronics, Measurement and Materials Characterization*. John Wiley and Sons, 2004.
- [5] S. Serfaty, Nathalie Haziza, Luc Darrasse, Siew Kan. Multi-turn split-conductor transmission Line resonators, *Magnetic Resonance in Medicine*, 38: 687-689, 1997.

Biosensors Based on Magnetic Nanoparticles

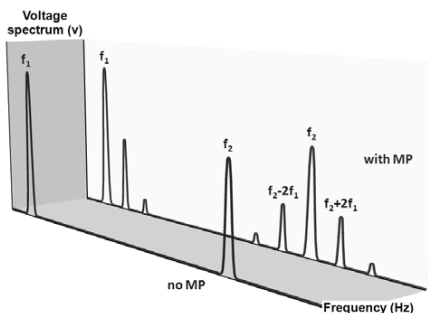
P.I. Nikitin¹, J.A. Khodakova¹, M.P. Nikitin^{1,2}, A.V.Orlov^{1,2}

¹A.M. Prokhorov General Physics Institute, Russian Academy of Sciences, Moscow, Russia

²Moscow Institute of Physics & Technology, Moscow, Russia

Novel highly sensitive magnetic biosensors have been developed based on magnetic nanoparticles (MP) used as labels and 3D porous filters which allow direct analysis of complex liquids such as neat milk, whole blood, drinks, water used for washing vegetables or meat, etc. For many complex liquids the biosensor does not require preliminary sample preparation and is compatible with large sample volume, which leads to sensitivity increase due to direct immunoenrichment of the antigen on the solid phase.

MP are detected at combinatorial frequencies by non-linear magnetization [1] as shown in the figure. The related readers can detect as little as few ng of MP [2,3] and direct comparison with radioactive technique for MP based on ⁵⁹Fe isotope demonstrated similar sensitivities of both methods [4]. Thus, the proposed biosensor approach allows realizing main advantages of old assays based on radioactive isotopes, but in much more safe and affordable ways. The combination of 3D filters and MP removes many kinetic limitations intrinsic to antigen interaction with antibody layer immobilized on 2D flat surface of standard immunoassay (ELISA) or GMR biochips. In our experiments, for optimization of the assay protocol an original optical biosensor instrument Picoscope® was used as proposed in [2,3].



As an example, several toxins produced by *Staphylococcus aureus* such as Staphylococcal Enterotoxin A (SEA), Toxic Shock Syndrome Toxin (TSST) have been detected directly in neat milk with no sample preparation, which is obligatory in standard methods. A detection limit (LOD) for TSST in 30 ml of neat milk was as low as 4 pg/ml, which is ca. 50 times better, than for ELISA. The assay time for such sample (2 hours) is less than that of ELISA (3-14 hours). For express 25 min-long procedure, using standard 0.15 ml sample volume the LOD

was 0.1 ng/ml, which is ca. 2-5 times better, than for standard, much longer methods. The developed assay has wide dynamic range (>3 orders of magnitude for both concentration and signal) as well as large angle of the signal dependence on concentration, which is close to its theoretical maximum of 1.0 in log-log scale. This allows obtaining reliable results for both low and high concentrations. The developed biosensor permits fast immunofiltration of antigens from complex samples, reduces the assay time and allows analyzing practically unlimited sample volumes.

References

- [1] P.I. Nikitin, P.M. Vetoshko, Patent RU 2166751 (2000), EP 1262766 publication (2001).
- [2] P.I. Nikitin, P.M. Vetoshko, T.I. Ksenevich, Sensor Letters, 5 (2007) 296-299.
- [3] P.I. Nikitin, P.M. Vetoshko, T. I. Ksenevich, J. Magn. Magn. Mater., 311 (2007) 445-449.
- [4] M.P. Nikitin, M. Torno, H. Chen, A. Rosengart, P.I. Nikitin. J. Appl. Phys, 103 (2008) 07A304.

Neel Effect toroidal current sensor

Eric-Vourch¹, Yu Wang¹, Pierre-Yves Joubert², André couderette³, Lionel Cima³

¹SATIE, ENS Cachan, CNRS, Universud, 94 235 Cachan Cedex, France

²IEF, Université de Paris-Sud, CNRS, 91 405 Orsay, France

³Neelogy S.A. 191, Avenue Aristide Briand 94230 Cachan France

The measurement of current is an important stake for the energy conversion, the energy management and the energy storage systems. Many sensor technologies exist such as shunts, Hall effect probes, fluxgate sensors or Rogowski coils, which exhibit different features from one to another (for example regarding the sensitivity, the dynamic range, the bandwidth, the only AC or the both AC and DC operation, the size, the weight, the implementation facility,...) [1,2]. Neel effect[®] sensors are based on a magnetic field transducer made up of magnetic nanoparticles embedded in a flexible plastic matrix [3]. Due to the superparamagnetic behavior of the nanoparticles, the transducer features a non-linear magnetization characteristic. Advantage can be taken of this non-linearity in order to accurately measure low as well as high currents. On the other hand, the possibility of building flexible sensors is also an advantage as it enables easy to install sensors to be designed. By superposing a sinusoidal magnetic field excitation to the DC or AC (slowly varying with respect to the excitation) magnetic field induced by the current to measure, a time varying magnetic flux density is sensed by the coil wound over the transducer. Thus, an electromotive force (EMF) appears at the output of the sensor. It has been demonstrated [4] that given the non linearity of the magnetic characteristic of the transducer, the amplitude of the component of the EMF at the second order harmonic of the excitation frequency is an odd function of the current to measure. This function, which is monotonous over a large range, enables measuring currents over ranges in the order of hundreds or thousands of Amperes, depending of the characteristics of the transducer.

Here we report on a Neel effect sensor featuring a toroidal topology and an excitation and measurement configuration using a single coil. This configuration is chosen so as to enable the EMF component at the first harmonic of the excitation frequency f_{ex} to be removed, and so that the output signal consists in the suitable component, that is, that at $2f_{ex}$. After presenting the concept of such a sensor, characterizations of a device are performed at different excitation frequencies. The obtained results show that with this particular device DC currents can be measured over a range [-150 A to 150 A].

References

- [1] Ziegler, S., Woodward, R.C., Iu, H.H.C., Borle, L.J.: 'Current Sensing Techniques: A Review', IEEE Sensors Journal, 2009, 9, (4), pp. 354-376
- [2] Ripka, P., 'Electric current sensors: a review', Meas. Sci. Technol., 2010, 21 112001
- [3] Lenglet L 2007 Current & magnetic field sensors, control method & magnetic core for said sensors, Billanco Patent WO2007042646 (A1).
- [4] E. Vourch, P.-Y. Joubert, L. Cima Analytical and numerical analyses of a current sensor using non linear effects in a flexible magnetic transducer. Progress In Electromagnetics Research Journal, PIER 99, 323-338, 2009

Note: Neel Effect is a trade mark and a patented technology that belongs to Neelogy SA.

Effective Power Signal Filtering using LC Filters with Air Core Coils

J. A. Somolinos¹, R. Morales², C. Moron³ and A. Garcia³

¹ Dpto. Sistemas Oceánicos y Navales, ETSI Navales (UPM), Madrid, Spain

² E.T.S.I. Industriales, University Castilla-La Mancha, Albacete, Spain

³ Dpto. Tecnología en la Edificación, E.U. Arquitectura Técnica (U.P.M.), Madrid, Spain

Computer controlled power supplies are usually expensive when high performance (wide voltage range, low ripple factor and low response time) is required. This paper presents a simple and effective system based on a V/f inverter combined with a three-phase bridge rectifier and a LC power filter. Figure 1 shows the general topology of the proposed system.

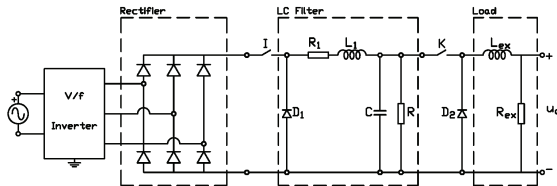


Figure 1. General view of the proposed system

Because of the widely variable frequency range of the V/f inverter when a wide range of voltage is required, amorphous or ferromagnetic core coils are avoided, and air core coils become an excellent solution to increase the efficiency of the power system. Figures 2 and 3 show the time responses of the output voltage from a 0-200 V (up to 20 A) power supply coupled with a 10 Ω inductive load. This power supply is controlled with a 0-10V analog input signal. Good time responses (less than 100 ms) and good ripple factor (less than 1%) without any overshooting are achieved, even when low voltage is required (lower frequency). Figures 4 and 5 show their corresponding frequency responses for 1 and 10V input signals. Additionally, experimental results are presented.

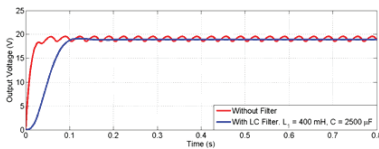


Figure 2. Time responses with $U_{in} = 1$ V

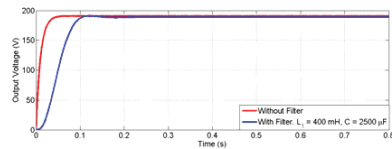


Figure 3. Time responses with $U_{in} = 10$ V

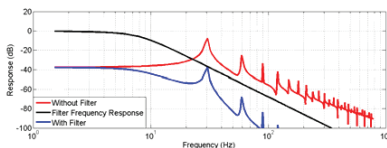


Figure 4. Frequency response with $U_{in} = 1$ V

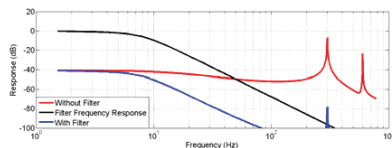


Figure 5. Frequency response with $U_{in} = 10$ V

Experimental Analysis of Magnetic Losses in a Three Phase Embedded Electrical Transformer

M. Aissaoui, D. Moussaoui, A. Oudina

Ecole Militaire Polytechnique, Bp 17 Bordj el Bahri, 16111 Alger, Algérie

The aim of the present work is to investigate a recently developed model for the prediction of core losses in an embedded electrical transformer operating at 400Hz and discuss the model's accuracy when contrasted to experimental results. The considered model combines the traditional technique of losses separation theory with the transformer electrical equations. However, excess losses are not considered in the model. Previous work indicates that the model gives reasonable results for specific operation conditions, and in particular when the air gap is overestimated. The cross section of the lamination strip is subdivided into several slices to take into consideration the skin effect. The electrical transformer model is based on the following equations:

$$U(t) = R I_k + L \frac{dI_k}{dt} + N \frac{d\phi_m}{dt} \quad (1)$$

$$H(B_k)lm + \frac{B_k}{\mu_0} 2\delta = \xi(t) + \alpha \frac{dB_1}{dt} + \beta \frac{dB_2}{dt} + \gamma \frac{dB_3}{dt} \quad k=1, 2, 3 \quad (2)$$

The theoretical losses are obtained by calculating the static hysteresis from the measured B(H) curve while the dynamic losses are obtained from the eddy-current formula together with Eqs. 1 and 2. The experiments are performed by feeding the transformer through a three-phase converter, which was designed in the laboratory specifically for the present work see Fig.1. The frequency of the converter can reach 500Hz. Contrasting the obtained results with experimental results shows that the model (Figure 2) considered improves accuracy over other models available in the literature.

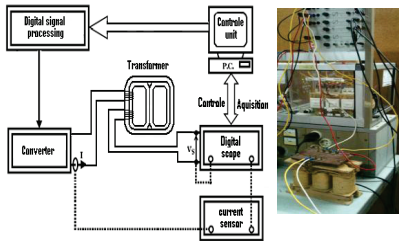


Fig. 1. Loss measurement bench.

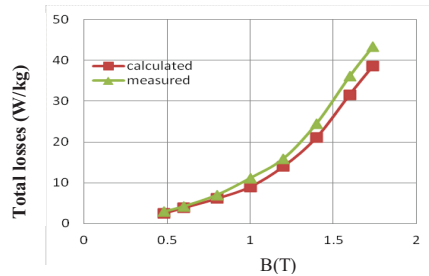


Fig. 2. Measured and predicted total losses in iron core as function of magnetization at 400 Hz.

Reference

- [1] V. Podlogar, B. Klopcic, G. Stumberger, D. Dolinar: Magnetic Core Model of a Mid-frequency Resistance Spot Welding Transformer. IEEE Trans. On Magnetics, Vol. 46, No. 2, (2010), 602-605.

Impulse Current Transformer with Nanocrystalline Core

Radek Prochazka¹, Jan Hlavacek¹, Karel Draxler², Milan Fryml³

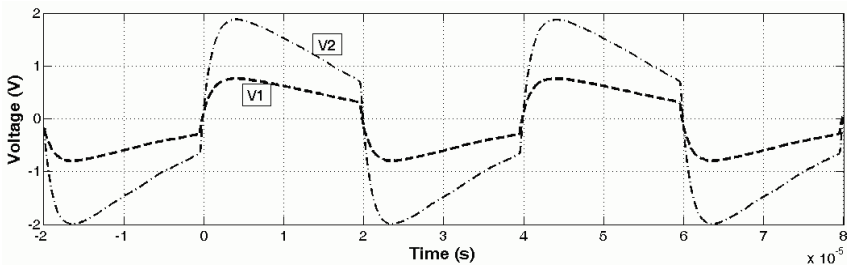
¹Department of Electrical Power Engineering, Faculty of Electrical Engineering, Czech Technical University in Prague, Prague, Czech Republic

²Department of Measurement, Faculty of Electrical Engineering, Czech Technical University in Prague, Prague, Czech Republic

³Authorized Metrological Center, KPB Intra s.r.o., Bucovice, Czech Republic

The paper deals with proposal and behavior of current transformer for impulse current transfer at a frequency of 25 kHz. One of the main requirements is the insulation of primary and secondary circuit assuming the operating voltage of primary side of 25 kV. In practice the transformer must withstand the voltage of 50 kV. The secondary side of transformer is loaded by real burden of 200 VA and composite error of current must not exceed 10 %. The time shift between the primary and secondary current is also important. Preliminary proposal was realized with the assumptions that the frequency of fundamental harmonic is 25 kHz. The main parameters and characteristics will be determined from measurements.

The measurement circuit was set up in order to measure transformer parameters. This circuit consists of RF power amplifier (800 W, 10 kHz - 3 MHz) supplied from function generator. To measure primary current the coaxial shunt $R_1 = 0.1 \Omega$ was used. The current on secondary side of transformer (total real burden 40 Ω) was measured by coaxial shunt of $R_2 = 0.2 \Omega$. Output voltage waveforms from shunts were measured by digital scope, see following figure.



The composite error can be expressed by formula: $\varepsilon_c = \frac{I_2 - I_1}{I_1} 100 = \left(\frac{V_2 R_1}{V_1 R_2} - 1 \right) 100$ (%), where I_1 , I_2 a V_1 , V_2 are rms values of currents resp. voltages at shunts. The ratio of shunt resistances $R_1/R_2 = 0.41$ was determined from dc calibration. Assuming that the rms values of voltages were measured by Agilent 8458A voltmeter and both coaxial shunts are frequency independent up to 500 kHz, the composite current error did not exceed the value of 6% in the range of 10% - 120% of transformer rated current.

References

- [1] de Carvalho Batista, T.; Luciano, B.A.; Freire, R.C.S.; Catunda, S.Y.C.; "Current transformer with nanocrystalline alloy core for measurement," Instrumentation and Measurement Technology Conference (I2MTC), 2011 IEEE, pp.1-4, 10-12, May 2011
- [2] Draxler K. - Styblikova R.: Use of nanocrystalline materials for current transformer construction. Journal of Magnetism and Magnetic Materials 1996, vol.157-8, pp. 447 – 448

Comparison of functional characteristics of miniature, double axis fluxgate sensors in Vacquier and Foerster configurations

Piotr Frydrych¹, Roman Szewczyk², Jacek Salach¹, Krzysztof Trzcinka²

¹Institute of Metrology and Biomedical Engineering, Warsaw University of Technology, Warsaw PL-02-525, Poland

²Industrial Research Institute for Automation and Measurements (PIAP), Warsaw PL 02-486, Poland

Fluxgate sensors made in PCB technology became common solution for miniature magnetometers. Due to small dimensions they are suitable for surface magnetic field scanning [1]. Thanks to low power consumption [2] such sensors are also suitable for electronic mobile devices [3]. Recently developed in PCB technology, miniature fluxgate sensors commonly use Vacquier configuration. However, alternative Foerster configuration seems to be forgotten. However Foerster type fluxgates can be suitable especially for miniature two axis fluxgate sensors [4].

This paper presents the results of research on possibility of development of miniature fluxgate sensors in Foerster configuration. These results are compared with fluxgate sensors characteristics in Vacquier configuration, which properties have already been tested [5].

Sensors in both configurations use the same core made of amorphous $\text{Fe}_{78}\text{B}_{13}\text{Si}_9$ alloys. During production process they were part of the same 7 layers printed board. Characteristics of both developed sensors were tested using the same experimental setup, which consist of three axis Helmholtz coils, fluxgate driving module with voltage/current transducer as well as selective nanovoltmeter. Results of measurements were analyzed considering sensitivity as well as in power consumption.

Presented research gives opportunity to further development of miniature two axis fluxgate sensors. Characteristics of both sensors and their power consumption parameters are important for optimization of fluxgate construction technology, which have already been investigated for material [6] and driving parameters [7].

References

- [1] Janosek, M. ; Ripka, P. ; Platil, A. : Magnetic markers detection using PCB fluxgate array. *J. of App. Phys.* 105 Vol. 7(2009).
- [2] Kubik, J. ; Pavel, L. ; Ripka, P. ; Kaspar, P. : Low-power PCB fluxgate sensor. *Sensors*, 2005 IEEE (2006) 432-435.
- [3] Vcelak, J. ; Petrucha, V. ; Kaspar, P. : Compact Digital Compass with PCB Fluxgate Sensors. *Sensors*, 2006. 5th IEEE Conference, (2007), 859 - 861.
- [4] http://techtransfer.ucc.ie/industry/documents/FluxgateleafletIV13_000.pdf
- [5] Frydrych, P. ; Szewczyk, R. ; Salach, J. ; Trzcinka, K. : Two-Axis, Miniature Fluxgate Sensors. *IEEE Trans. on Mag.* 48 Vol. 4, (2012), 1485 - 1488.
- [6] Frydrych, P. ; Szewczyk, R. ; Salach, J. ; Trzcinka, K. : Dependence of Functional Characteristics of Miniature Two Axis Fluxgate Sensors Made in PCB Technology on Chemical Composition of Amorphous Core. *Springer, Mechatronics, Part I*, (2012), 55-61.
- [7] Tipek, A. ; O'Donnell, T. ; Ripka, P. ; Kubik, J. : Excitation of PCB fluxgate sensor. *Sensors*, 2003. *Proceedings of IEEE*, Vol. 1, (2004), 647 - 650.

Optimization of driving current parameters for two axis fluxgate sensor

Piotr Frydrych¹, Roman Szewczyk², Jacek Salach¹, Krzysztof Trzcinka²

¹Institute of Metrology and Biomedical Engineering, Warsaw University of Technology,
Warsaw PL-02-525, Poland

²Industrial Research Institute for Automation and Measurements (PIAP), Warsaw PL 02-486,
Poland

Fluxgate sensors are intensively developed due to the fact, that they are used in navigation devices [1], nondestructive testing [2], safety and security applications [3] and many other branches where weak constant magnetic field measurements are necessary. Accuracy, sensitivity or level of energy consumption depends strongly on driving current parameters such as its shape, amplitude or frequency. Optimisation of driving parameters will help to achieve best functional parameters of sensors.

Paper presents the results on research of two axis miniature fluxgate sensor. Investigated sensor was made of seven layers PCB board. Frame shaped amorphous core made of amorphous $\text{Fe}_{78}\text{B}_{13}\text{Si}_9$ was used to measure magnetic field in two perpendicular directions. Frame-shaped core of investigated, miniature fluxgate sensor was made from amorphous alloy ribbon using photolithography technology. Core was placed in middle layer of 7 layers PCB board [4]. Measurements in each direction of fluxgate sensor were made simultaneously. Sensor characteristics were tested using three axis Helmholtz coils as reference magnetic field source. During the research three parameters of driving current were changed: its shape, amplitude and frequency. Due to three variables optimisation and time consuming characteristics testing, specialised computer controlled measuring setup was developed. This setup utilized National Instruments data acquisition and control card controlled by LabView. Method of optimisation of driving parameters utilised gradient-based optimisation algorithm. On the base of this algorithm optimal parameters of driving current were determined from the point of view of fluxgate sensor sensitivity maximisation.

References

- [1] Vcelak, J. ; Petrucha, V. ; Kaspar, P. : Compact Digital Compass with PCB Fluxgate Sensors. Sensors 2006 IEEE conference (2007), 859 - 861.
- [2] Gu Wei ; Chu Jianxin : A transducer made up of fluxgate sensors for testing wire rope defects. IEEE Trans. on Mag. 51 Vol. 1, (2002), 120 - 124.
- [3] Baglio, S. ; Ando, B. ; Malfa, S.L. ; Bulsara, A.R. ; Kho, A. ; Anderson, G. ; Longhini, P. ; In, V. : Advanced dynamic magnetometer for persistent surveillance. Waterside Security Conference (WSS), 2010, 1 - 4.
- [4] Frydrych, P. ; Szewczyk, R. ; Salach, J. ; Trzcinka, K. : Two-Axis, Miniature Fluxgate Sensors. IEEE Trans. on Mag. 48 Vol. 4, (2012), 1485 - 1488.

Noise Characteristics of Ferroprobe and Magnetic Microwire Four Channel Magnetometers of VEMA Series

J. Hudák¹, A. Čverha¹, P. Lipovský¹, R. Sabol¹, J. Blažek¹, D. Praslička¹, V. Moucha¹

¹Faculty of Aeronautics, Technical University of Kosice, Slovakia

The article deals with the summarization of results obtained by a comparison of four channel ferroprobe and magnetic microwires magnetometers of VEMA series [1]. Generally, the ferroprobe magnetometers are very common instruments used for weak stationary and low frequency magnetic fields measurement. The sensitivity of the ferroprobe is determined by a magnetic noise caused by a periodical magnetisation of its core [2]. Similarly, the origin of the magnetic noise in magnetic microwire sensors is in a periodical movement of the domain wall in the axial direction of the microwire [3]. In both cases the magnetic noise of sensors is determined by the core material and the core geometry, and it is practically inherent. Other sources of noise influencing the output signals of vector magnetometers are generated by fluctuations of voltages and currents in measurement chain electronics. Their level is usually dependent on the construction quality and by the used electronic components. Fluctuations of measured magnetic field background generated by nearby or distant sources and processes are also considered as noise and they influence the overall noise in the output signal of the vector magnetometer.

It is accepted, that the noise properties of magnetometers are sufficiently characterized by the power spectral density of the noise and the amplitude distribution. We compared the mean values, effective values, powers, probability distributions and the power spectral densities of the noise in the output signals of all four magnetometer channels. We also analyzed differential and correlation functions between the channels. The probes were placed in defined arrangements in a point, plane and space, where stationary and also low frequency magnetic field was generated. The sampling frequency was 1 kHz and the time interval of one analyzed data set was 1 s. We also performed 24 hour measurements, whereby the analyzed one-second data records were collected in five-minute intervals. The computed characteristics were visualized in the form of one, two and three dimensional graphs.

References

- [1] HUDÁK, Jozef - BLAŽEK, Josef - PRASLIČKA, Dušan - MIKITA, Ivan - LIPOVSKÝ, Pavol - GONDA, Patrik: Sensitivity of Vema-04.1 magnetometer. In: Journal of Electrical Engineering. Vol. 61, no. 7s (2010), p. 28-31. ISSN 1335-3632
- [2] BLAŽEK, Josef - HUDÁK, Jozef - PRASLIČKA, Dušan: A relax type magnetic fluxgate sensor. In: Sensors and Actuators A: Physical. Vol. 59, no. [1-3], p. 287-291. - ISSN 0924-4247
- [3] HUDÁK, Jozef - BLAŽEK, Josef - ČVERHA, Andrej - GONDA, Patrik - VARGA, Rastislav: Improved Sixtus-Tonks method for sensing the domain wall propagation direction. In: Sensors and Actuators A : Physical. Vol. 136, no. 2 (2009), p. 292-295. - ISSN 0924-4247

An offset temperature dependence of a fluxgate magnetometer and its compensation

PETRUCHA Vojtech

Department of Measurement, Faculty of Electrical Engineering, Czech Technical University in Prague, Czech Republic

The offset temperature dependence of a fluxgate magnetometer is given by many factors. Most important are properties of the fluxgate sensor and the stability of excitation and signal conditioning circuits. The offset temperature stability of a vectorially compensated magnetometer has been studied and measured. The magnetometer consists of three miniature ring-core fluxgate sensors which are embedded in a system of three vector compensation coils. The excitation is provided by H-bridge and specific output circuit (similar to [1]). The signal conditioning is based on synchronous detection of the second harmonic output signal. A method of the offset temperature dependence compensation presented in [2] has been intended for application in the design. The method is based on phase-shifting of detector control signals based on measurement of the excitation waveforms. The temperature dependence of the excitation coils resistivity is identified to be the main cause of change of excitation conditions which result in the offset temperature dependence. The phase-shift between the excitation control signal and excitation voltage across the three fluxgate sensors shows significant (almost linear) temperature dependence (see Fig. 1). There is a hysteresis visible in the graph which is caused by non-ideal placement of the reference temperature sensor. Unfortunately the first prototype of the vectorially compensated magnetometer does not provide any significant monotonous linear offset temperature dependence; rather high amplitude low frequency noise is present. This is probably caused by thermally induced mechanical stresses in the core. Two new prototypes of the fluxgate magnetometer have been manufactured and their properties will be measured soon. The results of this measurement and also other effects (influence of tuning capacitors) will be discussed in the paper.

References

- [1] O. V. Nielsen, J. R. Petersen, F. Primdahl, P. Brauer, B. Hernando, A. Fernandez, J. M. G. Merayo and P. Ripka: Development, construction and analysis of the 'Oersted' fluxgate magnetometer; 1995 Meas. Sci. Technol. 6. 1099
- [2] A. Cerman, J. M. G. Merayo, P. Brauer, F. Primdahl: Self-Compensating Excitation of Fluxgate Sensors for Space Magnetometers; I2MTC 2008 – IEEE International Instrumentation and Measurement Technology Conference, 2008.

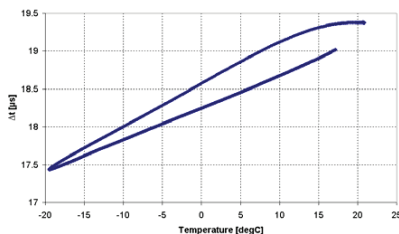


Fig. 1 Phase shift in the excitation circuit

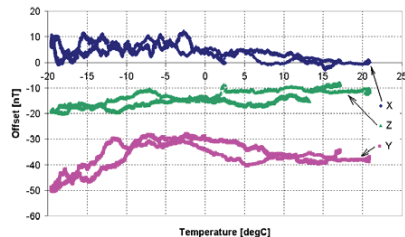


Fig. 2 Offset temperature dependence

Current measurement with a GMI sensor

Aktham ASFOUR, Jean-Paul YONNET and Manel ZIDI

Laboratoire de Génie Electrique de Grenoble (G2E Lab), UMR CNRS/INPG-UJF n°5529, Institut Polytechnique de Grenoble, ENSE3, St Martin d'Hères, France

The design and performance of a linear current sensor are presented. This sensor is based on a Giant Magneto-Impedance (GMI) element with a negative feedback. Figure.1 shows its block diagram. The sensing element is a 30 μm diameter GMI amorphous wire (Unitika Ltd). It is curled to a toroidal core of 2 cm diameter. Bias and feedback coils are wound around the core. The bias current is about 2.2 A, resulting in a bias field of 315 A/m. We developed conditioning electronics that consist of a square wave oscillator (3 MHz) based on a Schmitt trigger, a peak detector and a high gain amplifier with zero adjust. The GMI element is driven at an AC current of 5 mA peak-to-peak.

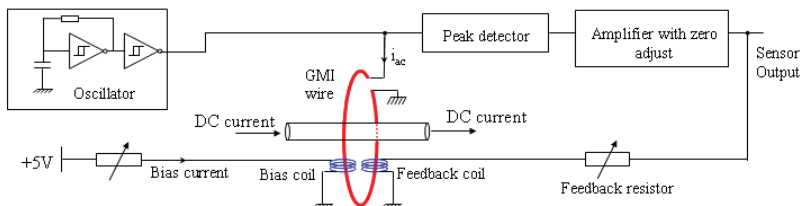


Figure. 1. A block diagram of the GMI-based current sensor

DC current measurements were performed. Results are shown on Figure. 2. With a high open-loop sensitivity of 25 V/A and a strong feedback, a good linearity is obtained in closed-loop within a range of $\pm 37\text{A}$. This measured sensitivity is about 0.27 V/A. The analysis of the closed-loop operation [1] gives a theoretical sensitivity of about 0.31 V/A, which is with good agreement with the measurement.

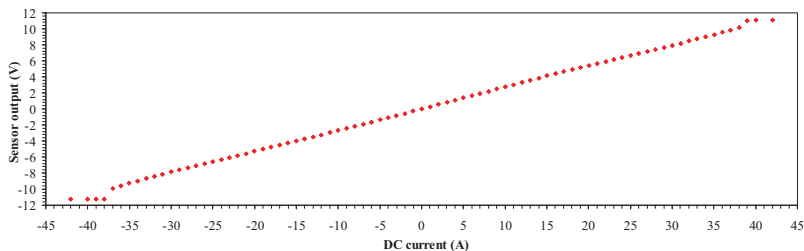


Figure. 2. Current measurements in closed-loop

The developed sensor could be used for applications that require relatively large measurement range such as power systems.

References

[1] K. Mohri, T. Uchiyama, L. P. Shen, C.M. Cai and L. V. Panina: Amorphous wire and CMOS IC-based sensitive micro-magnetic sensor (MI sensor and SI sensor) for intelligent measurements and controls. *J. Magn.Magn.Mater.*, vol. 249, (2002), 351-356.

Prediction of Giant Magneto Impedance on Co-Complex Coated Fe-Based Amorphous Wires Using Neural Network

Osman Caylak, Naim Derebasi

Uludag University, Department of Physics, 16059 Gorukle Bursa, Turkey

A change of the high frequency impedance of soft ferromagnetic materials under a static magnetic field and frequency called as giant magneto-impedance (GMI) effect. Recently, artificial neural networks (ANN) have successfully used for the prediction of magnetic performance in electromagnetic devices made from soft magnetic materials [1]. A giant magneto impedance effect was experimentally investigated on organic coated Co-complex Fe-based amorphous wires [2, 3].

The obtained data from these investigations was used for the training of the network. A 3-node input and 1-node output layer ANN model with 4 hidden layers and full connectivity between nodes was developed. The input parameters were sample properties, frequency and static magnetic field while output parameter was the GMI effect. A total of 3200 input vectors obtained from varied samples were available in the training set. The network was formed by a tangent hyperbolic transfer function in the hidden layer, sigmoid transfer function in output layer and 30 numbers of nodes in the hidden layers, after the performance of many models were tried. A set of test data different from training data set was used to investigate the network performance. The average correlation and prediction error of giant magneto impedance effect were found to be 99.6%, 0.4% for tested Co-complex Fe-based amorphous wires respectively. It is believe that the predictions from the model can be useful in GMI sensor design and applications.

References

- [1] Caylak O, Derebasi N and Meydan T, *Sensor Letters* 5, (2007), 123-125.
- [2] Caylak O and Derebasi N, *Journal of Optoelectronics and Advanced Materials*, 10 (11), (2008), 2916-2918
- [3] Peksoz A, Kaya Y, Taysioglu AA, Derebasi N and Kaynak G, *Sensors and Actuators A*, 159, (2010), 69

High Performance Current Sensor Utilising Giant Magnetoimpedance (GMI) in Co-based Amorphous Wires

Brett Fisher, Larissa Panina, Nick Fry and Des Mapps

School of Computing and Mathematics, University of Plymouth, Plymouth, UK

A Giant Magneto-impedance (GMI) non-contact sensor was developed to detect small currents and subsequently the leakage current between two current carrying conductors. A glass-coated amorphous wire with composition $Co_{66}Fe_{3.5}Cr_{3.5}Si_{11}B_{16}$ and a total diameter of $47.5\ \mu\text{m}$ was used as a GMI element. With an excitation frequency of 20 MHz, the wire of 5mm long showed an impedance change ratio greater than 100% between 0.6-1.2 Oe. The GMI wire is placed between two mu-metal washers. The sensor response does not depend on the position of the current carrying conductor in this chosen configuration. This also allows a small difference between two current carriers to be measured. High frequency excitation was realised by subjecting the wire to sharp pulsed current provided by a microcontroller. The characteristic frequency of the pulse excitation is in the range of 20 MHz. The use of microcontroller to drive the sensor was chosen to meet the requirements of the processing stage and to provide additional functionality with the same hardware. The excitation signal (pulse time and frequency) can be regulated to realise the best sensitivity for the GMI wire. Features including real-time digital filtering, data manipulation and the provision of a closed loop system can also be provided from the microcontroller. A leakage current simulation resulted in a resolution of a few mA for a carrier current of few Amperes, which is well below typical fault current levels of more than 10 mA. Therefore, it has been demonstrated the ability for high resolution current sensing based on pulse driven GMI element within a simple construction.

Differential Magnetic Permeability: A Tool for Coiled Giant Magneto-Impedance Design

Joël Moutoussamy¹, Christophe Coillot¹ and Gerard Chanteur¹

¹Laboratoire de Physique des Plasmas, CNRS - Ecole Polytechnique, France.

The present work is focused on high sensitivity (450-1300V/T) transverse coiled GMI transducers [1] manufactured with various magnetic materials, magnetically excited ($f < 50\text{kHz}$ and $I_{ac} < 10\text{mA}$, Fig 1) by an insulated coil which is also used for the measurement [2]. Two nanocrystalline films annealed under longitudinal and transverse magnetic fields (Fig 1), four different length (4-6-8-10cm) Ni-Fe films and one Mn-Zn thin ferrite core are studied through their impedance and their equivalent sensitivity (S_{equi}) [1] measurements at different frequencies and magnitudes of both the current (I_{ac}) excitation and the weak magnetic field (h_m , Fig 1). Because of the demagnetization and magneto crystalline anisotropies, the influence of the static magnetic field (H_0) is also investigated (Fig 2).

As reported in the previous study [1], the results have confirmed the primary role played by the derivative of the effective differential magnetic permeability (μ_{diff}) whatever the material used. As a consequence and from experimental results, analytic expressions of $\mu_{diff}(H_0, \omega)$ which are fitted with monotonous or double peak differential magnetic permeability are proposed and discussed first, from magneto crystalline and shape anisotropies considerations and secondly, from dynamic magnetization theory.

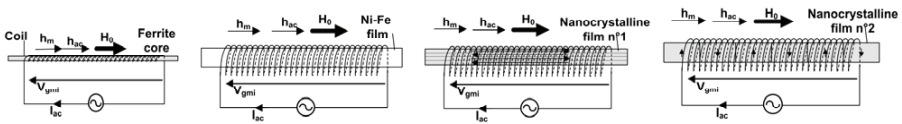


Figure 1: Coiled GMI transducers.

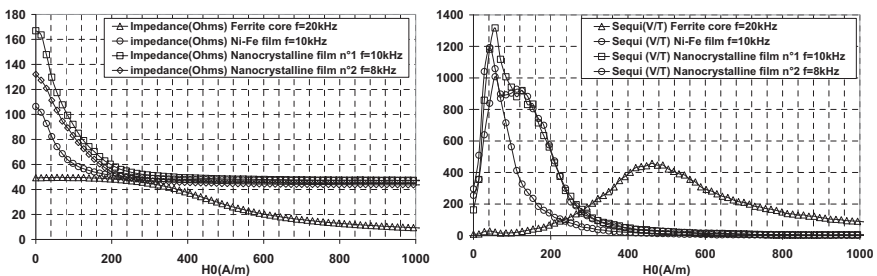


Figure 2: Impedance and equivalent sensitivity of various Coiled GMI ($L=10\text{cm}$, $I_{ac} < 10\text{mA}$).

References:

[1] J. Moutoussamy, C. Coillot, F. Alvès, G. Chanteur: Longitudinal and transverse coiled giant magneto-impedance transducers: principle, modelling and performances. Transducer'09 (Colorado-USA), (2009), 323-326.
 [2] M.Tibu, H. Chiriac: Amorphous wires-based magneto-inductive sensor for non-destructive control. Journal of Magnetism and Magnetic Materials, Vol. 320, (2008), 939-943.

AC characterization of magneto-impedance microsensors for eddy current non-destructive testing

T. Peng^{1,2}, J. Moulin¹, F. Alves², Y. Le-Bihan²

¹IEF, UMR 8622, Univ. Paris Sud/CNRS, Orsay, France

²LGEP, UMR 8507, Supelec/CNRS/ Univ. Paris Sud /UPMC, Gif-Sur-Yvette, France

Abstract: The application of magnetoimpedance (MI) sensors to eddy current non-destructive testing (NDT) involves high spatial resolution and AC field measurement capability. For this purpose multilayered MI microsensors (Finemet/Copper/Finemet) were fabricated by microfabrication process. Finemet (FeCuNbSiB) and copper thin films were deposited separately by RF and DC sputtering using bi-layers lift-off method. The SEM characterization shows that the upper magnetic layer has covered the copper track properly (Fig.1), which is a condition for high MI effect and high sensor sensitivity. A post-annealing step was achieved at 300°C for 1h under magnetic field, which led to induce a transversal anisotropy in the magnetic films. A method based on double amplitude demodulation was proposed for the AC sensitivity measurement. At a given excitation frequency, the microsensor was supplied by small magnetic field fluctuations (AC) around a DC polarization. After HF (excitation current frequency) then LF (magnetic field frequency) signal demodulations, the sensor sensitivity was obtained. According to these characterizations, the optimal excitation frequency was observed at 30 MHz, at which the sensor bandwidth reaches 6 kHz (Fig.2). The highest sensitivity arrived at 1300 V/T/A, which is in the same range comparing to DC method measurement. Due to the DC polarization larger than H_k , the sensor presents no hysteresis. Thus the sensitivity and the bandwidth are suitable for low frequency NDT applications aiming to detect flaws buried in conductive materials.

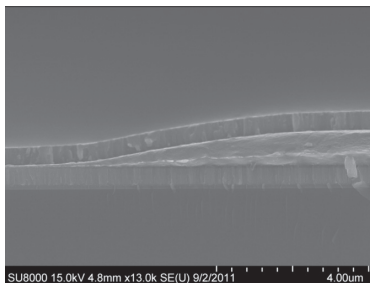


Fig1: Cross section of the micro sensor

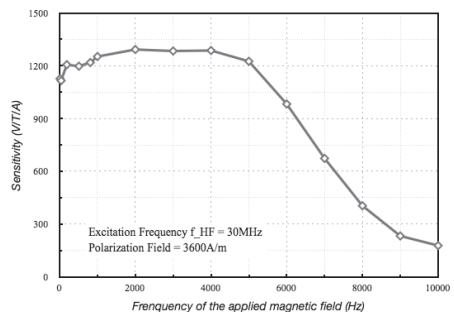


Fig.2: Sensor bandwidth characterization

FeNi-based Thin Film Meander Sensitive Elements for GMI Detectors

S.O. Volchkov¹, A.A. Yuvchenko¹, V.N. Lepalovskiy¹, V.O. Vas'kovskiy, A.P. Safronov², G.V. Kurlyandskaya^{1,3}

¹ Department of Magnetism and magnetic Nanomaterials, Ural Federal University, Ekaterinburg, Russia

² Department of Chemistry, Ural Federal University, Ekaterinburg, Russia

³ Departamento de Electricidad y Electrónica, Universidad del País Vasco, Bilbao, Spain

Giant Magnetoimpedance (GMI) is a considerable change of the complex impedance of soft ferromagnetic conductor under application of an external magnetic field [1]. Permalloy based thin film and multilayers were proposed for many technological applications as the sensitive elements of the detectors of small magnetic field for positioning, nondestructive testing, registration of magnetic labels in biosensing [1-2]. GMI sensitivity with respect to a magnetic field depends on a number of parameters like composition and effective magnetic anisotropy, resistivity and topology of the sensitive element. Sensitivity is a key parameter for the detection of the disturbances of an external magnetic field by magnetic markers in bioapplications or non-destructive testing. In the present work we have designed and studied the GMI-elements based on [FeNi(100 nm)/Cu(3 nm)]₄/FeNi(100 nm)/Cu(500 nm)/[FeNi(100 nm)/Cu(3 nm)]₄/FeNi(100 nm) multilayered structures prepared by magnetron sputtering. Meanders with different topology were fabricated by lithographic technique aiming to find better geometries for the detection of magnetic fields of a various configurations with focus on in biodetection and the ferrofluid dynamic studies. The width of the multilayer strip, number of turns of a meander and a distance between the strips were the parameters of variation. As the first step the GMI meander elements were carefully calibrated: the longitudinal GMI was measured in a microstrip line in a frequency range of 1 MHz to 500 MHz by Impedance Analyzer Agilent HP 4991A. As the second step both the frequency and the field dependences for the optimized frequency were measured in presence of the ferrofluids or iron spheres of 500 microns in diameter placed in certain configurations. For measurements with alcohol-based Fe₃O₄ ferrofluid a small bath was placed on the surface of the sensitive element. The stray field configurations were simulated by FEM-software.

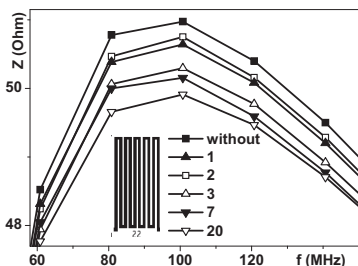


Fig. 1. The frequency dependence of GMI of meander sensitive element in presence of 1, 2, 3, 7 and 20 iron spheres and without them. Inset show the geometry of the meander.

As an example figure 1 shows selected frequency dependencies of the GMI element in presence of 1 to 20 iron spheres and without them. The impedance, Z , changes are additive at increase of the number of spheres in the range under consideration. Stray fields created by the iron spheres caused the impedance variations which also depended on the particular rearrangement of the spheres. These results can be used for fabrication of the magnetic keys or magnetic security tags.

[1] G.V. Kurlyandskaya, M.L. Sánchez, B. Hernando, V. Prida, P. Gorria, M. Tejedor, Appl.

[2] L. Chen, Ch.-Ch. Bao, H. Yang, D. Li, Ch. Lei, T. Wang, H.-Y. Hu, M. He, Y. Zhou, D.-X. Cui, Bios. Bioelectr. 26 (2011), 3246–3253.

The prospects of using film structures based on In-containing semiconductor materials in magnetic field sensors for thermonuclear reactor magnetic diagnostic systems

I.Bolshakova¹, L.Viererbl², I.Đuran³, N.Kovalyova¹, K.Kovarik³, Ya.Kost¹, O.Makido¹,
J.Sentkerestiová⁴, A.Shtabalyuk¹, F.Shurygin¹

¹Magnetic Sensor Laboratory, Lviv Polytechnic National University, Lviv, Ukraine

²Research Centre Rež, Rež near Prague, Czech Republic

³Institute of Plasma Physics, Prague, Czech Republic

⁴Faculty of Nuclear Sciences and Physical Engineering, Czech Technical University in
Prague, Prague, Czech Republic

The use of semiconductor sensors in magnetic field diagnostic systems of thermonuclear reactors is associated with a number of difficulties, among which the main is instability of sensor material parameters under irradiation with high-energy particles. However, In-containing materials can retain their parameter stability in radiation environment given a certain method of their obtaining and processing. Semiconductor sensors of magnetic field based on such materials may be promising for application under radiation conditions of thermonuclear fusion reactors, as they are characterized by a number of advantages allowing to enhance the accuracy of steady-state magnetic field measurement at long plasma burning pulses.

The work presents the results of investigation into the effect exerted by irradiation with high-energy particles (neutrons and electrons) on the parameters of semiconductor magnetic field sensors based on In-containing materials InSb and InAs. Using the on-line measurement method during sensors' irradiation, the dose dependences of their sensitivity change have been obtained. The effect of reactor neutron flux spectrum and irradiation temperature on the magnitude of sensor sensitivity change has been analyzed.

As a result of the analysis of the conducted investigation, it has been determined that semiconductor magnetic field sensors based on In-containing semiconductor materials InSb and InAs can be effectively applied in thermonuclear reactors magnetic diagnostic systems. However, in case of buffer layers presence in heterostructures based on indium arsenide, they become conducting under irradiation, and parameter stabilization becomes problematic for such sensors.

Spin accumulation from the spin Hall effect and the anisotropic effect studied using the effective mean-free-path model

Sui-Pin Chen¹, Ching-Ray Chang²

¹Department of Electrophysics, National Chiayi University, 60004, Chia Yi, Taiwan

²Department of Physics, National Taiwan University, 10617, Taipei, Taiwan

In presence of the spin Hall effect [1-4], there exists the spin-dependent scattering, and also the spin accumulation. The resulting spin accumulation can be specified by the difference between the spin-up and the spin-down chemical potentials. The difference can be easily derived by using the effective mean-free-path model [5], which is equivalent to the Boltzmann transport equation model [6]. In this paper, a nonmagnetic thin film system both with the spin Hall effect and with the anisotropic effect is investigated by use of the effective mean-free-path model. The thin film has the mean free path λ and the width w along the y -axis. The parameter P is used to specify the spin accumulation along the y axis. Our theoretical results in Fig. 1 show that the spin accumulation will be localized near both side edges, when the thin film has a large ratio of w/λ or has a large parameter a which is a measure for the anisotropy of the scattering [7].

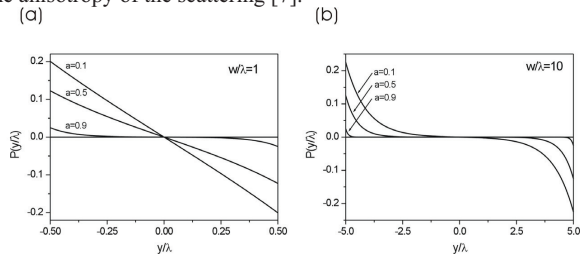


Figure 1: The relation of $P(y/\lambda)$ versus a for (a) $w/\lambda=1$ and (b) $w/\lambda=10$.

References

- [1] J. E. Hirsch: Spin Hall Effect. Phys. Rev. Lett. 83 Issue 9, (1999), 1834-1837.
- [2] S. Zhang: Spin Hall Effect in the Presence of Spin Diffusion. Phys. Rev. Lett. 85 Issue 2, (2000), 393-396.
- [3] Y. K. Kato, R. C. Myers, A. C. Gossard, and D. D. Awschalom: Observation of the Spin Hall Effect in Semiconductors. Science 306 Number 5703, (2004), 1910-13.
- [4] K. Nomura, J. Wunderlich, J. Sinova, B. Kaestner, A. H. MacDonald, and T. Jungwirth: Edge-spin accumulation in semiconductor two-dimensional hole gases. Phys. Rev. B 72 Issue 24, (2005), 245330.
- [5] S.-P. Chen, C.-R. Chang, T.-M. Hong, and C.-H. Lai: Spin accumulation from the Spin Hall effect studied using the effective mean-free-path model, IEEE Trans. Magn. 42 Number 10, (2006), 2667-2669.
- [6] S.-P. Chen and C.-R. Chang: Analytic solutions of the linear Boltzmann transport equation for multilayered systems. Phys. Rev. B 72 Issue 6, (2005), 064445.
- [7] Th. G. S. M. Rijks, R. Coehoorn, M. J. M. de Jong, and W. J. M. de Jonge: Semiclassical calculations of the anisotropic magnetoresistance of NiFe-based thin films, wires, and multilayers. Phys. Rev. B 51 Issue 1, (1995), 283-291.

Improved Quantum Well Hall Sensors for Micromagnetometry

V. Mosser¹, D. Seron¹, M. Konczykowski², S. Bansropun³
vincent.mosser@itron.com

¹ITRON France, Issy Technology Center,

52 rue Camille Desmoulins 92448 Issy-les-Moulineaux, France

²Laboratoire des Solides Irradiés, Ecole Polytechnique, 91128 Palaiseau, France

³Thales Research & Technology, 1 av. Augustin Fresnel, 91767 Palaiseau, France

For spatially resolved magnetometry applications, Hall sensors show the best resolution among all sensor types when the size decreases below a few μm [1]. We have implemented various improvements in the fabrication process of GaAs based Quantum Well Hall Sensors (QWHS): an amorphization implant instead of a mesa etching for delineating the shape of the Hall cross as well as improvement of the ohmic contacts.

Using an improved spinning current technique implementation [2], we achieve e.g. a resolution of $100\text{nT}/\sqrt{\text{Hz}}$ at 1Hz for devices with a $1.4\mu\text{m}$ active area, equivalent to a few 10^{-5} flux quantum.

These sensors, as well as integrated sensor arrays, are presently actively used in several research areas, including thermodynamics of magnetic noise in frozen ferrofluides [3], investigation of new pnictide materials [4], magnetization in molecular magnets [5], non-linear electrodynamics of vortex matter in High Temperature Superconductors [6], etc... which will exemplify the gains in performance for various operating conditions.

References

- [1] C. Dolabdjian, A. Qasimi, D. Bloyet and V. Mosser, "Spatial resolution of SQUID magnetometers and comparison with low noise room temperature magnetic sensors", *Physica C, Superconductivity and Applications*, **368**, 80-84 (2002)
- [2] V. Mosser et al, this conference
- [3] K. Komatsu, D. L'Hôte, S. Nakamae, V. Mosser, M. Konczykowski, E. Dubois, V. Dupuis, and R. Perzynski, "Experimental Evidence for Violation of the Fluctuation-Dissipation Theorem in a Superspin Glass" *Phys. Rev. Lett.* **106**, 150603 (2011)
- [4] M. Kończykowski, C. J. van der Beek, M. A. Tanatar, V. Mosser, Yoo Jang Song, Yong Seung Kwon, R. Prozorov, "Anisotropy of the coherence length from critical currents in the stoichiometric superconductor LiFeAs ", *Phys. Rev.* **B 84**, 180514(R) (2011)
- [5] S. Bahr, C.J. Milios, L.F. Jones, E.K. Brechin, V. Mosser and W. Wernsdorfer, "Influence of antisymmetric exchange interaction on quantum tunneling of magnetization in a dimeric molecular magnet Mn_6 ", *Phys. Rev.* **B 78**, 132401 (2008)
- [6] C. J. van der Beek, G. Rizza, M. Konczykowski, P. Fertey, I. Monnet, Thierry Klein, R. Okazaki, M. Ishikado, H. Kito., A. Iyo., H. Eisaki, S. Shamoto, M. E. Tillman, S. L. Bud'ko, P. C. Canfield, T. Shibauchi, and Y. Matsuda, "Flux pinning in $\text{PrFeAsO}_{0.9}$ and $\text{NdFeAsO}_{0.9}\text{F}_{0.1}$ superconducting crystals", *Phys. Rev.* **B 81**, 174517 (2010)

Shiftable Attenuation of Low Magnetic Fields Using a Magnetically Soft Layer on an Integrated Hall Sensor

Volker Peters, Philip Beran, Hans-Peter Hohe

Fraunhofer Institute for Integrated Circuits IIS, Erlangen, Germany

Integrated 3D-Hall-sensors can directly measure all three components of a magnetic field vector. They comprise a lateral Hall sensor for the field perpendicular to the chip surface and two vertical sensors for the horizontal field components.

A shortcoming especially of the vertical sensors is that residual offsets and noise prevent precise and temperature independent measurements in the range below $50 \mu\text{T}$. Yet this range is of special interest for applications relying on the earth field like electronic compasses.

We examined the possibility of attenuating external fields by using a coating of magnetically soft material for the purpose of calibrating offset and low frequency noise (Fig. 1). If this layer is driven into saturation by an integrated coil the external field becomes 'visible' for the sensor and can be measured offset-free (Fig. 2).

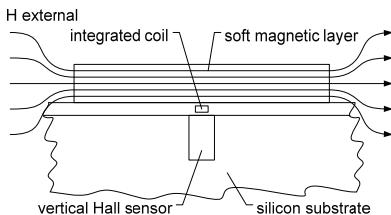


Fig. 1 – Basic sensor configuration

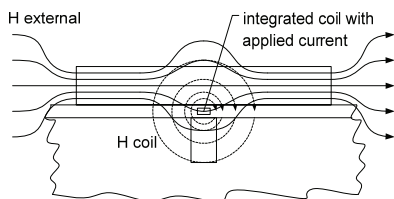


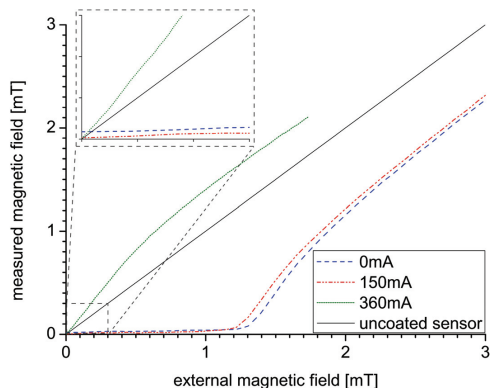
Fig. 2 – Layer in local saturation

As the integrated coil is able to saturate the coating very locally the unsaturated regions of it may act as concentrator of the external field and hence increase the sensitivity.

Different materials and geometries were modelled and simulated by an FEM tool and the approach was tested for feasibility. The results of the simulations were used to design an experimental IC and to choose a suitable material for the soft magnetic layer.

The measurement results prove our concept: In normal state the coating can attenuate external fields almost completely. During saturation phase the field concentration enhances the sensitivity for low fields. At higher fields the complete coating is saturated and the sensitivity decreases to its natural value.

Fig. 3 – Sensor signal versus external field at different saturation currents (normalised). The sensitivity of an uncoated sensor is shown as comparison.



Original induction sensors: orthogonal and cubic configurations.

Christophe Coillot¹, Mathieu Boda¹ and Joel Moutoussamy¹

¹Laboratoire de Physique des Plasmas, CNRS - Ecole Polytechnique, France.

Induction magnetometers remain unavoidable in many applications [1] because of their performances in terms of noise equivalent magnetic induction (NEMI) since few Hz, their simplicity and their strength. Nevertheless, their improvement remains marginal because of the limitation coming from their basic principle (induction law implies surface for flux measurement). In this paper we will present two original induction sensor configuration using ferromagnetic core which could permit significant improvements. On one side, we will present orthogonal search coil, how it works and some mathematical equations to describe it more deeply. In this sensor, the flux is canalized inside a “helical” ferromagnetic core (cf. Figure 1), then magnetic flux will induced a voltage through a winding orthogonal to the original magnetic field direction. On the other hand we will look at the “cubic induction sensor” (also called array of induction sensor, cf. Figure 2) which has been proposed in [2]. This induction sensor takes advantage of a large area to catch the flux of the magnetic field. The flux is then distributed inside 4 windings connected in series which permits to have lower inductance than a single induction sensor with same turn number.

We will compare expected performances to the one measured on prototypes. Thus, we will discuss the limitations of these designs for magnetic sensing applications.



Figure 1 : « helicore » of the orthogonal induction sensor.

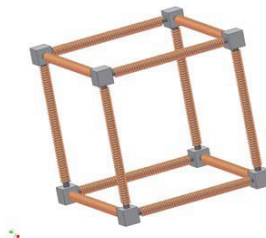


Figure 2 : Cubic induction magnetometer.

References

- [1] Christophe Coillot and Paul Leroy (2012). “Induction Magnetometers: Principle, Modeling and Ways of Improvement”, Magnetic Sensors - Principles and Applications, Dr Kevin Kuang (Ed.), ISBN: 978-953-51-0232-8, InTech, Available from: <http://www.intechopen.com/books/magnetic-sensors-principles-and-applications/induction-magnetometers-principle-modeling-and-ways-of-improvement>
- [2] J. Christian Dupuis, "Optimization of a 3-axis induction magnetometer for airborne geophysical exploration", Master's thesis, Dept. of Electrical and Computer Engineering, University of New Brunswick, (Fredericton, NB, Canada), 2003.

Metal detector signal imprints of detected objects

NOVÁČEK Petr¹, Ripka Pavel¹, Roháč Jan¹

¹Department of Measurement, Faculty of electrical engineering, Czech Technical University in Prague, Prague, Czech Republic

Increasing of a discrimination ability of metal detectors is one of the key activities in recent development of modern de-mining methods [1]. This ability improves a progress of humanitarian de-mining missions as well as it decreases injury risks of detector operators when this modern equipment is used. This paper presents an improved method which enables a usage of image processing during localization of metal objects and further extends the capability of modern metal detectors. Our approach deals with the detector signal dependency on a height above the ground (distance from detected object) [2]. In this paper we present creating detector signal intensity map around detected objects.

The metal detector signal amplitude and phase change with a height and also with lateral distance from the detected object. The signal depends also on the object characteristics such as its size, shape, conductivity, and permeability. Especially, the conductivity and permeability are crucial factors, because they cause signal phase shift. Furthermore, when a signal height profile is known, it is also possible to estimate the type of a detected object material. Moreover, signal intensity maps database can be made by detector movement in constant height above different objects of interest, which represents signal imprints of the objects [3]. These imprints can be then compared with a measured one and thus additional improvement of precision of the object observation and identification can be obtained. To provide a sufficient precision in object identification is our main aim, because it is a key factor particularly when unexploded ordnance is observed and a human operator is in a risk.

The experimental results were obtained using ATMID [4] metal detector using also position information which was measured by a distance sensor mounted on the detector search head and by an external optical position system. The position system was able to measure with a sub-pixel resolution and approx. 1mm standard deviation. The ATMID detector was further equipped with a signal acquisition electronics and PC communication interface. The position system was synchronized by the acquisition unit. Based on reached results, when proposed method was applied with signal height profile known, we proved the method capability to estimate the detected object material, size, and distance, as well as its shape. According to reached results we can say that the proposed method leads to a better ability of differentiation between metal scraps and dangerous objects such as explosive remnants of wars.

References

- [1] L. S. Riggs. Discrimination experiments with the U.S. army's standard metal detector. *Radio Sci.* 39(4), 2004.
- [2] P. Novacek, P. Ripka, O. Pribula and J. Fischer. Mine detector with discrimination ability. *JEE* 61(7), pp. 141-143. 2010.
- [3] P. Verlinde, M. Acheroy, G. Nesti and A. Sieber. Preparing the joint multi-sensor mine-signatures project database for data fusion. 2001, .
- [4] Schiebel. *ATMID all Terrain Mine Detector Maintenance Manual MT5001/16/010E* 2003.

Step Response Identification of Metallic Targets by Numerical Simulation

ZOLTAN Polik¹

¹Department of Telecommunication, Szechenyi Istvan University, Gyor, Hungary

The classical approach of proximity sensing [1] is an essentially harmonic excitation of a sensing head and the detection of the energy loss, frequency change or a phase shift resulted by the perturbing effect of an approaching metallic target. However, numerous methods are emerging to exploit the time domain response of objects to be detected by means of single-pulse or repetitive excitation and time independent analysis of an induction signal captured by a coil or differential coil systems [2]. Transient analysis provides more independent information as compared to the harmonic analysis and may lead to the design of smart sensors with particular properties of material independent or material selective proximity sensing.

The paper deals with the identification of different materials (e.g. aluminum, steel and fictive materials) on the base of their step response measured by a gradiometric coil arrangement from the aspect of numerical simulations [3]. The electrical conductivity and the magnetic permeability were varied independently to unveil the specific contributions of these two material parameters. It was found that the amplitude, the zero crossing points and the overshoot of the gradiometric voltage signal are characteristic to the respective target material. Fig. 1 shows the simulated responses of the aluminum and steel targets for different sensor-to-target distances.

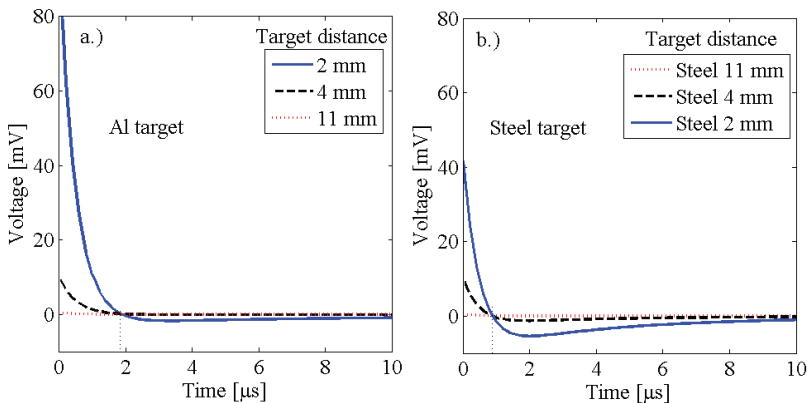


Fig. 1. Responses of the aluminum and steel targets for different sensor-to-target distances

References

- [1] S. Fericean, R. Droxler: New Noncontacting Inductive Analog Proximity and Inductive Linear Displacement Sensors for Industrial Automation. *IEEE Sensors Journal*, Vol. 7. No. 11. (2007), 1538 - 1545.
- [2] M. J. Gill: Measuring proximity of a metal object. UK Patent Application, GB 2 200216 A (1988).
- [3] J. M. Jin: *The Finite Element Method in Electromagnetics*. Wiley, New York, (2002), 780p.

Improving the Magnetolectric Response of Laminates Containing High Temperature Piezopolymers.

GUTIÉRREZ Jon¹, Lasheras Andoni¹, Barandiarán Jose Manuel¹, Vilas Jose Luis², San Sebastián María² and León Luis Manuel²

¹Departamento Electricidad y Electrónica and ²Departamento Química Física, Facultad de Ciencia y Tecnología, Universidad del País Vasco UPV/EHU, P. Box 644, E-48080-Bilbao, Spain

Artificial magnetolectric (ME) structures as 2-2 type laminates (one magnetostrictive, the other piezoelectric) show a strong ME coupling arising via the interaction between magnetic and piezoelectric constituents through the elastic deformation. Extremely high ME coefficients have been found when such heterostructures were made of iron-based Metglas alloys and PVDF piezoelectric polymer [1]. In a recent work [2] we reported the good magnetolectric performance of such type of laminate composite device when using Vitrovac 4040[®] ($\lambda_s \approx 8$ ppm) as the magnetostrictive component and the 2,6(β -CN)APB/ODPA (poli 2,6) polyimide as the piezoelectric one. This is a new class of high temperature piezopolymer. We measured at the magnetoelastic resonance of the laminate and at room temperature 0.35 V/cm.Oe and a sensitivity to applied magnetic field of 45.4 mV/Oe; those values kept practically constant up to 85 °C.

Searching for an improvement on the ME response of such laminate composites, we have modified both constituents: first, the magnetostrictive one by using Metglas 2826, an alloy that has higher magnetostriction value ($\lambda_s \approx 12$ ppm) than Vitrovac 4040[®]. Pieces of this alloy in the ribbon form have been thermally treated at high temperature to get stresses-relief conditions and also to get a perpendicular domain structure in the ribbons when they are heated under applied magnetic field. The main consequence of such thermal treatments has been to achieve a piezomagnetic coefficient of $d_{33} = 1.5 \times 10^{-6}$ /Oe for the stress-relief sample, higher than the measured one in the as-cast state for this alloy.

Concerning the performance of the piezoelectric constituent, a series of nitrile containing polyimide copolymers were obtained by reaction of the 4,4'-oxydiphtalic anhydride (ODPA) with a mixture of two aromatic diamines, namely 1,3-Bis-2-cyano-3-(3-aminophenoxy)phenoxybenzene (diamine 2CN) and 1,3-Bis(3-aminophenoxy)benzene (diamine 0CN). Such copolyimide has better mechanical and piezoelectric response than the poli 2,6 polymer; as an example, a 50/50 ratio mixture shows twice the remnant polarization than the poli 2,6 polymer alone for the same polarizing high voltage.

We present and discuss here results showing the ME performance of these laminate composites at room and also high temperature, showing that an appropriate election of the characteristics of both magnetic and piezoelectric constituents makes these magnetolectric devices suitable for high temperature applications.

References

- [1] J. Zhai, S.X. Dong, Z. Xing, J. Li and D. Viehland, Appl. Phys. Lett. 89 (2006), 083507.
- [2] J. Gutiérrez, J.M. Barandiarán, A. Lasheras, J.L. Vilas, M. San Sebastián and L.M. León, Key Engineering Materials 495 (2012), 351-354.

Investigation of the near-carrier noise for a strain-driven ME laminates by using cross-correlation techniques

X. Zhuang¹, M. Lam Chok Sing¹ and C. Dolabdjian¹

¹Groupe de Recherche en Informatique, Image, Automatique et Instrumentation de Caen (GREYC), CNRS UMR 6072-ENSICAEN, Université de Caen Basse Normandie, 14050 Caen Cedex, France

The near-carrier noise around the longitudinal mechanical resonance of magneto-electric (ME) laminates has been investigated. A composite ME sample [1] is driven by an AC electric field applied on the piezoelectric material along its longitudinal direction at a frequency close to its resonance. The ME thin film response to these excitations can be sensed by either a charge detection using a classical charge amplifier or an electromotive force detection using a coil surrounding the sample. Each amplified output is followed by a synchronous detector. We named this two demodulation techniques as piezo-electric (PP) and piezo-magnetic (PM), respectively. The resulting output low frequency noise levels correspond to the noise appearing around the carrier frequency. These noise levels determine the ME sensor performance by using such modulations. In order to understand the origin of the near-carrier noise, we have designed an experimental setup and observed, simultaneously, the direct low frequency noise and the noise after the PP and PM demodulations. The corresponding equivalent magnetic noise spectral density curves are shown in Figure 1. Cross-correlating noise measurements have also been done. The first result analysis shows that the sensed noises around the carrier are independent of the direct measured low frequency noise of the ME sample. Furthermore, the noise levels near the carrier and obtain by the two modulation techniques have a correlation higher than 50 %. This make us think that the mechanical strain induced by the carrier can be the main cause of the equivalent magnetic sensed noise levels by using PP or PM technics.

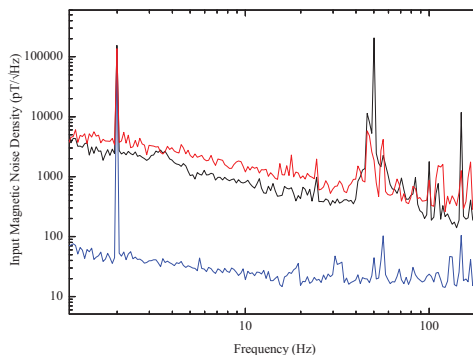


Figure 1: Comparison of the direct equivalent magnetic noise floor (black curve) and the equivalent magnetic noise given by the PP technic (red curve) and PM technic (blue curve) after demodulation.

Reference

[1] J. Das, J. Gao, Z. Xing, J. F. Li, and D. Viehland: Enhancement in the field sensitivity of magnetoelectric laminate heterostructures. *Appl. Phys. Lett.*, Vol. 95, (2009), 092501.

Magneto-Elastic Sensors for the Detection of Pulse Waves

C. Hlenschi, S. Corodeanu, H. Chiriac

¹National Institute of Research and Development for Technical Physics, Iasi, Romania

The pulse wave magnetoelastic sensor for cardiovascular applications is based on the magnetoelastic response of the amorphous magnetic microwire (100 μm in diameter) whose permeability changes, as a result of the strain produced by the pulsating blood vessels. The electrical output is amplified and filtered by an electronic system. The signal is displayed on a computer using an acquisition board.

The system allows the detection of the arterial stiffness, of the vascular tone and, in case of using two sensitive elements, the detection of the pulse wave velocity for a more precise evaluation of the arterial stiffness. The sensor has 0.5 mm in diameter and 5-10 mm in length (Fig. 1), and is fixed in a special bracelet that assures a good contact with the skin and the blood vessels.

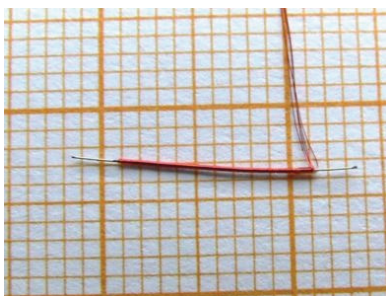


Fig. 1. The active element of the magneto-elastic sensor for the detection of the pulse waves.

Inductive Stress Sensor based on Magnetic Bistability of FeSiBP amorphous microwires

J. Olivera^{1,2}, R. Varga², M. Hernández¹, G.A. Badini-Confaloni³, M. Vázquez³

¹Acoustic Applied Center and Non-destructive Testing, CSIC-UPM, Madrid, Spain.

²Institute of Physics, Faculty of Science, U.P.J.S, Kosice, Slovakia

³Materials Science Institute of Madrid, CSIC, 28049 Madrid, Spain

The magnetic bistability effect exhibited particularly by magnetic amorphous microwires has been a topic of growing interest during the last few years [1]. One of its main technological interests is related with the Large and single Barkhausen Jump (LBJ) that takes place under magnetic field above some critical value (called the switching field). Drastic change of the magnetization at applied magnetic fields just above the switching field can be measured by simple induction method during LBJ [2]. Due to the strong magnetoelastic anisotropy, the switching field depends on magnetoelastic energy determined by the strength of the internal stresses, applied stresses and magnetostriction constant [3]. This gives us a possibility of employ positive magnetostriction microwires as a stress sensor.

In the given manuscript the role of different dimensions, composition and measuring frequency in controlling the magnitude of Stress dependence of Switching field have been investigated. Positive magnetostriction glass-coated amorphous microwires with nominal composition $\text{Fe}_{78}\text{Si}_9\text{B}_{11}\text{P}_2$ with a total diameter equal to $50\mu\text{m}$ and two metallic core diameter ($8\mu\text{m}$ and $20\mu\text{m}$), and $\text{Fe}_{76}\text{Si}_9\text{B}_{10}\text{P}_5$, for ratios of the metallic nucleus diameter to the total microwire diameter (0.82, 0.66). We show that it's possible to modify the magnetoelastic behavior of the sensor with different magnetostriction constant and variation of internal stresses through changing the microwires geometry.

References

- [1] M. Vázquez, H. Chiriac, A. Zhukov, L. Panina, and T. Uchiyama, *Phys. Status Solidi A* 208, No. 3, (2011), 493–501
- [2] H. Chiriac, T. A. Óvári, *J. of Optoelectronics and Advanced Materials* Vol.4, No.2, June 2002, 367-371.
- [3] V. Zhukova, M. Ipatov, and A. Zhukov, *Sensors*, No. 9, (2009), 9216-9240.

Magnetoelastic Characteristics of FeNi-based Amorphous Ring-shaped Cores under Uniform Compressive and Tensile Stresses

SALACH Jacek¹, SZEWCZYK Roman², BIENKOWSKI Adam¹, JACKIEWICZ Dorota¹

¹Institute of Metrology and Biomedical Engineering, Warsaw University of Technology,
Warsaw, Poland

²Industrial Research Institute for Automation and Measurements, Warsaw, Poland

Magnetoelastic Villari effect is connected with the changes of flux density B achieved in the magnetic core, for given magnetizing field H_m , when it is subjected to mechanical stresses σ generated by external forces [1]. Magnetoelastic properties of the magnetic materials may be described either by $B(H)_\sigma$ characteristics, which represent the influence of both tensile and compressive stresses on magnetic hysteresis loops of the material.

Way in which material reacts on the stresses σ should be connected with Le Chatelier's principle [2] and determined by value of magnetostriction λ of material. It should be indicated, that for iron and iron-nickel based amorphous alloys, positive value of magnetostriction up to 35 $\mu\text{m}/\text{m}$ can be observed. In such a case, for stresses σ parallel to the magnetizing field H direction, increase of flux density B under tensile stresses should be observed. However, under compressive stresses σ , value of flux density B should decrease for given value of magnetizing field H . This effect is described theoretically, however its seems not to be verified experimentally for compressive and tensile stresses in soft amorphous alloys.

Paper presents methodology of generation of uniform, compressive or tensile stresses in ring-shaped amorphous alloys core [3, 4]. In this methodology the set of special nonmagnetic, cylindrical backings was used. These backings enabled the core to be wound as well as creates the possibility of generation of uniform compressive and tensile stresses σ .

Using this methodology $B(H)_\sigma$ characteristics were experimentally determined for iron-nickel Metglas 2826 MB3 amorphous alloy. On the base of these results, the Le Chatelier's principle was experimentally confirmed in the case of magnetoelastic $B(H)_\sigma$ characteristics for both compressive and tensile stresses.

References

- [1] B. D. Culity „Introduction to magnetic materials“ Addison Wesley, 1972.
- [2] V. E. Iordache, E. Hug „Effect of mechanical strains on the magnetic properties of electrical steels“ Journal of Optoelectronics and Advanced Materials 6 (2004) 1297.
- [3] A. Bieńkowski, R. Szewczyk, Patent (Poland) P-345758, 2001.
- [4] J. Salach, A. Bieńkowski, R. Szewczyk, Patent (Poland), P-370124, 2004.

Calibration of the 3D coil system's orthogonalities

Zikmund A.¹, Ripka P.¹

¹Faculty of Electrical Engineering, Czech Technical University, Prague, Czech Republic

A magnetic tracker requires a 3-axial orthogonal coil system as a source of the magnetic field which is sensed by a magnetic sensors. Ideally, the three source coils should be perfectly orthogonally aligned, which is difficult to achieve. The coil bobbins and the support system can be machined very precisely, however the position of individual turns in multi-turn coils is not precisely known. In [1], the magnetic tracker was presented and it was discovered (Fig. 2) that the non-concentricity and angular non-alignment of the coil system affects the result precision. The non-concentricity error (Fig. 1.) can be easily suppressed by corrections.

To measure the non-orthogonalities between the source coils and apply correction for these is the next step. We describe two different methods of the measurement of angles between the coils.

The first method uses the precisely defined rotations of the coil system. Each coil of the system is excited at a specific directional position. During these excitations the magnetic field is measured with the 3-axial magnetometer in the constant distance. In this way we get as many measured values as needed for the calculation of the non-orthogonal angles.

The second method is also based on the rotation of the coil system but the coils are positioned in the homogeneous field of the Helmholtz coil which is excited by AC current. The induced voltage in the individual coils is measured. The measured voltages are used for calculation of the angles.

Both methods discovered the angular misalignment of the current 3D excitation coil system. Based on calibration angles between the coils we are able to apply the correction in the magnetic tracker.

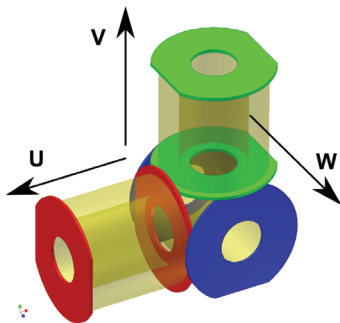


Fig. 1. The Coil system arrangement.

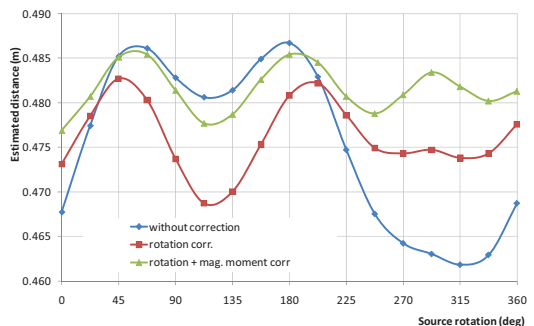


Fig. 2. Error of magnetic tracker after correction of magnetic moment and non-identical centers of the coils.

References

- [1] A. Zikmund, P. Ripka: Magnetic Tracker with High Precision. *Procedia Engineering* [online]. 2011, vol. 25, no. 25, p. 1617-1620.

Investigation of Magnetic Nanoparticles for Biomedical Applications

I.L. Nikitina¹, M.V. Yuriev², P.M. Vetoshko³, P.I. Nikitin¹

¹General Physics Institute, Russian Academy of Sciences, Moscow, Russia

²Moscow Institute of Physics & Technology, Moscow, Russia

³Institute of Radioengineering and Electronics, RAS, Moscow, Russia

Biomedical applications of magnetic nanoparticles (MP) continue to expand due to unique properties of these nanoagents: possibility to be guided and heated by external magnetic field. Besides, MP can be quantified with high sensitivity by external magnetic field even in opaque medium or living body [1-4]. MP are considered to be potentially successful agents for diagnosis of different disorders such as atherosclerosis and cancer, and therapy of cancer (via hyperthermia), anemia, etc. However, their biocompatibility and non-toxicity suggest their suitability for *in vivo* thernagnostic purposes. The choice of the proper MP for each particular application significantly depends on their pharmacokinetic behavior in living body. In terms of pharmacokinetics the most crucial characteristics for nanoagents are their blood clearance and their biodegradation and/or clearance from the organism. To study such parameters of different MP, we have improved our method of non-invasive MP detection in blood and organs of small animals by non-linear magnetization [1-4]. For the study, several promising MP with different biochemical properties were selected with Picoscope® [5], which was used for real time detection of consequent binding of MP with known receptors on the microscopic glass slip surface by measuring the layer thickness change (averaged over the sensor's surface) at a picometer scale. We investigated influence of the following MP parameters on the dynamics *in vivo*: nanoparticle size, coating, concentration and injected amount, anesthesia, number of injections, etc. For the study of MP dynamics in blood flow of mice the tail of a mouse was placed in the induction coil of the device. After retroorbital MP injection (near the eye of the mouse), the MP blood concentration dynamics in tail arteries and veins were recorded in real-time with 3 sec resolution. In some variations of the experiment (large MP doses, certain MP coatings, etc.) the concentration curves were complex and could not be fitted with a single exponential curve. The developed method allows non-invasive recording of the MP dynamics in the blood with high time resolution and sensitivity. For non-invasive study of MP degradation in organs of mice after intravenous injection of MP the mouse was scanned by external coils which detected MP on combinatorial frequencies [4]. During two months the signal in the liver region was recorded for every mouse and MP degradation curve was plotted for every mouse. Non-invasiveness of the measurement procedure allowed carrying out more humane experiments using and sacrificing much less mice than it would be necessary for invasive studies. Influence of coating, size and dosage of MP on the degradation dynamics was investigated. The developed methods and acquired data can be used for understanding kinetics of MP clearance and degradation by organs of reticulo-endothelial systems and for the development of biomedical agents based on MP and other nanoparticles.

References

- [1] P.I. Nikitin, P.M. Vetoshko, Patent RU 2166751 (2000), EP 1262766 publication (2001).
- [2] P.I. Nikitin, P.M. Vetoshko, T. I. Ksenevich, J. Magn. Magn. Mater., 311 (2007) 445-449.
- [3] M.P. Nikitin, M. Torno, H. Chen et al. J. Appl. Phys, 103 (2008) 07A304.
- [4] M.P. Nikitin, P.M. Vetoshko et al. J. Magn. Magn. Mater., 321 (2009) 1658-1661.
- [5] P.I. Nikitin, B.G. Gorshkov et al. Sensors and Actuators B 111-112 (2005) 500-504.

Magneto-optical Sensitive Elements for Single Magnetic Nanoparticle Detection

Vladimir Skidanov, Petr Vetoshko and Alexandr Stempkovskiy

Institute for Design Problems in Microelectronics RAS, Moscow, Russia

Biological and medical applications require high space resolution of high sensitive magnetometers. Enhancement of space resolution is necessary to reveal freely flowing magnetic nanoparticle. Space resolution of modern types of sensitive magnetometers (SQUID, alkali vapor) is no better than few millimeters due to temperature adjustment facilities while GMR-sensors with micrometer scale dimensions aren't sensitive enough to feel remote magnetic nanoparticle and can detect only captured magnetic label [1]. Traditional types of fluxgate magnetometer need coils and magnetically soft core those are principal obstacles for sensitive elements miniaturization [2]. Experimental methods used to reveal nanoparticles by their various magnetization reversal characteristics [3] need no less than few nanograms ($10^4 - 10^5$ nanoparticles). The only way to resolve the space resolution problem is to remove temperature facilities or coils and to use optical signal from sensitive element with micrometer scale dimensions. In addition magnetometer construction should possess micrometer scale distance between sensitive element and freely flowing nanoparticle under investigation. Bi-substituted epitaxial garnet films $(\text{BiLu})_3(\text{FeGa})_5\text{O}_{12}$ with uniaxial anisotropy and high faraday rotation are used for production of sensitive elements with one or two straight domain walls inside. Magnetization reversal parameters and sensitivity to external magnetic field of elements with various shapes (Fig. 1) were investigated experimentally.



Fig. 1. Microphotographs of sensitive elements saturated in opposite directions:
a – bridges $30 \times 60 \mu\text{m}$, b – squares $60 \times 60 \mu\text{m}$, c – rings $90/30 \mu\text{m}$.

Elements exhibit almost step-like switching characteristic with saturation field ~ 200 A/m. Sensitivity ~ 1 nT / $\text{Hz}^{0.5}$ of magneto-optical fluxgate sensor is achieved which is restricted by photodiode noise yet. Absence of coil possesses to reveal alone magnetic nanoparticle $10^{-15} - 10^{-17}$ g ($10^3 - 10^5$ nm^3) if it can be arbitrary located within $10 \mu\text{m}$ vicinity of garnet surface. Localized random electric current pulses at level 1-0.1 nA in micrometer size muscles and nerves can be investigated *in vivo*.

References

- [1] V.C. Martins, F.A. Cardoso, J. Germano, S. Cardoso, L. Sousa, M. Piedade, P.P. Freitas and L.P. Fonseca: Femtomolar limit of detection with a magnetoresistive biochip. *Biosensors and Bioelectronics* 3, issue 8, (2009), 2690-2695.
- [2] M. Janosek and P. Ripka: PCB sensors in fluxgate magnetometer with controlled excitation. *Sensors and Actuators A: Physical* 151, (2009), 141-145.
- [3] M. Nikitin, M. Torno, H. Chen, A. Rosengart, P. Nikitin: Quantitative real-time *in vivo* detection of magnetic nanoparticles by their nonlinear magnetization. *Journal of Applied Physics* 103, (2008), 07A304.

A Magnetic Based Displacement-to-Frequency Transducer

A. Garcia¹, C. Morón¹, E. Tremps¹, M.J. López¹ and P. Ramirez²

¹Sensors and Actuators Group, E.U. Arquitectura Técnica (U.P.M.), Madrid, Spain

²Sensors and Actuators Group, E.U. Informática (U.P.M.), Madrid, Spain

Inductive Sensors LVDT (Linear Variable Differential Transformer) is one of the most used sensor in displacement measurements due to the advantages offered by it: electrical insulation between the sensor and measurement electronics; its hardness that allows to use in unclean or unfavorable environments and its reliability that allow it to make measurements with an accuracy greater than 1/10.000.

But, it have some disadvantage as their dimensions (the range of the LVDT' s measure is always less than ½ of the total length of the windings) or the associated measurement electronics complexity (it is needed to detect voltage and phase to discriminate the direction and magnitude of displacement and the requirement of a good stabilization of the working frequency, as being a system of mutual induction amplitude depends on the frequency of the driving signal) [1-5].

In this work it is shown a new displacement-to-frequency transducer based on the variation of the inductance of a coil, when the magnetic core (sensor nucleus) is partially or completely inserted in a single coil. This transducer is based in a Colpitts' oscillator circuit that shows low manufacturing price, and a great immunity to noise. We used a tank circuit with a parallel configuration because it can be used at lower frequencies and enables to make a direct analysis.

The sensor was designed using four coils of different sizes and also with different number of turns but with the same self-inductance ($L = 39.5 \mu\text{H}$). In this way, the electronic circuit can be the same for diferent sensor cores. So, as the sensor has a dynamic range equal to the length of the inductance, the core sensor (coil with his ferromagnetic core) can be exchanged with the same measurement electronic system. In this way, the range of measurement is only determined by the core sensor selected, using the same electronics for all sensor cores. The obtained sensibility is superior to 1/100.000.

References

- [1] P. Ripka. Magnetic Sensors. Artech, 2001.
- [2] A. Hernando, M. Vázquez and J.M. Barandiarán. J. Phys. E: Sci. Instrumen, p. 1129, 1988.
- [3] J. Salonen, M. Björkqvist, J. Paski. Sensors and Actuators A, p. 438, 2004.
- [4] R. Ali, D.R. Mahapatra, S. Gopalakrishnan. Sensors and Actuators A, p. 424, 2004.
- [5] P. Zivojinovic, M. Lescure, H. Tap-Béteille. Sensors and Actuators A, p. 273, 2004.

Wireless magnetic position sensing system composed of multi channels digitizer for realtime monitoring

S. Hashi¹, T. Kuboki¹, K. Ishiyama¹, S. Yabukami², T. Ozawa², K. Takashima¹, Y. Kitamura¹, Y. Itoh³, H. Kanetaka⁴

¹Research Institute of Electrical Communication, Tohoku University, Sendai, Japan

²Faculty of Engineering, Tohoku Gakuin University, Tagajo, Japan

³Web Design Unit, Osaka University, Suita, Japan

⁴Department of Biomedical Engineering, Tohoku University, Sendai, Japan

We previously proposed and developed a wireless magnetic position sensing system that uses LC resonant magnetic markers (LC markers), which was considered as a useful candidate for detecting invisible objects [1]. It can not only detect the position of the LC marker as a magnetic dipole, but also the orientation of the LC marker. However, because of the requirement of multi channels equipment for the system, a discussion about detection speed has not been done in detail. In the present paper, we evaluated the detection speed of the proposed system composed of multi channels digitizer.

The system is composed of measurement apparatus and a coil assembly that consists of an exciting coil and a pick-up coil array. The exciting coil and the pick-up coil array were integrated into one board. The pick-up coil array consists of 25 pick-up coils placed at intervals of 45 mm on an acryl board. Each coil consists of 100 turns of polyester enameled copper wire (PEW) wound around an acryl bobbin of 25 mm in diameter. The exciting coil consists of 13 turns of PEW around a 390 × 390-mm square acryl frame. The marker consists of a Ni-Zn ferrite core 3 mm in diameter and 15 mm long with 300 turns of wound coil, and a chip capacitor 560 pF, representing a LC series circuit designed for a resonant frequency of 191 kHz. The final size of the marker is 4 mm in diameter and 15 mm long.

The measurement apparatus composed of multi channels digitizer, which has 25 simultaneous analog inputs at 2 MS/s per channel with 16-bit resolution, was constructed. When the number of data sample is set to 2,000 points, the data acquisition time is theoretically 1 ms. Evaluation result is as follows. The total capturing speed of the system was around 22 Hz (one capturing per second) under synchronized operation of 25 digitizers. A classification of total time is as follows: the time for voltage acquisition was about 1 ms, the time for FFT analysis to obtain the amplitude of induced voltage was 25 ms, and the time of about 15 ms was needed for convergence calculation of inverse problem (one marker). As a result, in order to gain the measurement speed of the system, it was clearly found that the further optimization for FFT analysis and convergence calculation was required.

Acknowledgements

This study were supported in part by Strategic Information and Communication R&D Promotion Programme (SCOPE) in the Ministry of Public Mngement, Home Affairs, Posts and Telecommunications (MPHPT) and the Japan Society for the Promotion of Science (JSPS) through Grants-in-Aid for Scientific Research (B) No. 23300044.

References

[1] S. Hashi, M. Toyoda, S. Yabukami, K. Ishiyama, Y. Okazaki, K. I. Arai, H. Kanetaka: Wireless magnetic motion capture system using multiple LC resonant magnetic markers with high accuracy. *Sens. Act. A: Phys.*, 142, No. 2, (2008), 520-527.

Position detection using magnetoimpedance sensor array for designing *in situ* reconfigurable sensor networks

M. Ipatov¹, V. Zhukova¹, J. Gonzalez¹, A. Zhukov^{1,2}

¹Dpto. de Física de Materiales, Universidad del País Vasco (UPV/EHU), San Sebastián, Spain
²IKERBASQUE, Basque Foundation for Science, 48011 Bilbao, Spain

We have investigated the application of magnetoimpedance (MI) effect in amorphous microwires for absolute position detection and demonstrated that the MI elements arranged in 1D and 2D arrays can be used for contactless proximity and position sensing of magnetic label attached to the detecting object. Owing to the high sensitivity of MI elements to the stray magnetic field produced by the magnetic label, the required density of the MI elements can be rather low that allows designing low-cost *in situ* reconfigurable sensor networks. Moreover, we demonstrate that the number of MI elements required for position detection can be further reduced and their separation can be increased by using the symmetry breaking effect of dc bias current on magnetoimpedance in microwire with helical anisotropy [1]. The application of bias current to the microwire with a high angle α of deviation of anisotropy easy axis from transversal direction (high helical anisotropy) can considerably affect the impedance dependence on external magnetic field. For example, it was demonstrated that for the microwire of the same composition in which a helical anisotropy with $\alpha = 35^\circ$ was induced, the application of bias current transforms symmetric MI dependence in a highly asymmetric [1, 2]. Then we use a cross-checking of two MI curves with properly selected bias current for determination of the magnitude and the sign of the external magnetic field in the extended range much higher than the microwire anisotropy field. An example of application 2D proximity and position sensing device for wireless power transfer is also considered.

References

- [1] M. Ipatov, V. Zhukova, J. Gonzalez, A. Zhukov: Symmetry breaking effect of dc bias current on magnetoimpedance in microwire with helical anisotropy: Application to magnetic sensors. *J. Appl. Phys.* 110 (2011) 086105.
- [2] M. Ipatov, A. Chizhik, V. Zhukova, J. Gonzalez, A. Zhukov: Correlation of surface domain structure and magneto-impedance in amorphous microwires. *J. Appl. Phys.* 109 (2011) 113924.

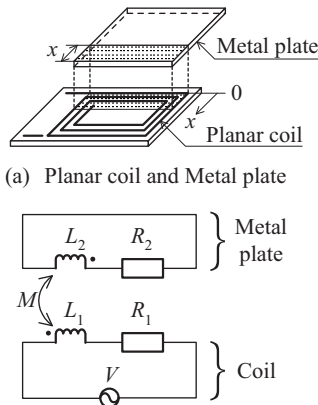
Consideration of planar coil inductance for thin type displacement sensor

Hiroyuki Wakiwaka¹, Yasuyuki Hattori¹, Daisuke Ito¹, Kunihiisa Tashiro¹, Hisashi Yajima², Tatsuya Hosaka², Takehiko Kanazawa², Nobuhiro Fujiwara²

¹Faculty of Engineering, Shinshu University, Nagano, Japan

²Product development division-3, SMC Corporation, Ibaraki, Japan

The sensors in which the measurement range is wide in the thin type are necessary so that the thin actuator may contain the sensor. The planar coil is suitable as a displacement sensor for the equipment integration. However, the theoretical formula for the inductance of the square planar coil still has few examples [1]. Then, we derived theoretical formula for the inductance of the square multilayer planar coil. We assumed the metal plate as a coil. Figure 1 shows the outline of over view and equivalent circuit. The mutual inductance M represent the mutual inductance of metal plate and planar coil. The resistance R_2 represent the resistance of metal plate. We define the displacement x as the displacement of metal plate. M and R_2 are function of x . We derived theoretical formula for the resistance and inductance of the square planar coil from the equivalent circuit. The metal plate was displaced and resistance and inductance were measured. The theoretical value was compared with the measured value, the inductance characteristic followed the characteristic which inductance of the metal plate L_2 was set to 110 ~ 120 nH. Figure 2 shows the comparison result. The resistance characteristic followed the characteristic which L_2 was set to 110 nH and added offset of 0.1 Ω .



(b) Considering the metal plate a coil

Fig.1 Principle

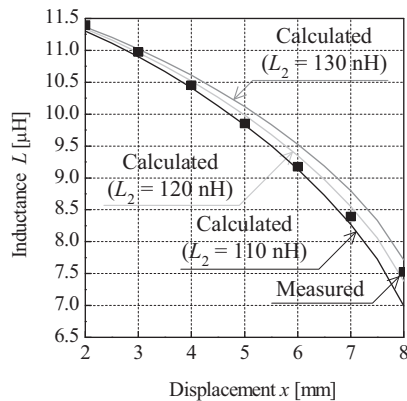


Fig.2 Characteristics of inductance vs. displacement.

References

[1] A. Tanaka, K. Ishida, N. Takehira: A New Approximate Equation of Self-Inductance of Multi-Layer Rectangular Coil (For Longer Coils). IEEE Japan. Vol.113-A No. 5, (1993), 428-429.

Optimization of a SQUID gradiometer for use in unshielded environment

O. Baltag, M.C. Rau

Medical Bioengineering Department, University of Medicine and Pharmacy “Grigore T. Popa” Iasi, Romania

One of the research directions in the gradiometers manufacturers is interested to find new solutions for the implementation of systems that must operate in unshielded environments. The biomagnetic fields are so small that they are buried in electromagnetic noise. The majority of biomagnetometric installations have a special concept and construction which only permit their utilization in shielded rooms. The SQUID type magnetometers used in such installation have a high sensitivity and low electromagnetic immunity against the surrounding electromagnetic noise which determine the utilization of SQUID magnetometers in shielded environment [1]. Reduce the effects of the electromagnetic ambient can be done by several methods:

- balancing the SQUID sensors which forms the gradiometer system [2],
- use of higher order SQUID gradiometers – 2nd or 3rd order and [3]
- application of external compensatory magnetic fields.

Limited accuracy and errors in the construction of a gradiometer lead to geometrical flaws. Balancing sensors is possible up to certain technological limits which refers to the geometrical and axial identity of the coils.

Electronic balancing is another solution used in SQUID gradiometer systems which have independent sensors.

The work presents the theoretical and technical solutions on optimization of a SQUID gradiometer system for use in an unshielded electromagnetic environment.

The solution relates to the use of a system for automatic compensation by means of a negative feedback reaction.

References

- [1] Y.P. Ma, J.P. Wikswo, magnetic shield for wide bandwidth magnetic measurements for nondestructive testing and biomagnetism, *Rev. Sci. Instrum.*, 62, (11), (1991), 2654-2661.
- [2] H.J.M. Brake, Z. Dunajski, W.A.G. van der Mheen, J. Flokstra, Electronic balancing of multichannel SQUIDS magnetometers, *J. Phys.E: Sci. Instrum.* 22 (1989), 560-564.
- [3] S.A. Uzunbajakau, A.P. Rijpma, H.J.M. Brake, M.J. Peters, Optimization of a third-order gradiometer for operation in unshielded environments, *IEEE trans. On Applied Superconductivity*, 15 No. 3, (2005), 3879-3885).

A New Calibration Method for a 2nd order SQUID Gradiometer System

Baltag O., Rau M.

Medical Bioengineering Department, University of Medicine and Pharmacy “Grigore T. Popa” Iasi, Romania

The paper presents theoretical and experimental results of a study on a new method for calibrating a 2nd order SQUID gradiometer. 1st order gradiometers are easily calibrated and verified because the magnetic field generator is easily to constructed and calibrated – Helmholtz type coils or magnetic dipoles. For calibrating a 2nd order gradiometer must generate a magnetic fields whose spatial variation corresponding to the second order spatial derivative [1]. These fields are relatively difficult to obtain using a set of Helmholtz coils [1], [2]. The proposed method refers to the generation of magnetic fields using a number of coils equal to the number of SQUID sensor gradiometers. These coils comprise, in volume, each sensor. Circulating currents through the coils that produce magnetic fields in the volume sensor has a spatial variation corresponding to the second order spatial derivative. It presents the mathematical model used in the fields and gradient calculation. Coil configuration can be extended to produce a first order gradient. The experimental results confirm the validity of the mathematical model described in this paper.

References

- [1] S.G. Lee, C.S. kang, J.W.Chang, A square loop Helmholtz coil system for the evaluation of a single layer second order high T_c SQUID gradiometer, *Physica C*, 460-462, (2007), 1472-1474.
- [2] A.C., Bruno, P.C. Ribeiro, Spatial Fourier calibration method for multichannel SQUID magnetometers, *Rev. Sci. Instrum.* 62, (1991), 1005–1009.

Bias-voltage controlled tunneling resistance in a magnetic tunneling junction with an inserted thin metallic layer

Sui-Pin Chen

Department of Electrophysics, National Chiayi University, Chia Yi, Taiwan

The topic of spin-dependent tunneling (SDT) in a magnetic tunneling junction (MTJ) continues to receive considerable attention, in regard both to its fundamental physics and its potential applications. SDT in an MTJ is characterized by the tunneling resistance (TR). An MTJ consists of an FM₁-I₃-FM₄ structure, where FM₁ and FM₄ are ferromagnetic electrodes and I₃ is a thin insulator. The change of SDT in the MTJ is measured by the tunneling magnetoresistance (TMR) ratio. In the FM₁-I₃-FM₄ MTJ, SDT is extremely sensitive to the interface structures between the insulator and each electrode. Thus, modulating one of the interfaces can change SDT. One way to achieve this is to insert a thin nonmagnetic (M₂) layer between one of the ferromagnetic electrodes, FM₁ or FM₄, and the insulator I₃. The M₂-inserted MTJ is the FM₁-M₂-I₃-FM₄ structure. The inserted M₂ layer leads to a severe alteration of the interface, thus resulting in a dramatic effect on SDT, the TR, and the TMR ratio.

The excellent experimental work of Yuasa et al. shows how the TMR is affected by the inserted Cu metal in a high-quality Co-Cu-Al₂O₃-NiFe MTJ. [1] A distinct attenuated oscillation of the TMR ratios with increasing the Cu thickness is observed at room temperature when the inserted Cu thickness is less than to 29Å. This reveals that the phase coherence of the spin-polarized electron across the Cu layer is conserved after multiple reflections occur at the Co/Cu and the Cu/Al₂O₃ interfaces, if the Cu thickness is much shorter than 29Å, the phase-relaxation length. Thus, in the FM₁-M₂-I₃-FM₄ MTJ where the M₂ thickness is much shorter than the phase-relaxation length, the phase of the electron plays a crucial role in the TMR ratio, the TR, and SDT. Another noteworthy experimental effect from the inserted M₂ layer is that the dependence of the applied bias voltage on the TMR effect in the FM₁-M₂-I₃-FM₄ MTJ is much larger than that in the FM₁-I₃-FM₄ MTJ. This implies that the phase of the electron across the M₂ layer is sensitive to the bias voltage applied to the FM₁-M₂-I₃-FM₄ MTJ.

Here, we adopt the spin-polarized free-electron model [2] and extend our previous work [3] to investigate how SDT, the TR, and the TMR are affected by the bias voltage in terms of the phase factor of an electron across the M₂-inserted MTJ. We find a new method of changing the tunneling resistance. Unlike the traditional method of varying the magnetizations configuration between the two ferromagnetic layers, the proposed method uses the polarity of the bias voltage with a small strength to change the tunneling resistance in the FM₁-M₂-I₃-FM₄ MTJ. Under suitable conditions, we show that both tunneling resistance changes resulting from the polarity of the bias voltage and from the magnetizations configuration are equal in magnitude, and are larger than that in a conventional FM₁-I₃-FM₄ MTJ.

References

- [1] S. Yuasa, T. Nagahama and Y. Suzuki: Spin-Polarized Resonant Tunneling in Magnetic Tunnel Junctions. *Science* 297 No. 5579, (2002), 234-237.
- [2] S. Zhang and P. M. Levy: Magnetoresistance of Magnetic Tunnel Junctions in the Presence of a Nonmagnetic Layer. *Phys. Rev. Lett.* 81 Issue 25, (1998) 5660-5603.
- [3] S.-P. Chen: Tunable tunneling magnetoresistance in a ferromagnet-metal-insulator-ferromagnet tunneling junction, *J. Appl. Phys.* 107 Issue 9, (2010), 09C716.

Behavior of DC tolerant current transformers in wide frequency range

MLEJNEK Pavel, KAŠPAR Petr

Department of Measurement, Faculty of Electrical Engineering,
Czech Technical University in Prague, Prague, Czech Republic

Understanding of behavior of CTs at frequency above nominal is important in applications where amplitude and phase of higher harmonics are measured, e.g. in energy quality testers or modern energy meters. The amplitude of particular harmonics can be used for detection of disturbance of CT as was described in our previous paper [1].

In order to investigate, three samples of linear DC tolerant CT from three manufacturers have been tested in frequency range from 50 Hz up to 5 kHz. Basic parameters of these sensors are reported in Table 1.

All measurements have been carried out with same conditions: 10 A primary current, 7.5 Ω burden resistor (even for TD120L despite it causes higher phase error than declared by manufacturer) and acquiring 11 frequency points in logarithmic scale.

The comparison of three samples from different manufacturers is shown in Fig. 1. The phase displacement at 50 Hz corresponds to the specification and decreases with increasing frequency: it is due to lower magnetizing current at higher frequency.

Manufacturers usually do not specify ratio errors because CTs have to be anyway calibrated in final product (e.g. energy meter) during final setup. Therefore, all ratio errors were normalized to -0.5% at 50 Hz and the changes in frequency range can be observed in figure below. The same effect (mentioned above) causes decrement of ratio errors for higher frequency.

Phase displacement at self resonant frequency and higher slightly depends on position of primary turn in the hole. According to position the phase error can change polarity.

Theoretical background and results from more detailed measurement and comparison of these linear CTs with dual core CTs will be discussed in full paper.

Table 1: Specification of tested DC tolerant CT

Manufacturer	Vacuum - schmelze	Magnetec	Tachwatrans
Type	4626X131	MB-361-01	TD120L
Current range	100 A	100 A	510 A
DC tolerance	100 A	100 A	120 A
Turns ratio	1:2500	1:2500	1:2500
Phase error	3.3 deg	5.1 deg	3.3 deg
Burden	7.5 Ω	7.5 Ω	1 Ω

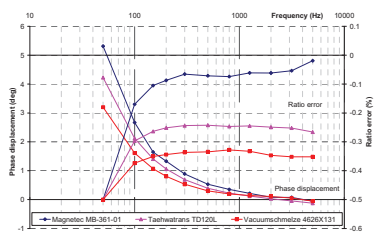


Fig. 1: Phase displacement and ratio error of CTs with 10A primary current.

References

- [1] P. Mlejnek, P. Kašpar, Detection of Disturbance of Working Conditions of Current Transformer in Energy Meter for Reduction of Unauthorized Current Consumption, PEDS 2009 – The Eighth International Conference on Power Electronics and Drive Systems, (2009) 284 – 287, ISBN 978-1-4244-4166-2.

Tuesday, July 3

ORAL SESSION

FLUXGATE, INDUCTION, SCALAR MAGNETOMETERS

Recent developments in space magnetometry

MAGNES Werner

Space Research Institute, Austrian Academy of Sciences, Graz, Austria

Resource requirements of scientific instruments for space applications, such as volume, mass and power, must constantly be reduced while the measurement performance must be at least kept the same.

During the last years, the Space Research Institute of the Austrian Academy of Sciences has been involved in the development a front-end ASIC (Application Specific Integrated Circuit) for magnetic field sensors as well as in the development of a new quantum-optic scalar magnetometer. The ASIC has jointly been developed with the Fraunhofer Institute for Integrated Circuits in Germany and the scalar magnetometer, respectively, with the Institute of Experimental Physics at the Graz University of Technology.

The Magnetometer Front-end ASIC (MFA), which is mainly designed for fluxgate sensors, reduces the required power for the active readout electronics by a factor of 10 as well as the area needed on a printed circuit board by a factor of 3-4 compared to magnetic field instruments e.g. aboard Venus Express (ESA). The concept of the MFA is based on a combination of the readout electronics of a conventional fluxgate magnetometer with the control loop of a delta-sigma modulator in order to get an optimized signal-to-noise ratio with a reasonable oversampling factor [1]. A first space magnetometer equipped with the MFA will fly aboard the 4-satellite NASA mission called Magnetospheric Multiscale (launch in 2014).

The scalar magnetometer, which is also called Coupled Dark State Magnetometer (CDSM), is a special kind of optically pumped magnetometer. This means that the energy from a light source is used for exciting electrons in an atom for measuring the magnitude of the surrounding magnetic field. In case of the CDSM, the optical source is a specially modulated laser light, which excites Rubidium atoms stored in a glass cell [2]. The measurement of the magnetic field is based on a quantum-interference effect called Coherent Population Trapping (CPT) in conjunction with the Zeeman Effect in free atoms. The measurement of magnetic fields is reduced to a frequency measurement which can be done with highest accuracy.

Advantages of the CDSM are a straightforward sensor design (no excitation coils, mechanisms and active electronics parts), a high dynamic range of more than 6 decades and its omni-directional measurement capability. The sensor just consists of a 1 cm³ big glass cell containing a few micrograms of an alkali metal (rubidium 87) in a buffer gas, two fibre couplers with polarisation optics and a cylindrical housing. A first verification in space will take place aboard a Chinese science mission in 2016.

References

- [1] Magnes, W., M. Oberst, A. Valavanoglou, H. Hauer, C. Hagen, I. Jernej, H. Neubauer, W. Baumjohann, D. Pierce, J. Means, P. Falkner: Highly integrated front-end electronics for spaceborne fluxgate sensors. *Meas. Sci. Technol.*, 19, (2008), 115801, doi:10.1088/0957-0233/19/11/115801
- [2] Lammegger, R.: Method and device for measuring magnetic fields. Patent, (2008), WO 2008/151344 A3

Beat interferences in fundamental mode orthogonal fluxgates

Ichiro Sasada, Feng Han, Shoumu Harada

Dept. of Applied Science for Electronics, Kyushu University, Kasuga, Japan

The fundamental mode orthogonal fluxgate (OFG) [1] has a very low noise level, for example, a few $\text{pT}/\sqrt{\text{Hz}}$ in the frequency range above 10 Hz. The sensor head can be made very thin, for example, assembled in an 8 mm outer diameter plastic pipe by using an amorphous wire core. Therefore they can be used to make a sensor array to image magnetic field distribution. By using a U-shaped wire core to which dc biased ac excitation current is fed, the magnetic field interference to other electronic devices are made minimum [2]. Due to the high sensitivity of OFG, however, tiny but still substantial (several hundreds pT) sinusoidal oscillations are visible in the output when two OFGs are placed closely in parallel in the magnetic shield. Frequencies of such oscillations are found exactly the difference of two frequencies of ac excitation currents to the sensor head and higher harmonics of the difference frequency. The interference can be described as a beat of excitation magnetic fields. Such interferences should be suppressed in the case of biomagnetic fields imaging, because they are usually very small. We will show that using the same excitation frequency for all the sensor heads is a simple solution to suppress beat interferences where beat interferences are converted to tiny dc components (equivalently small offsets). We will also show sensor head array having 16 channels on a 3 cm grid.

References

- [1] I. Sasada: Orthogonal fluxgate mechanism operated with dc biased excitation, *Journal of Applied Physics*, Vol. 91, No. 10, pp. 7789 (2002).
- [2] I. Sasada, M. Murakami: Fluxgate Magnetometer Electromagnetically Compatible with the First-Order SQUID Gradiometer, presented at Intermag2009, CR-04, Sacramento, USA

Orthogonal fluxgate with annealed wire-core

M. Butta, I. Sasada

Dept. Of Applied Science for Electronics and Materials, Kyushu University, Fukuoka, Japan

One of the main sources of noise in fluxgate sensors is Barkhausen noise originated in the magnetic core. It has been demonstrated that adding dc bias to the excitation current of orthogonal fluxgate strongly contributes to decrease the Barkhausen noise and in turn the sensor noise [1]. When dc bias is added the flux is gated only in one direction and the magnetization is always saturated; as a result domain wall movement does not occur, instead the magnetization only rotates. In this case the fundamental harmonic of the voltage induced in the pick-up coil is used as an output signal.

The key point for noise reduction is to use large ac current in order to achieve large sensitivity, avoiding however an ac current large enough to bring the core out of saturation at the timing of the lowest amplitude of the total current. From this point of view the ideal core for an orthogonal fluxgate in fundamental mode has the saturated portion of BH loop very wide, which corresponds to large circumferential anisotropy.

In order to fulfill this requirement we modified the BH loop of Co-based amorphous magnetic wire (120 μm diameter) by annealing it under the effect of dc current passing through the wire. Annealing is performed in a temperature-controlled furnace (Joule effect is negligible). A circular magnetic field is generated inside the wire by the dc current; when the current exceeds 75 mA the core is saturated in circumferential direction and annealing induces circular anisotropy in the wire [2]. We studied the dependence of anisotropy by changing both duration and temperature of annealing as well as dc current to the wire. Generally a longer duration or higher temperature of annealing increase the circumferential coercivity; however, for temperature higher than 230°C further increment of coercivity is not observed. This is probably because the annealing temperature gets closer to Curie temperature (about 310°C). The sensitivity of the sensor decreases when we increase circular anisotropy of the core by annealing, as expected by the model of the sensor [3].

Annealing is mainly useful for noise reduction. We studied the noise at 1 Hz of sensors based on as cast wire and annealed wire (30 minutes, 200 °C) for different values of ac excitation current and keeping dc bias always 48 mA for both wires. The sensor based on as cast wire reaches minimum noise at ~25 mA ac (about 3 pT/ $\sqrt{\text{Hz}}$), then the noise rises because ac current becomes too large and the core can not be kept in saturation. On the contrary annealed wire reaches its minimum noise at ~45 mA ac (about 1.7 pT/ $\sqrt{\text{Hz}}$), since the core is still saturated due to large circular anisotropy. By properly choosing annealing parameter we can induce in the core circular anisotropy large enough to suppress Barkhausen noise but not too large to kill sensitivity.

References

- [1] Paperno E., Suppression of magnetic noise in the fundamental-mode orthogonal fluxgate - Sens. Act. A 116. - 2004. - pp. 405-409.
- [2] Berry B.S., Prichet W.C., Magnetic annealing and directional ordering of an amorphous ferromagnetic – Physical review letters, Vol. 34, Iss. 16, pp. 1022-1025, 1975
- [3] Sasada I., Orthogonal fluxgate mechanism operated with dc biased excitation - J. Appl. Phys., vol. 91

Noise and drive field amplitude in RQ-tape-wound toroidal fluxgate sensors

BUTVIN P.¹, Janošek M.², Butvinová B.¹, Ripka P.², Chromčíková M.³, Švec P.¹

¹Institute of Physics, Slovak Academy of Sciences, Bratislava, Slovak Republic

²Dept. of Measurement, Faculty of Elec. Eng., Czech Tech. Univ., Praha, Czech Republic

³VILA Joint Glass Ctr. Inst. Inorg. Chem SAS, TnUniv. A. Dubček, Trenčín, Slovakia

The correlation between noise and drive field in fluxgate-type magnetic field sensors is still a live theme for many years [1]. Though not universally accepted, the notion of small-scale “defect structures”, which are difficult to remagnetize and cause drive field non-uniformity is still considered in more recent literature [2]. Modern rapidly quenched (RQ) soft-magnetic ribbons are already well characterized and fulfilling sufficiently the most of the established material requirements (low magnetostriction, handy to make symmetric ring cores etc.), they provide an advantageous possibility to test the above notion once more. There are metallic glasses exhibiting relatively homogeneous and intrinsic-stress free (if properly annealed) structure and nanocrystalline materials with inherent microscopic structural (and magnetic as well) heterogeneity. Both the materials are of the same form and show well tailorable magnetic properties for quite similar magnetic anisotropy to be induced. Apart from the unknown scale of the “defect structures”, the two material classes promise at least qualitatively the difference necessary to test the above notion.

Small ring cores have been wound of 2.5 mm wide RQ ribbons using two different low-magnetostrictive materials: a Co-Fe-Cr-B-Si metallic glass (MG) and a nanocrystalline Fe-Nb-Cu-B-Si “Finemet” (FM). Mostly 10-wrap ring cores were put into MACOR machinable-ceramics sheaths and annealed in axial magnetic field to acquire comparable transversal (relative to ribbon long axis) magnetic anisotropy. The vastly different Curie temperature as well as the necessity to attain partially crystalline structure of FM required accordingly significant difference in annealing temperature for the materials. The other large difference (~50%) is the saturation induction, thus a compromise between comparable anisotropy energy density and effective permeability was sought. Nevertheless, there are still other material disparities that are hard to balance: The low annealing temperature (260°C) necessary for the MG did not safely minimize macroscopic bending stress. The higher temperature for FM brings the risk of building so-called macroscopic heterogeneity capable of deteriorating uniformity of the desired transversal induced anisotropy.

Both the materials showed sensor noise to vary with the amplitude of drive field – noise is reduced (below 7 pT/√Hz@1 Hz for MG) by larger amplitude (10 kA/m p-p). Although the noise was generally higher for FM sensors, the difference and its variation with systemic changes of FM cores (e.g. crystalline share) do not support clearly the idea of principal similarity between small-scale “defect structures” and FM inherent microscopic heterogeneity. Thus the effort to improve FM noise by manipulating the other material properties (macroscopic ones inclusive) is worth further try.

References

- [1] D. Scouten: Sensor Noise in Low-Level Flux-Gate Magnetometers, IEEE Trans. Mag., Vol. 8, No. 2 (1972), 223-231
- [2] G. Mussman, Y. Afanassiev: Fluxgate sensors for space research, part 3.4, Books on Demand, Nordstedt (2010), 90-97

Measurement of DC currents in the power grid by current transformer

RIPKA P.¹, Draxler K.¹, Styblíková R.²,

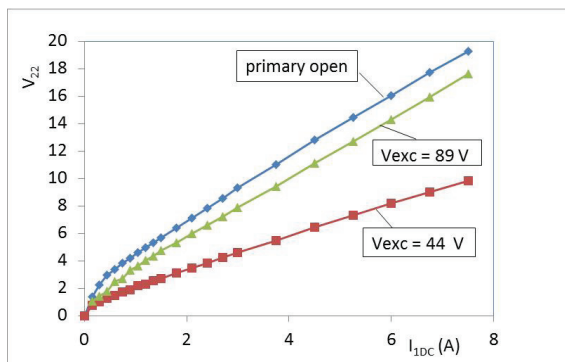
¹ Czech Technical University, Prague, Czech Republic

² Czech Metrology Institute, Prague, Czech republic

Geomagnetic storms induce DC telluric currents and also currents in pipelines and power networks. These currents may cause saturation of transformers resulting in tripping of protective relays and possible blackout. Prediction of magnetic storms and monitoring of DC currents can prevent problems. It would be very expensive to mount DC current sensors inside the existing 200 – 700 kV substations. Therefore the industrial requirement is to use existing current transformers to monitor also DC currents.

In our case the available transformer type CLA 2.2 had 500 A/5A current ratio and the rated output load of 5VA, corresponding with 0.2 Ω load resistor. To be able to measure the primary DC current I_{DC} even without AC component (which was not possible in [1]), we applied 370 Hz AC sinewave excitation into the secondary winding of the current transformer and created fluxgate current sensor. As our excitation source had low impedance, the excitation voltage was practically undistorted sinewave. Instead of measuring the output voltage, we measured 2nd harmonic component in the excitation current (using 0.2 Ω sensing resistor) by SR 830 lock-in amplifier.

The measured values are shown in Fig. 1 for short-circuited primary circuit and two amplitudes of the excitation voltage. The third characteristics was measured with open primary circuit. This is not a realistic condition, but the working point in real power grid will be always between the mentioned two extreme cases (short-circuit and open). The influence of the primary impedance is less than 10%, which is negligible for practical applications. Also the influence of the amplitude of the primary AC current is negligible for small current values below 50A, which is typical range of the measured currents.



References

[1] P. Ripka, P. Kaspar, P. Mlejnek: Current transformer can detect DC current component, SMM 2011

Tuesday, July 3

ORAL SESSION

MAGNETOELECTRICITY, AMR

Induction magnetometer using a low noise ASIC from sensor to ADC: design, performances and limitation.

Amine RHOUNI¹, Gérard SOU¹, Christophe COILLOT² and Paul LEROY²

¹L2E Laboratory of Electronics and Electromagnetism, UPMC Univ, Paris, France.

²LPP Laboratory of Plasmas Physics, CNRS - Ecole Polytechnique, Palaiseau, France.

Induction magnetometers are essential in many applications ([1], [2] & [3]) due to their performance, their low Noise Equivalent Magnetic Induction (NEMI) since a few Hz, robustness, ease of implementation and low power consumption.

In this paper, we will first briefly introduce the principle of the search coil magnetometer with feedback flux. Then, we will present the designed low noise ASIC preamplifier ($3\text{nV}/\sqrt{\text{Hz}}$) and $10\text{fA}/\sqrt{\text{Hz}}$ @1kHz) in $0.35\mu\text{m}$ CMOS technology dedicated to the frequency range kHz - MHz. Modelization and performances of the ASIC (called MagIC2, cf. Figure 1) will also be detailed.

A complete modelization of the NEMI of this circuit associated with an inductive sensor (10cm length) will be presented. Modeled and measured NEMI will be compared. The role of the imaginary-part of the ferromagnetic core permeability in the measured NEMI will be discussed. We will show that a NEMI of about $6\text{fT}/\sqrt{\text{Hz}}$ can be achieved making possible the observation of the lightning electromagnetic signatures, but which remains insufficient for the study of electromagnetic waves that present an interest for the space weather as the whistlers [3]. The prospects to improve performances to achieve this goal will be addressed. The way to evaluate the digitization number of bits will be discussed. The objective of the digitization being to take advantage of the instrument sensitivity and thus to restore the output noise fluctuations.

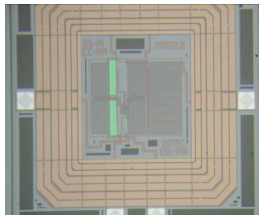


Figure 1 Photography of the low noise preamplifier ASIC chip (1mm x 1mm)

References

- [1] Le Contel O. , Roux A., Coillot C., Bouabdellah A., de la Porte B., Alison D., Rucco S., Angelopoulos A., Bromund K., Chaston C. C., Cully C., First results of the THEMIS Search Coil Magnetometer (SCM), *Space Sci. Rev.*,doi: 10.1007/s11214-008-9371-y, 2008.
- [2] M. Hayakawa, K. Hattori, K. Ohta, Monitoring of ULF geomagnetic variations associated with Earthquakes, *Sensors*, Vol. 7, (2007), 1108-1122.
- [3] Lichtenberger J., Ferencz C., Bodnár L., Hamar D. and Steinbach P. (2008). Automatic whistler detector and analyzer system: automatic whistler detector. *J. Geophys. Res.* **113**, A12201, doi: 10.1029/2008JA013467.

Temperature characteristics of resonance magnetolectric interaction in PZT/Ni disk resonators

D.V. Chashin, D.A. Burdin, N.A. Ekonomov, and Y.K. Fetisov

Moscow State Technical University of Radio Engineering, Electronics and Automation,
Moscow, Russia

Magnetolectric (ME) interaction in laminated structures consisting of ferromagnetic (FM) and piezoelectric (PE) layers is intensively studied because of prospects of its applications in high sensitive magnetic field sensors, low-power autonomous electrical generators, and electrically tuned signal processing devices [1]. The interaction arises from combination of magnetostriction of FM layer and piezoelectricity of PE layer due to mechanical coupling between the layers and results in generation of electrical voltage u across the structure which magnitude is proportional to the external magnetic field.

This paper describes for the first time measured temperature characteristics of resonance ME interaction in disk resonators consisting of lead zirconate-titanate (PZT) and nickel (Ni) layers. The resonators with diameter of 25 mm and thickness of 0.6 mm were fabricated by bonding PZT and Ni disks with epoxy glue or by using electrolytic Ni deposition on one side of the PZT disk. The resonators were placed in tangential dc magnetic field $H=0-200$ Oe and excited with tangential ac magnetic field $h\cos(2\pi ft)$ ($h=0-2$ Oe, $f=10$ Hz-200 kHz). The generated ac voltage u was measured for different temperatures in the range of 200 - 360 K.

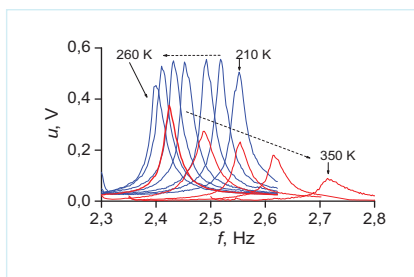


Fig. 1

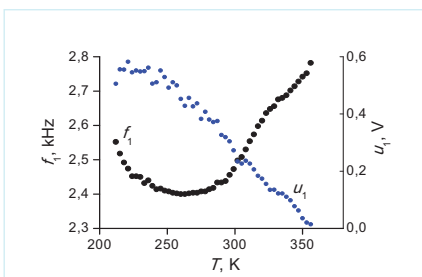


Fig. 2

Figures 1 and 2 show typical evolution of the PZT/Ni resonator line and corresponding dependences of the resonance frequency f_1 and maximum generated voltage u_1 as temperature increases from 210 K to 350 K. It was shown that change of the frequency is due to decrease in the Young's modulus of the layers with increase in the temperature and due to difference in the coefficients of thermal expansion of the layers which produces static deformation of the resonator. The magnitude of ME voltage at the resonance frequency gradually drops with increase in the temperature because of increase in the dielectric constant of the PZT layer. The results obtained may be used for thermo-stabilization of characteristics of ME magnetic field sensors.

The work was supported by the Ministry of Education and Science of Russia and the Russian Foundation for Basic Research.

References

[1] C.-W. Nan., M.I. Bichurin., S. Dong. D. Viehland, and G. Srinivasan: Multiferroic magnetolectric composites: historical perspective, status and future directions. J. Appl. Phys., v.103, (2008). 131101.

New magnetoelectric composite structures for magnetic field sensors

L.Y. Fetisov¹, N.S. Perov¹, A.V. Medvedev², G. Srinivasan³, G. Srinivasulu³

¹Magnetism division, Faculty of Physics, Moscow State University, Moscow, Russia

²FOMOS-Materials, Moscow, Russia

³Physics Department, Oakland University, Rochester, Michigan, USA

Recently, one can see great interest in developing magnetic field sensors based on magnetoelectric effect in multiferroic structures consisting of magnetostrictive and ferroelectric layers [1]. The sensors operate due to combination of magnetostriction which changes dimensions of magnetostrictive layers under external magnetic fields and piezoelectric effect in ferroelectric layers which generate electric voltage across the sample. The ME sensors have several advantages in comparison with the others (Hall sensors, magnetoresistance sensors, etc.), including high sensitivity at room temperature [2], large frequency range, and linearity of the voltage vs magnetic field dependence. Till now the ceramics PZT and PMN-PT were used as ferroelectrics for magnetoelectric structures.

This paper describes new layered magnetoelectric structures where piezoelectric layers are used instead of ferroelectric ones. Such piezoelectrics as langatate ($\text{La}_3\text{Ga}_{5.5}\text{Ta}_{0.5}\text{O}_{14}$), quartz, and katangasite ($\text{Ca}_3\text{TaGa}_3\text{Si}_2\text{O}_{14}$) possess the following advantages: lack of hysteresis, large enough piezoelectric module together with small dielectric permeability, high acoustical quality factor and temperature stability. These piezoelectric materials were produced by "FOMOS-Materials" company in Moscow. Magnetoelectric characteristics for structures with mentioned above piezoelectrics and permendur layers were measured in the frequency range 20 Hz – 200 kHz and magnetic fields up to 1.2 kOe at the room temperature. It was shown that magnetoelectric coefficient for permendur - langatate structures is an order of magnitude higher than for permendur - PZT structures and reaches $\alpha_E \sim 700 \text{ V}\cdot\text{Oe}^{-1}\cdot\text{cm}^{-1}$ under acoustical resonance conditions [3]. In addition, langatate-based structures have orders of magnitude smaller magnetic noise in the low frequency range. For structures permendur-katangasite $\alpha_E \sim 4.3 \text{ V}\cdot\text{Oe}^{-1}\cdot\text{cm}^{-1}$ and for structures amorphous magnetic-quartz $\alpha_E \sim 2 \text{ V}\cdot\text{Oe}^{-1}\cdot\text{cm}^{-1}$.

The research was partially supported by the Ministry of Education and Science of Russia, the Russian Foundation for Basic Research, and the National Science Foundation of the U.S.

References

- [1]. Ce-We Nan, M.I. Bichurin, S. Dong, D. Viehland, and G. Srinivasan: Multiferroic Magnetoelectric composites: Historical perspective, status, and future directions. *Appl. Phys. Lett.* V. 103, (2008), No. 031101.
- [2]. X.W. Dong, B. Wang, K.F. Wang, J.G. Wan, J.-M. Liu: Ultra-sensitive detection of magnetic field and its direction using bilayer PVDF/Metglas laminate. *Sensors and Actuators A.* No. 153 (2009), 64-68.
- [3]. G. Sreenivasulu, L. Y. Fetisov, Y.K. Fetisov and G.Srinivasan: Piezoelectric single crystal langatate and ferromagnetic composites: Studies on low-frequency and resonance magnetoelectric effects. *Appl. Phys. Lett.* V. 100, (2012), No. 052901.

Investigation of the role of crystallographic texture on the sensitivity of AMR thin film sensors

Andras Bartok¹, Laurent Daniel¹, Thierry Baudin², Adel Razek¹

¹Laboratoire de Génie Électrique de Paris, Gif sur Yvette, France

²Institut de Chimie Moléculaire et des Matériaux d'Orsay, Orsay, France

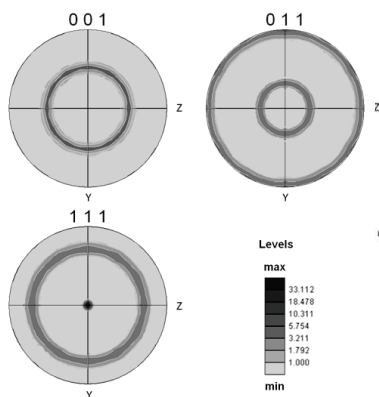
AMR sensor is one of the most widely deployed magnetic field sensors due to its high sensitivity and flexibility of design. In the applications where the quantitative measurement of a magnetic field is necessary (contactless current measurements, electric compasses) these sensor elements are typically thin permalloy films with strong magnetic anisotropy axis. Their preferred fabrication method is electron beam evaporation where the deposition is usually performed in an applied magnetic field. This process creates a so-called fiber crystallographic texture (*Figure a*) inducing an uniaxial anisotropy in the film plane (x - y plane).

This texture ensures the direction of the magnetization along the anisotropy axis (x) in absence of external field. Thanks to this effect a sensitive direction can be defined (y) and the sensor will be no more sensitive for the small field perturbation in other directions. In this context the quality of the texture is a key factor for the sensing properties of thin film AMR sensors.

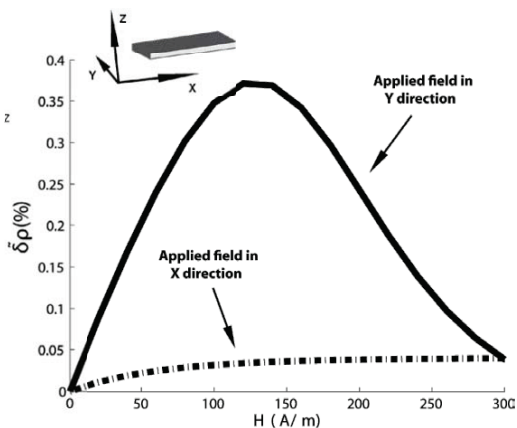
Numerical AMR models are mostly based on micromagnetic calculations. If the effect of the microstructure on the overall AMR properties is to be investigated these methods are not relevant as the number of degrees of freedom and interactions are growing quickly with the number of magnetic moments.

A micro-macro approach for AMR effect is proposed, including microstructural data such as crystallographic texture. It is useful in order to provide a design tool for thin film sensors accounting for.

In this paper, the sensing properties of a $\text{Fe}_{11}\text{Ni}_{89}$ film are computed using different calculated fiber crystallographic textures. The role of the sharpness of the crystallographic texture on the sensing properties (*Figure b*) is discussed.



a) Pole figures of fiber texture



b) Change of resistivity with change of applied magnetic field

Tuesday, July 3

ORAL SESSION

MAGNETIC MICROWIRES

Amorphous and nanocrystalline microwires

Horia Chiriac

National Institute of Research and Development for Technical Physics

The abstract has not been received.

Micromagnetic modelling on high frequency response of amorphous microwires

J. Torrejón^{1,2}, A. Thiaville¹, A. L. Adenot-Engelvin³ & M. Vazquez².

¹Laboratoire de Physique des Solides, Univ. Paris-Sud, CNRS , 91405 Orsay, France.

²Instituto de Ciencia des Materiales, CSIC, 28049 Madrid, Spain

³CEA, DAM, Le Ripault, 37260 Monts, France

The glass-coated microwires, fabricated by quenching and drawing technique [1], are attractive materials over a very wide frequency range as a consequence of the several applications [2]: high frequency inductors, broadband skin antennas, microwave filters, noise suppressors, and radar absorbing materials. The ultrarapid solidification process confers an amorphous structure, which provides a very soft magnetic behaviour as a consequence of the absence of strong magnetocrystalline anisotropy. The presence of glass cover is an important source of internal stresses in the microwires. Such stresses together with its magnetostriction govern the magnetic structure of microwires, both are included in the magnetoelastic anisotropy.

The magnetic behaviour of amorphous glass-coated microwires has been modelled by quasi-analytical 1D micromagnetics. Co-based alloys with negative magnetostriction present a noticeable circumferential anisotropy where an axial core responds to the minimization of exchange energy. The theoretical approach is based on one-dimensional micromagnetic model where exchange, magnetoelastic and magnetostatic energies are considered. We assume that magnetization profile varies only along radial direction and magnetoelastic anisotropy does not depend to the radial coordinate, corresponding to dominant glass cover induced stresses. The model evaluates firstly the static properties. Solving the variational problem that leads to Euler-Lagrange equation, we estimate the size of the core and the axial hysteresis loops as a function of radius, exchange coefficient and anisotropy constant [3].

The model was extended to high frequency dynamics under axial ac field. The microwave permeability has been computed as a sum of eigenmodes. These modes are obtained as solution of a Schrödinger equation where the potential derives from static solution. Finally, comparison with experimental measurements (applying the a.c. field in a coaxial APC7 setup) shows the important role of the skin effect for thicker wires. Macrospin model is also explored in order to evaluate the roles of exchange constant and radius.

References

[1] M. Vazquez, in *Handbook of Magnetism and Advanced Magnetic Materials*, vol. 4, edited by H. Kronmuller and S. Parkin. Wiley, Chichester, UK, (2007) pp. 2193-2296.

[2] M. Vazquez, A. L. Adenot-Engelvin, *J. Magn. Mater.* **321** (2009) 2066

[3] J. Torrejón et al; *J. Magn. Mater.*, **323** (2011) 283.

Presentation: **Oral**

Topic: **Modelling and simulation**

Tailoring the switching field dependence on external parameters in magnetic microwires

R. Varga¹, J. Gamcova¹, P. Klein¹, A. Zhukov², M. Vazquez³

¹Institute of Physics, Fac.Sci., UPJŠ, Park Angelinum 9, 041 54 Košice, Slovakia

²Department Fisica de Materiales, Fac. Quimica, San Sebastian 20080, Spain

³Instituto de Ciencia de Materiales de Madrid, CSIC, 28049 Madrid, Spain

Amorphous glass-coated microwires with positive magnetostriction are characterized by a magnetic bistability. Their magnetization can reach only two values (+ M_s or- M_s) and switching between the two values runs through the single Barkhausen jump when the external field approaches the value of switching field H_{sw} .

The switching field of magnetic microwires is extremely sensitive to external parameters (like temperature, mechanical stress, frequency of applied magnetic field, etc...) the feature that can be successively employed in various sensors construction.

The switching field in amorphous microwires has two contributions: magnetoelastic and another one arising from structural relaxation [2]. These two contributions have different sensitivity to the external parameters [3] which gives us opportunity to tailor the overall sensitivity of the switching field to stress, temperature, magnetic field according to desired conditions.

In this contribution we show the experimental results on the tailoring the temperature, stress and frequency dependence of glass-coated bistable microwires by selecting the proper chemical composition or by properly selected thermal treatment. In such a way, the strong stress dependence of the switching field can be obtained by annealing out the stress introduced by production. On the other hand, no stress dependence appears in the same composition when annealing at high temperatures as a result of inducing the additional stress by glass-coating. Similarly, the linear temperature dependence of the switching field can be obtained by properly annealing of microwire, meanwhile no temperature dependence appears in the same microwires when the frequency of the exciting field is adjust adequately.

Support by the project NanoCEXmat Nr. ITMS 26220120019, Slovak grant APVV-0266-10 and VEGA grant No.1/0076/09 is acknowledged.

References

- [1] M. Vázquez, in *Handbook of Magnetism and Advanced Magnetic Materials* edited by H. Kronmüller and S. Parkin, (Wiley, New York, 2007), Vol. 4, p. 2193.
- [2] R. Varga, K. L. Garcia, A. Zhukov, M. Vazquez, P. Vojtanik, *Appl. Phys. Lett.* **83**, 2620 (2003).
- [3] R. Varga, A. Zhukov, M. Ipatov, J. M. Blanco, J. Gonzalez, V. Zhukova, P. Vojtanik *PHYSICAL REVIEW B* **73**, (2006), 053605.

Effects of annealing treatment on microwave properties of amorphous FeSiB-base microwires

EL KAMMOUNI Rhimou, Badini-Confalonieri Giovanni and Vázquez Manuel

Institute of Material Science of Madrid, CSIC, 28049 Madrid, Spain

The influence of thermal treatments in ribbon-shaped metallic glasses was systematically studied years ago paying particular attention to their static magnetic properties. In this regard, samples become magnetically harder upon thermal treatments above the crystallization temperature, while softness is improved in some cases when nanocrystalline structure is achieved. More recently, studies were also focused on wire-shaped samples.

The present study deals with the influence of annealing treatments on the microwave electromagnetic response of magnetic microwires with an objective of tuning the characteristics (i.e., frequency) of the ferromagnetic absorption properties [1,2]. Amorphous Pyrex-coated Fe₇₆Si₁₃B₁₁ microwires were fabricated by quenching and drawing technique having metallic and total diameter in the range of 18 and 26 μm. They were subsequently annealed under controlled atmosphere at temperature from 100°C to 700°C for 1h. The effect of thermal treatments (i.e., coercivity) was firstly checked by analyzing the low-frequency hysteresis loops by fluxmetric and VSM induction techniques. The ferromagnetic resonance spectrum was then investigated from power absorption measurements in a Network Analyzer in the frequency range from 10MHz to 18GHz. The linear shift of FRM frequency with square root of the applied static field is interpreted considering the Kittel equation. The effective anisotropy field is in addition observed to increase with annealing temperature. Finally, the influence of the presence of a second external electroplated polycrystalline CoNi microlayer in the treatments is analyzed. In this case, a second absorption peak ascribed to the new magnetic phase is observed together with an additional shift in the effective anisotropy field.

[1] R. El kammouni, G. Infante, J. Torrejon, M.R. Britel, J. Brigui M. Vázquez, Phys. Stat. Sol. A 208 (2011) 520.

[2] J. Torrejón, G.A. Badini-Confalonieri, and M. Vázquez, J. Phys. D: Appl. Phys. 43 (2010) 145001.

Tuesday, July 3

POSTER SESSION TP1 - TP45

Performance Comparison of Two Different Tubular Linear Actuators for the Active Accelerator Pedal Application

Young-Kyoun Kim, Jeong-Jong Lee, and In-Soung Jung

Korea Electronics Technology Institute, Yatap-Dong, Seongnam, Korea

Recently, the needs of motorization in vehicle system have increased as a wide range of reasons, such as a vehicle safety, convenience and energy consumption. An Active Accelerator Pedal (AAP) is one of them. The AAP is installed in the accelerator pedal in the vehicle. Unlike conventional mechanical pedal, it is generally run by an electric actuator generating resistance or vibration force against drivers' foot press force [1]-[2].

Previous AAP utilized rotary motor with mechanical gear system which brings unexpected breakdown and failure. To overcome the troubles by mechanical parts, linear actuator is utilized. Since the pedal press is linear motion, the active pedal system with linear motor does not need the gear system. This paper described both analysis and design of two different tubular linear actuators for the AAP application. Their designs are optimized to satisfying the requirement of the actuator such as a high force density and a low detent force, and then a performance comparison of them is conducted based on the same dimensions. Finally, the validity of all results is confirmed by both analysis results and experimental results.

In this paper, the slotless tubular linear actuator is qualitatively compared with the slotted tubular linear actuator. Fig. 1 shows the basic structure of two different tubular linear actuators. The slotted tubular actuator consists of a slotted tubular stator wounded coils and a mover mounted permanent magnets, and slotted stators are made up of four pieces and their surfaces are faced with the mover surface with four poles mounted permanent magnets respectively. The slotless tubular linear actuator consists of a mover mounted permanent magnets and a stator wounded coils, and the magnet is made up of two poles magnetized to radial direction, and the slotless stator coil are excited in two phase.

In this study, two different types actuator is design for the AAP, and then their performance comparison is qualitatively investigated. Fig. 2 shows the comparison of analysis results of their thrust force. In full paper, the more detail of the performance comparison included experimental results will be presented.

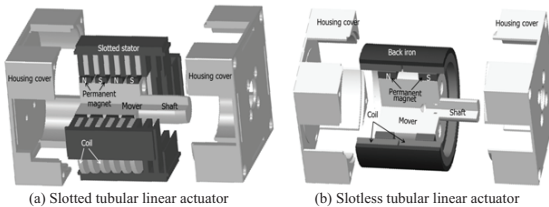


Fig. 1 Configuration of two different types of tubular linear actuator

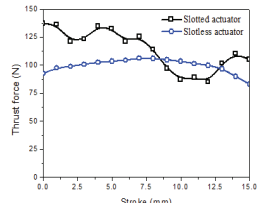


Fig. 2 Comparison of thrust force of them

References

- [1] M. Hjalmdahl, and A. Varhelyi, "Speed regulation by in car active accelerator pedal Effects on speed and speed distribution," IATSS RESEARCH, vol.26, no.2, pp. 60-66, 2002.
- [2] http://www.nissan-global.com/EN/NEWS/2008/_STORY/080804-02-e.html, "WORLD FIRST ECO PEDAL HELPS REDUCE FUEL CONSUMPTION," Nissan ECO Pedal system to be commercialized by 2009.

Magnetically actuated rotary walking of superparamagnetic particle chains on a solid surface

Chiun Peng Lee¹, Shin Yi Tsai¹, Zung Hang Wei¹, and Mei Feng Lai²

¹ Department of Power Mechanical Engineering, National Tsing Hua University, Taiwan

² Institute of Nanoengineering and Microsystems, National Tsing Hua University, Taiwan

It is known that the chain structure of superparamagnetic particles, which are in micro and nano scale, forms under an external field, and these chain structures can make response to the field variation even without field gradient. Based on this important benefit, the rotating magnetic particle chains have been widely applied for numerous purposes [1, 2]. In this paper, we demonstrate and analyze the behavior of the rotary walking superparamagnetic particle (10 nm diameter Fe_3O_4 particles) chains on a solid non-magnetic surface.

Figure 1 shows the sequential OM images of the particle chain walking on the solid surface. From our experiment results, we found that the ratio of the distance d (see Fig. 1(c)) that the particle chain can go via a 180-degree rotation to the chain length L is a function of rotational frequency ω and strength of external field, and the largest d is observed the same with the chain length, which means the $d/L = 1$. The relationships between d/L and ω are shown in Fig. 2. From this figure, it is obvious that the d/L decreases as the rotating frequency is increasing. It can be explained by the force diagram of the walking particle chain shown by the insect in Fig. 2. When the particle chain is rotating under a uniform rotary external field H , in addition to the itself caused gravity force F_g and the viscose drag force F_{drag} , the rotation is also dominated mainly by the frictional force F_{fric} . For the case that the external field strength being a constant and rotating slowly (< 0.5 Hz), the F_g is larger than the y-component of the F_{drag} , and it causes a large enough F_{fric} to prevent the sliding between the chain and the substrate. In contrast, when the external field rotates faster, the y-component of F_{drag} becomes stronger and makes the particle chain floats during the rotation. Once the floating occurs, the chain slides on the substrate and in consequence the chain's walking step is always shorter than the chain length. The faster the rotation is, the stronger the drag force and the smaller the d/L will be.

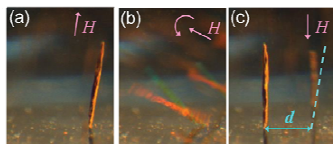


Figure 1 Sequential images of the walking chain. $H = 54$ Gauss, $\omega = 3.5$ Hz, $d/L = 0.65$.

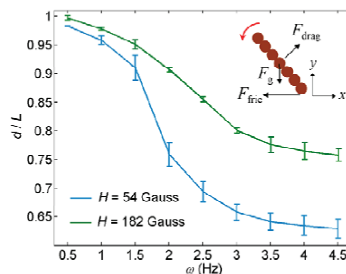


Figure 2 d/L at different ω and H . The error bars are the standard deviation of experimental data.

References

- [1] T. Roy, A. Sinha, S. Chakraborty, R. Ganguly, I. K. Puri: Magnetic microsphere-based mixers for microdroplets. *Phys. Fluids* 21, (2009), 027101.
- [2] C. E. Sing, L. Schmid, M. F. Schneider, T. Franke, A. Alexander-Katz: Controlled surface-induced flows from the motion of self-assembled colloidal walkers. *Proc. Natl. Acad. Sci. USA*, 107, (2010), 535-540.

Cogging Torque Reduction of Surface Permanent Magnet Motor with Asymmetric Stator Slots

Jeong-Jong Lee¹, Se-Hyun Rhyu¹, Young-Kyoun Kim¹, , In-Soung Jung¹

¹ Intelligent Mechatronics Research Center, Korea Electronics Technology Institute, Korea

By the development of automotive electronics, the number of parts that make up a small electric motor, the role of these kinds is also increasing. Recently high performance vehicle is needed various small motor for automatic system and economical driving. The small electric motor will be more important in automotive industry. And, the more simple structure of the motor reduces production costs.

This paper presents the method for cogging torque reduction in the small electric motor applied to the automotive actuator. In general case, the cogging torque of the motor is very sensitive to the output torque in the actuator with high gear ratios. The motor with 8-pole and 6-slot is simple for production. However, the large cogging torque is not much use. In order to reduce the cogging torque, the asymmetric slot has been applied to the motor. Many papers were published about analysis methods of the cogging torque in electric machines. The analytical method and FEM analysis has been used many paper [1][2]. In this paper, we used the FEM analysis for cogging torque.

Figure 1 shows the analysis model with 8pole-6slot. The cogging torque frequency is 24-period per one mechanical rotation. Figure 2 show the cogging torque according to teeth width. Maximum torque of this motor is 4mNm. Therefore, the cogging torque is critical value of torque pulsation. In the paper, the method of cogging torque reduction is suggested with special shaped. Other interesting result and detailed descriptions on experiments and analysis will be included in the full paper.

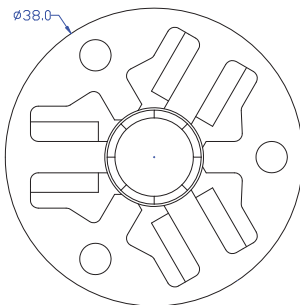


Fig. 1 Analysis model (8pole/6slot)

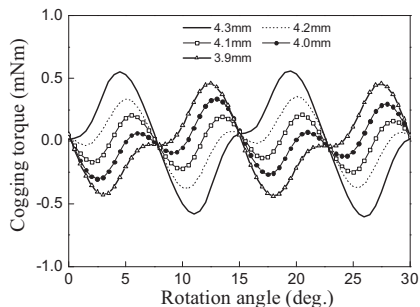


Fig. 2 Cogging torque according to teeth width

References

- [1] L. J. Wu, Z. Q. Zhu, David A. Staton: Comparison of Analytical Models of Cogging Torque in Surface-Mounted PM Machines. IEEE Trans. on Industrial Electronics, Vol. 59, No. 4, pp. 2414-2425, Jun 2012.
- [2] J. J. Lee, Y. K. Kim, S. H. Rhyu, I. S. Jung, S. H. Chai, J. P. Hong: Hysteresis Torque Analysis of Permanent Magnet Motors Using Preisach Model. IEEE Trans. On Magnetics, Vol. 48, No. 2, pp. 935-938, Feb. 2012

Comparison Between The Performances of The Conventional and The Augmented Railgun

M. Abdallah¹, H. Lahrech¹ and H. Mohellebi²

¹Electromagnetic Systems Laboratory, EMP, Bordj El-Bahri, Algiers 16111, Algeria.

²Electrical Engineering Laboratory, Tizi-Ouzou University, Tizi-Ouzou, 15 000, Algeria

E-mail: abdelmedi@yahoo.fr, isl.lahrech@gmail.com, mohellebi@yahoo.fr

The aim of this paper is the comparison between the performances of the Conventional Railgun (CRG) and the Augmented Railgun (ARG). The contact between the current's bridge and the rails of the launcher gives an important heat caused by Joule's effect and friction. This contact creates plasma, this transition can be avoided by increasing the resistance of the current's bridge. The problem is how to solve the plasma's problem without losing the current intensity because we need it to increase the propulsion's force? This can be simply obtained by applying an external magnetic field to the bridges of the current of the projectile (Fig. 1). The augmented railgun is presented as a launcher (CRG) reinforced by a second pair of rails, the prototype proposed is of small gauge (20 cm of length and 15 mm of diameter). The power supply of the launcher consists of condensers's benches delivering of the current with two separate circuits: the inner circuit associates the projectile, and the outer circuit generating the additional magnetic field. The force acting on the bridge of current is [1]:

$$F_p = \frac{\partial W_c}{\partial x} = \frac{1}{2} \frac{\partial L_1}{\partial x} I_1^2 + \frac{\partial W_{12}}{\partial x} I_1 I_2 \quad (1)$$

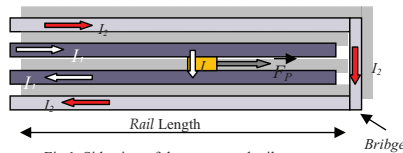


Fig.1. Side view of the augmented railgun

Inductance of the outer circuit L_2 and Inductance of the projectile L_p , do not vary when the projectile moves. In equation (1), W_c is the magnetic coenergy, I_1 and I_2 are the electrical currents in inner and outer circuit respectively and L_1 is the inductance of the inner circuit. The results obtained are given in figure 1 and figure 2. The speed can reach the value of 1.01 km/s as shown in Fig.1. The evolution of the force on the projectile is carried out as the function of the displacement (Fig.2). It should be note that a 40 kN of propulsion force is obtained.

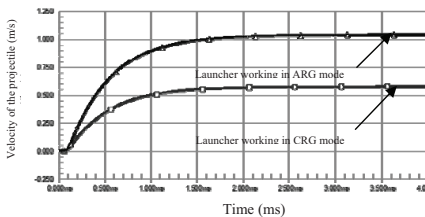


Fig.1. Comparison between the projectile's velocities in the launcher working in CRG & ARG

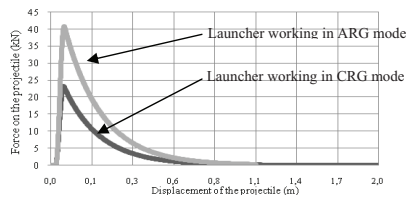


Fig. 2. Comparison between the projectile's forces in the launcher working in CRG & ARG

The augmentation of rails represents a solution to improve the projectile propulsion. The simulation shows that the increase in the rails allows an increase in the propulsion force with a rate of 60%. While the execution we met the problem of heating due to the strong concentration of current. To solve this problem we used the pre-accelerator to propel the projectile and feed the rails at the same time.

References

- [1] M. Coffo, J. Gallant, "Modelling Of A Parallel Augmented Railgun With PSPICE Validation Of The Model And Optimization Of The Augmenting Circuit," IEEE transactions on magnetics, vol 35, no 1, january 2007.

Electronic control of the switched reluctance motors

C. Morón¹, E. Tremps¹, P. Ramirez², A. Garcia¹, J.A. Somolinos³

¹Dpto. Tecnología de la Edificación, E.U. Arquitectura Técnica (U.P.M.), Madrid 28040, Spain

²Dpto. S.I.A., E.U. Informática (U.P.M.), Ctra. Valencia Km. 7, Madrid 28031, Spain

³Dpto. Sistemas Oceánicos y Navales, ETSI Navales (UPM), Madrid, Spain

In this work contributions are made to the Electronic Control of the Switched Reluctance Motors (SRM) to a given margin of power between 0.25 -10 kW. A low-cost drive of the SRM which permits regulation of speed with constant commutation angles is proposed. The control of this drive has been built by means of analogical and digitally discrete components. With respect to the sensors, a single current sensor has been used and the position/speed sensor built by means of three optical-interrupters and a slotted disc. Regarding the basics of this drive, we have studied how some motor parameters such as efficiency and acoustic noise have been influenced by the different strategies of control which were mainly built by different types of regulators (Pulse-Width Modulation PWM, Hysteresis, PWM with current regulation) with some characteristic parameters focusing on the motor's operation, such as efficiency and acoustic noise.

Also a platform is presented for a design of the digital SRM drives by using as a base the Dspace Ace kit 1104 CLP. On this platform, three different alternatives of averaging torque control have been developed for SRM starting from the signals coming from three optical-interrupters: (a) Online control of the turn-on and turn-off angles for variable speed applications which does not depend on curves of magnetization but on a few parameters of the motor. (b) A control that includes a performance turn off optimizer in which starting from the turn-on and turn-off conduction obtained from the aforementioned control modifying itself online by means of an algorithm in order to minimize input power and maximize performance. (c) The third alternative tries to maximize efficiency from a table, experimentally obtained, which picks up the turn-on and turn-off angles minimizing the drive input power in distinct operational zones with margins of speed pre-established. An efficiency and electrical consumption comparison between the results obtained applying different digital control alternatives and with a commercial vector-controlled induction motor drive of the same size is included.

Design Analysis and Experimental Validation of a Double Rotor Synchronous PM Machine Used for HEV

PIŠEK Peter¹, Štumberger Bojan^{2,3}, Marčič Tine¹, Vrtič Peter³

¹TECES, Research and Development Centre for Electrical Machines, Maribor, Slovenia

²Faculty of EE&CS, University of Maribor, Maribor, Slovenia

³Faculty of Energy Technology, University of Maribor, Maribor, Slovenia

The paper presents a new rotary actuator – the double rotor permanent magnet synchronous machine (DRPMSM), which is to be used in hybrid electric vehicles (HEVs) as a four-quadrant drive system. The focus in this paper is placed on the electromagnetic design, construction and the experimental validation of the proposed DRPMSM. In this work the radial-radial electric machine concept with one permanent magnet per pole on the outer rotor has been employed. Other designs were proposed in [1]-[3], however deeper investigations still need to be reported. For this reason special attention in this work was paid to the investigation of the most appropriate stator-slot/outer-rotor pole/inner-rotor-slot number combination because of the newly proposed outer rotor design. Six different slot-pole-slot combinations were investigated and compared in detail. The machines' performances were evaluated based on post-processing of results from time-stepping finite element analyses. From all results comparison it was elaborated that the combination 36-8-36 was the most appropriate. It's distinguished by low harmonic distortion in the back electromotive force, high average torque with low ripple and low power loss in the iron core material of the DRPMSM. A machine prototype based on the 36-8-36 design has been manufactured and tested in the generator and motor mode of operation. The agreement between calculated and measured machine performance characteristics is good.

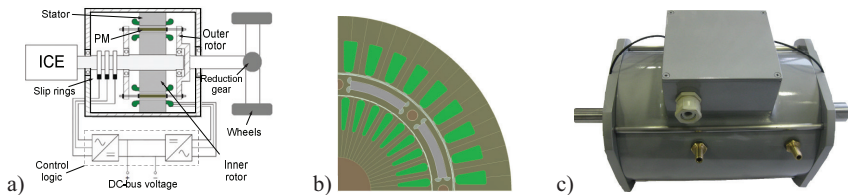


Fig.1. a) Principal layout of the DRPMSM drive b) Cross section diagram c) Assembled DRPMSM prototype

References

- [1] S. Eriksson and C. Sadarangani, "A four-quadrant HEV drive system", Proc. IEEE 56th Vehicular Technology Conf., vol. 3, pp. 1510-1514, Sept. 2002.
- [2] R. Liu, H. Zhao, P. Zheng, X. Gan, R. Zhao and B. Kou, "Experimental evaluation of a radial-radial-flux compound-structure permanent-magnet synchronous machine used for HEVs", IEEE Trans. Magn., vol.45, pp. 645-649, Jan. 2009.
- [3] M. Aubertin, A. Tounzi, and Y. Menach, "Study of an electromagnetic gearbox involving two permanent magnet synchronous machines using 3-D-FEM," IEEE Trans. Magn., vol.44, pp. 4381-4384, Nov. 2008.

Design Consideration for High Power Density and Fast Response Permanent Magnet Brushless DC Actuator

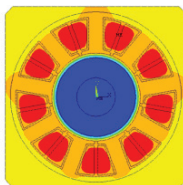
Yu Tang, Yongxiang Xu, Jibin Zou

Department of Electrical Engineering, Harbin Institute of Technology, Harbin, China

Recently the high power density and fast response permanent magnet brushless DC actuator is widely studied. The volume of actuator is limited, but the output torque of the actuator should be matched the requirement. So the design consideration for high power density permanent magnet brushless DC actuator is important for designers. In the other respects, the actuator should follow the control signal as soon as possible. So in the practical design, the high power density and fast response should be considered in the same time.

In this paper, a high power density and fast response PM brushless DC actuator is designed. The actuator volume is limited. The combination of pole number and slot number is selected to get the high power density. After the analysis, the 8-pole and 9-slot actuator is selected as the design model for the further analysis. Then the design considerations for the fast response are analyzed through FEM method. The electrical time constant and mechanical time constant are main factors for the consideration. In order to get the fast response, the actuator's rotor is designed carefully, because the rotor inertia is mainly determined by the rotor structure. Then the actuator inductance is computed through the FEM. The inductance can affect the actuator's electrical time constant. The impact of these design factors on the actuator's characters is analyzed in this paper as well. Because the power density of the actuator is high, the actuator's temperature rise should be considered carefully. So the thermal FEM analysis is carried out to ensure the design.

The model actuator is fabricated. The experiment results prove that the model actuator fulfill the design requirement. The design considerations presented in the paper are valuable for the similar design.



49.744 54.998 58.447 62.798 67.351 71.583 75.655 80.207 84.537 88.91

Thermal FEM analysis result



Experimental system

References

- [1] Chunting Chris Mi, Gordon R. Slemon, Richard Bonert: Minimization of Iron Losses of Permanent Magnet Synchronous Machines. IEEE Trans on Energy Conversion, 20 No. 1, (2005), 121-127.

Magnetic and magnetostrictive measurements of RE doped cobalt ferrite bulks and thin films

Georgiana Dascalu,¹Mihai Sergiu Stratulat,¹Ovidiu Florin Caltun,¹Cristian Focsa²

¹Faculty of Physics, Alexandru Ioan Cuza University, 700506 Iasi, Romania

²Laboratoire de Physique des Lasers, Atomes et Molécules (UMR CNRS 8523), Université Lille 1 Sciences et Technologies, 59655 Villeneuve d'Ascq cedex, France

Ferrite materials with spinel structure are of great scientific interest and technological importance in electronics and optoelectronics, in microwave industry, in fabrication of sensors because of their low cost, easily manufacturing and remarkable electric and magnetic properties. This type of ferrite also exhibits a large magnetostriction coefficient ($\lambda_s \sim 110 \cdot 10^{-6}$) [1-3] thus making it a good candidate for sensors and actuators applications.

The present study was focused on the influence of rare earth (Dy, Gd, La) addition on the magnetic and magnetostrictive properties of cobalt ferrite bulk materials and thin films deposited by Pulsed Laser Deposition (PLD). The deposition process was performed in a stainless steel vacuum chamber at a pressure of 10^{-2} mbar. For the target ablation it was used the second harmonic (532nm) of a 10 ns Nd-YAG laser with a repetition rate of 10 Hz. The energy density was $10\text{J}/\text{cm}^2$ and the target-substrate distance was kept at 2.5cm for all the samples. In every set of depositions, only the substrate temperature was varied from room temperature to 600°C .

The structural characteristics of the targets and thin films were investigated using Raman spectroscopy, X-Ray diffraction and the hysteresis loops were plotted by means of a vibrating sample magnetometer. For the bulk materials we used the strain gauge method for magnetostriction measurements. The magnetostriction coefficient of the thin films deposited on an elastic bronze strip was obtained using a homemade set-up based on the cantilever method.

In bulk materials, the addition of RE cations in the preparation process determined the formation of RE orthoferrite as a second phase and the magnetostriction curves indicated a decrease of the saturation magnetostriction coefficient and of the negative slope ($d\lambda/dH$) at low magnetic fields. The XRD diffractograms and Raman spectra for thin films indicated the formation of a single spinel phase. The shift of the [311] diffraction peak observed for RE doped cobalt ferrite thin films suggested an increase in lattice parameter due to the inclusion of cations with high ionic radii. The VSM hysteresis loops of the thin films obtained for both in-plane and out-of-plane configurations indicated an increase in coercive field as the substrate temperature was augmented and also an increase in magnetic moment when the Fe ions were substituted by RE cations with a higher magnetic moment.

References

- [1] L. M. Boutiuc, I. Dumitru, O. F. Caltun, M. Feder, V. Vilceanu, Coprecipitated Cobalt Ferrite for Sensors, *Sens. Lett.* 7 (2009) 244-246;
- [2] P. Kumar, S.K. Sharma, M. Knobel, M. Singh, Effect of La³⁺ doping on the electric, dielectric and magnetic properties of cobalt ferrite processed by co-precipitation technique, *J. Alloy. Compd.* 508 (2010) 115–118;
- [3] Lijun Zhao, Hua Yang, Xueping Zhao, Lianxiang Yu, Yuming Cui, Shouhua Feng, Magnetic properties of CoFe₂O₄ ferrite doped with rare earth ion, *Mater. Lett.* 60 (2006) 1-6;

Improved magnetostrictive properties of manganese substituted cobalt ferrite for automobile torque sensor applications

G. Dascalu¹, O. F. Caltun¹, G. S. N. Rao², B. Parvatheeswara Rao³, K. H. Rao³

¹Dept. of Physics, Al. I. Cuza University, Iasi, Romania,

²Dr. V. S. Krishna Govt. Degree College, Visakhapatnam, India

³Dept. of Physics, Andhra University, Visakhapatnam, India

Terfenol and Samfenol are widely considered as materials for applications of automobile torque sensors, but they are characterized by high magnetic anisotropy high Curie temperature, low strain derivative, brittle and thus unable to withstand substantial amount of tension. Alternately, cobalt ferrite is preferred for automobile stress or torque sensor applications due to its large values of negative magnetostriction and moderate positive anisotropy, appreciable tensile strength and good ductility besides its low cost and easy processability. In general, large strain derivative, low Curie temperature, reasonable saturation magnetization, minimum magnetomechanical hysteresis and good magnetostriction are some of the desirable characteristics for a material to work as stress or torque sensor [1]. Substituted cobalt ferrites offer the kind of flexibility to tailor the required properties for use in automotive and other torque sensing applications.

Since the strain derivative/response is the figure of merit for a material to be used in the mentioned applications, the aim of the study is to improve the magnetostrictive properties of manganese substituted cobalt ferrite. A series of samples with composition $\text{CoMn}_x\text{Fe}_{2-x}\text{O}_4$ ($x = 0.00$ to 0.60) has been prepared by conventional ceramic technique. Structural and magnetic characterizations were made using X-ray diffraction and built-in Curie temperature set-up, respectively. Magnetization measurements were made using VSM and the magnetostrictive properties were studied by tensile strain gauge method.

Manganese substituted cobalt ferrites have shown maximum strain derivative values as compared to pure cobalt ferrite which make the materials promising for magnetostrictive sensing applications. The strain derivative has been observed to increase for higher substituent concentrations in $\text{CoMn}_x\text{Fe}_{2-x}\text{O}_4$ and this behavior has been attributed to the decreased anisotropic contribution of Co^{2+} ions. The observed decrease in coercivity in $\text{CoMn}_x\text{Fe}_{2-x}\text{O}_4$ system has been attributed to the decrease in magnetocrystalline anisotropy caused by the migration of Co^{2+} ions into tetrahedral sites. The observed variations are explained on the basis of cation site occupancies and its valence states.

References

[1] I. C. Nlebedim, Y. Melikhov, I. C. Nlebedim, Y. Melikhov, J. E. Snyder, N. Ranvah, A. J. Moses, D. C. Jiles, *J. Appl. Phys.* 109, 07A908 (2011)

Deposition and Etch Technologies for High Volume Manufacturing of Magnetic Sensors

Adrian J. Devasahayam, Frank Cerio and Katrina Rook

Veeco Instruments Inc., Plainview, New York, USA

The demand for magnetic sensors is increasing exponentially driven by several emerging applications such as the automotive sector, digital compasses for smart phones and tablets, gaming and various industrial applications like non-contact position sensing, torque measurements, angle and current sensing¹. This surging demand requires low cost sensors fabricated by proven high volume manufacturing techniques. In this paper, we will describe key technologies required for deposition and etching of such sensors. We will focus on innovations uniquely required for magnetic materials such as optimized magnetron designs and substrate magnetic alignment as well as ion beam etching technologies needed for etching complex magnetic materials while maintaining critical dimensions.

Typical magnetic sensors utilize Anisotropic Magneto-Resistance (AMR), Giant Magneto-Resistance (GMR) or Tunneling Magneto-Resistance (TMR) in increasing order of sensitivity and complexity in manufacturing. Sputter deposition is typically used to deposit these materials but requires adaptation of magnetrons, substrate fixtures and other hardware components for magnetic materials. These are optimized for uniform magnetic properties of coercivity, anisotropy, $\Delta R/R$ and other properties over the full wafer size (up to 8"). Film uniformities as low as $1\%3\sigma$ are obtained. In this paper we will describe the impact of hardware design on these key film properties.

Patterning of magnetic materials presents some unique requirements. These materials are not easy to etch by standard dry etching techniques (RIE). RIE typically results in corrosive by-products which can cause down-stream device reliability issues. Additionally, chemistries suitable for etching multi-layer, multi-element stacks are not readily available and do not have the required flexibility for different magnetic materials. Ion beam etching has been the technique of choice for etching magnetic materials. We have developed unique technologies for high volume manufacturing with special emphasis on critical dimension control, large area film uniformity and low energy etching. These film parameters are directly impacted by the ion source and grid design of the etching system. We have also developed integrated secondary ion mass spectroscopy (SIMS) for end point control, which is important for accurate etch control for multi-layer film stacks. In this paper we will describe how these hardware features are essential for good device yields.

References

[1] MEMS Journal, January 2012

Mean field model for ferromagnetic nanowire arrays

Costin-Ionuț Dobrotă, Alexandru Stancu

Faculty of Physics, “Alexandru Ioan Cuza” University of Iasi, 700506, Romania

The growing scientific interest in the magnetic properties of the ferromagnetic nanowires is motivated by their potential applications in high-sensitivity magnetic sensors [1] and microwave devices [2]. The magnetic behavior of the nanowire arrays is essentially influenced not only by the hysteretic properties of individual wires, but also by the magnetic interactions between wires which depend both on their geometrical properties as well as on the array characteristics, such as shape, dimension and lattice constant.

A good choice for magnetic characterization in order to obtain valuable information about ferromagnetic entities from a system, referring to the coercive and interaction field distributions, is the first-order reversal curves (FORC) method [3]. The Preisach model provides the connection between these distributions and the FORC diagram revealed in experiments, but more sophisticated Preisach-type models must be used to describe complex FORC distributions obtained for ferromagnetic nanowire arrays.

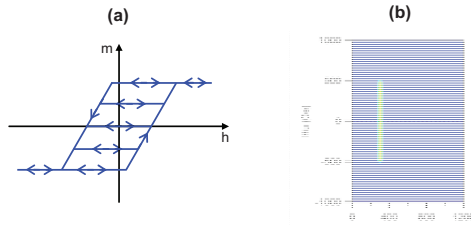


Figure (a) PKP symmetrical hysteron, (b) FORC diagram of the PKP symmetrical hysteron

In this paper, we present a model based on Preisach-Krasnosels’kii-Pokrovskii (PKP) symmetrical hysterons [4] which is able to describe, in a simple manner, specific FORC distributions for nanowire arrays. As a general characteristic of ferromagnetic nanowire arrays, if the applied field is along the wires, their FORC diagrams have a specific shape consisting of a narrow distribution of coercive fields and a wide and flattened distribution of interaction fields with steep extremities, denoting the presence of the mean interaction field in the system (see Figure). Different local interaction mean fields are responsible for these FORC distributions and we can obtain these distributions if we take into account lower interaction fields acting on the peripheral wires from the array.

Acknowledgement

This work was partially supported by the European Social Fund in Romania, under the responsibility of the Managing Authority for the Sectorial Operational Programme for Human Resources Development 2007-2013 [grant POSDRU/88/1.5/S/47646].

References

- [1] P. D. McGary *et al.*, *J. Appl. Phys.*, vol. 99, p. 08B310, 2006.
- [2] B. K. Kuan *et al.*, *Appl. Phys. Lett.*, vol. 94, pp. 202505, 2009.
- [3] I. D. Mayergoyz, *Mathematical Models of Hysteresis and Their Applications*, Elsevier, Amsterdam/Boston, 2003.
- [4] R. V. Iyer, X. Tan, *IEEE Contr. Syst. Mag.*, vol. 29, pp. 83-99, 2009.

Metamaterials sensor for electromagnetic nondestructive evaluation

A.Savin¹, D.Faktorová², R.Steigmann¹, R.Grimberg¹

¹National Institute of Research and Development for Technical Physics, Iasi, ROMANIA

²University of Žilina, Slovak Republic

The development of the modern science and technology imposes the use of new materials with especially properties and in the same time, the use of the materials already known in extreme conditions. In all these cases, a rigorous quality control is imposed, both during their processing as well as during the in-service inspection. In the case in which the material is conductive or it is a composite material reinforced with conductive fibers, the electromagnetic nondestructive evaluation procedures are itself recommended.

In these systems, an electromagnetic field, usually generated, function on frequency, by the coils circulated by alternative currents or antennas, will action over the object to be controlled. The reception is done with the same circuit elements. Because the distances between the emission part, the object to be controlled and the reception part are small, comparable with the wavelength of the incident field, the system functions in near field, its specific being the existence of evanescent waves, waves with extremely rapid dumping reported to distance. The evanescent waves are carrier of information which allows the obtaining of special spatial resolution, fact used nowadays, in Scanning Near Field Optical Microscopy (SNFOM). In the range of radiofrequency and microwaves, in order to handle the evanescent waves, electromagnetic metamaterials can be used [1] and circuit elements - metamaterials lens type.

In this paper is presented the performances of a new electromagnetic sensor [2], [3] at the nondestructive evaluation of different types of materials as carbon fiber reinforced plastics, steels in order to detect hydrogen delayed cracks specific to the oil industry, metallic strips grating in printed circuits boards. In all situations, a spatial resolution superior than of the classical detection methods.



Figure 1. Macrograph (200X) of a region with crack. The opening of the crack is in the micrometer range.

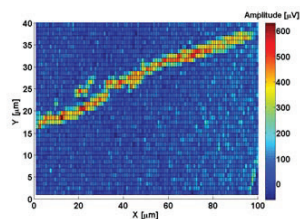


Figure 2. The signal delivered by the transducer (amplitude) at the scanning of 100x40 μm² region containing a crack.

References

- [1] J.B.Pendry, D.Schurig, D.R Smith:. Controlling Electromagnetic Fields, *Science*, 312, (2006), 1780-1782
- [2] R. Grimberg, A. Savin, R. Steigmann, Electromagnetic imaging using evanescent waves, *NDT and E International*, 46, (2012), 70-76
- [3] R.Grimberg, G.Y.Tian, High Frequency Electromagnetic Non-destructive Evaluation for High Spatial Resolution using Metamaterial, *Proceedings of Royal Society A*, in Press 2012

Anisotropy Field in Ni Nanostripe Arrays

Flores A. G.¹, Raposo V.¹, Iñiguez J.¹, Zazo M.¹, Redondo C.², Navas D²

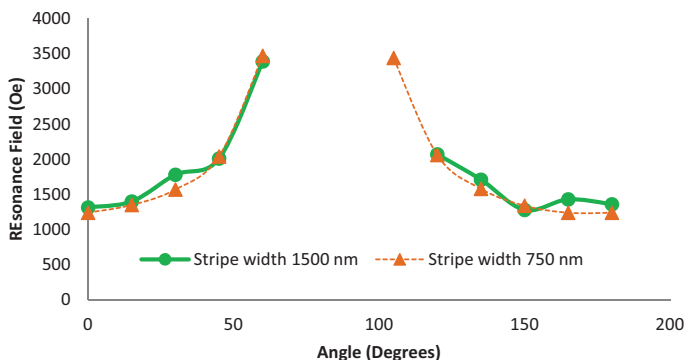
¹ Departamento de Física Aplicada, Universidad de Salamanca, E-37071, Salamanca, España

² Departamento de Química Física, Universidad del País Vasco, Barrio Sarriena s/n, 48940 Lejona (Vizcaya), Spain

Nanostructures of periodic arrays have recently been intensively studied due to their singular magnetic properties and their potential application in high density perpendicular recording media, magnetic sensors or microwave devices. In nanostripe arrays, the coupling mechanism between wires has an important effect in the reversal mechanism of the magnetization and its knowledge could be useful in tuning the magnetic properties of the system. To understand magnetization processes in these materials it should be considered the intergrain exchange coupling, magnetic dipolar interactions and the anisotropy fields. The anisotropies fields of nanostripe arrays can be investigated by various techniques. One of these techniques is the ferromagnetic resonance spectroscopy due to the fact that the resonance field depends directly on the anisotropy field strength and its angular spread. In order to understand the dynamic phenomena in these samples nanostripe arrays of Ni have been prepared by interference lithography. The film thickness is of 45 nm for a lattice period of 2.7 μm and the stripe width of:



Ferromagnetic resonance measurements have been carried out at a frequency of 9.54 GHz as a function of H . The sample was placed in a rectangular cavity in such a position that the angle between the applied field H and the film plane can be adjusted from 0° to 180° . The spectra show several absorption lines. The angular dependence of the resonance field are shown in the following Figure:



As it can be seen, the resonance field of the absorption peak increases upon changing the angle from parallel (0°) to perpendicular (90°) to the film plane. This behaviour can be explained by the relation between resonance field, frequency and anisotropy field determined by demagnetizing factors and magnetization angle respect to the sample easy axis direction after energy minimization.

Dependence of Ferromagnetic Resonance Field with Diameter Sample in Permalloy Nanodot Arrays

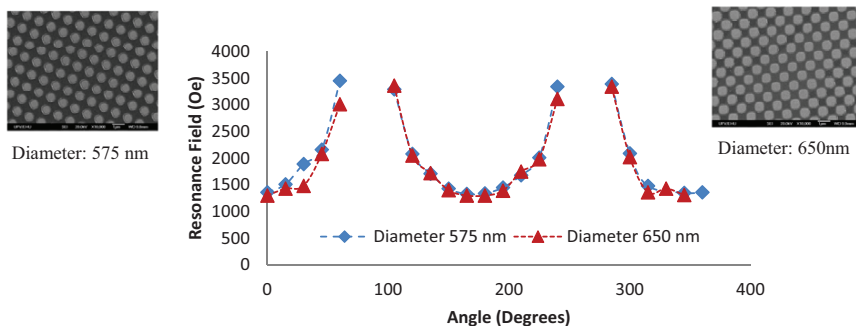
Flores A. G.¹, Raposo V.¹, Iñiguez J.¹, Zazo M.¹, Redondo C.², Navas D.²

¹ Departamento de Física Aplicada, Universidad de Salamanca, E-37071, Salamanca, España

² Departamento de Química Física, Universidad del País Vasco, Barrio Sarriena s/n 48940 Leioa – Bizkaia

Dynamic properties of magnetic nanostructures have recently been intensively studied due to their potential application in high density perpendicular recording media, magnetic sensors or microwave devices. To understand magnetization processes in these materials it should be considered the intergrain exchange coupling, magnetic dipolar interactions and the anisotropy fields. The anisotropies fields can be investigated by various techniques. One of these techniques is the ferromagnetic resonance spectroscopy due to the fact that the resonance field depends directly on the anisotropy field strength and its angular spread. In order to understand the dynamic phenomena in these samples dot arrays of Permalloy have been prepared using interference lithography. The film thickness is of 50 nm for a lattice period of 1 μm and the dot diameters of 575 nm and 650 nm.

Ferromagnetic resonance measurements have been carried out at a frequency of 9.54 GHz as a function of H. The sample was placed in a rectangular cavity in such a position that the angle between the applied field H and the film plane can be adjusted from 0° to 180°. The spectra show several absorption lines. The angular dependence of the resonance field are shown in the following Figure:



As it can be seen, the resonance field of the absorption peak increases upon changing the angle from parallel (0°) to perpendicular (90°) to the film plane. This behaviour can be explained by the relation between resonance field, frequency and anisotropy field determined by demagnetizing factors and magnetization angle respect to the sample easy axis direction after energy minimization.

Fabrication and Properties of CoFe_2O_4 -PZT Magnetoelectric Thin Films

GIOUROUDI Ioanna¹, ALNASSAR Mohammed², GRÖSSINGER Roland³, KOSEL Jürgen²

¹Institute of Sensor and Actuator Systems, Vienna University of Technology, Vienna, Austria

²Division of Physical Sciences and Engineering, King Abdullah University of Science and Technology, Thuwal, Kingdom of Saudi Arabia

³Institute of Solid State Physics, Vienna University of Technology, Vienna, Austria

Magnetoelectric (ME) thin film materials have great potential for application in microdevices such as sensors and actuators, high density information storage devices, transducers for magnetic-electric energy conversion and energy harvesting modules. By combining piezoelectric and magnetostrictive thin films, the potentialities of these materials increase. In this paper, double-layer magnetoelectric CoFe_2O_4 (CFO)/ $\text{PbZr}_{0.52}\text{Ti}_{0.48}\text{O}_3$ (PZT) thin films were prepared on Si (100) substrates via pulsed laser deposition (PLD). Their thickness was analyzed using Atomic Force Microscopy (AFM) and their phase structure was characterized by X-ray Diffraction (XRD). The morphologies of the films were examined by scanning electron microscopy (SEM). The double-layer thin films exhibit both good ferromagnetic and piezoelectric properties. A piezoelectric evaluation system, aixPES, with TF2000E analyzer component was used for the electric hysteresis measurements of the thin films and a vibrating sample magnetometer (VSM) was employed to characterize their magnetic properties. The magnetization dependence on the magnetic field was measured at room temperature by applying a magnetic field up to 12 kOe. The coercivity of the composite was about 1kOe. The coexistence of the ferroelectric PZT and ferromagnetic CFO phases in the composite thin films generates an ME effect, which is studied in detail and representative results will be shown and discussed.

Structural studies, low field magnetic properties and application of amorphous FeCoMoCuB alloys

Mariusz HASIAK¹, Marcel MIGLIERINI^{2,3}, Mirosław ŁUKIEWSKI⁴, Jerzy KALETA¹

¹Institute of Materials Science and Applied Mechanics, Wrocław University of Technology, Wrocław, Poland

²INPE, Slovak University of Technology, Bratislava, Slovakia

³RCPTM, Palacky University, Olomouc, Czech Republic

⁴ELHAND Transformatory, Lubliniec, Poland

Amorphous FeCo-based alloys are very interesting because present good soft magnetic properties at higher temperatures. The unique combination of soft magnetic properties offers opportunities to apply these alloys in electrical industry.

In this paper we present the results of microstructure and magnetic properties investigations as well as design and production process of chokes core switch mode power supply made from $(\text{Fe}_x\text{Co}_y)_76\text{Mo}_8\text{Cu}_1\text{B}_{15}$ alloys ($x/y = 1, 3, 6$ and 9). The samples in form of thin ribbons 5 mm width and about 20 μm thick were obtained by rapid quenching method on a single roller. The room temperature examination of microstructure of the as-quenched samples was performed by several methods such as Mössbauer spectroscopy, X-ray diffractometry as well as Atomic Force Microscopy (AFM) and Lateral Force Microscopy (LFM). From the obtained results we can conclude that all investigated samples in the as-quenched state were fully amorphous. Moreover, the beginning of crystallization and peak of primary crystallization temperature for the sample with Fe/Co ratio $x/y = 1/1$ are of 695 K and 719 K, respectively [1]. Our analysis of $(\text{Fe}_x\text{Co}_y)_76\text{Mo}_8\text{Cu}_1\text{B}_{15}$ alloys ($x/y = 1, 3, 6$ and 9) alloys extends the recent studies on the FeCoMoCuB system [2, 3].

The investigation of magnetic characteristics was focused on choosing optimal initial parameters for simulation process of parameters for chokes core. Full procedure describing the design of chokes for switch mode power supply allows to understand this process in detail. The results obtained from numerical analysis of choke core such as core losses and temperature, winding losses were compared with the same parameters obtained for commercial materials such as FINEMET, METGLASS and Fe-3.2% Si alloys.

Analysis of the magnetic properties of $(\text{Fe}_x\text{Co}_y)_76\text{Mo}_8\text{Cu}_1\text{B}_{15}$ alloys ($x/y = 1, 3, 6$ and 9) alloys shows that the investigated alloys can be applied in electrical industry as highly sensitive device.

This work was partially supported by the grants SK-PL-0013-09, VEGA 1/0286/12, and CZ.1.05/2.1.00/03.0058.

References:

- [1] I. Škorvánek, J. Marcin, J. Turcanová, J. Kováč, P. Švec, FeCo-based soft magnetic nanocrystalline alloys, *Acta Electrotechnica et Informatica*, **10** (3), 14-18 (2010).
- [2] C.F. Conde, J.S. Blázquez, V. Franco, A. Conde, P. Švec, D. Janičkovič, Microstructure and magnetic properties of FeMoBCu alloys: Influence of B content, *Acta Materialia* **55**, 5675-5683 (2007).
- [3] M. Hasiak, M. Miglierini, M. Łukiewski, J. Kaleta, Microstructure, magnetic properties, and applications of Co-rich HITPERM-type amorphous alloys, **48** (4) 1665-1668 (2012).

Microstructure and magnetic properties of amorphous FeCo-based alloys with different Fe/Co ratio

Mariusz HASIAK¹, Marcel MIGLIERINI^{2,3}, Agnieszka ŁUKIEWSKA⁴,
Józef ZBROSZCZYK⁴, Jerzy KALETA¹

¹Institute of Materials Science and Applied Mechanics, Wrocław University of Technology,
Wrocław, Poland

²INPE, Slovak University of Technology, Bratislava, Slovakia

³RCPTM, Palacky University, Olomouc, Czech Republic

⁴Institute of Physics, Częstochowa University of Technology, Częstochowa, Poland

Amorphous FeCuNbSiB (FINEMET) and Fe(Zr,Hf,Nb)BCu (NANOPERM) magnetic materials are very interesting because of their excellent soft magnetic properties. The role of small addition of Mo, Nb, Hf, Mn, and Ti on microstructure and magnetic properties has been reported in several papers, e.g. [1]. Partial replacement of Fe atoms by Co atoms in NANOPERM-type alloys leads to changes in the structures and increase of magnetic inductions at elevated temperatures [2, 3]. The aim of this paper is to study structural changes and low field magnetic properties of amorphous $(\text{Fe}_1\text{Co}_x)_{76}\text{Mo}_8\text{Cu}_1\text{B}_{15}$ alloys ($x = 1, 2$ and 3). All samples were produced by rapid quenching on a single roller in a form of thin ribbons. The amorphicity of the alloys was checked at room temperature by X-ray diffractometry and Mössbauer spectroscopy in transmission geometry. Magnetic characterization of amorphous $(\text{Fe}_1\text{Co}_x)_{76}\text{Mo}_8\text{Cu}_1\text{B}_{15}$ alloys ($x = 1, 2$ and 3) was done by investigations of magnetic after-effect, initial magnetic susceptibility, as well as tangent losses. The magnetic after-effect was investigated by decomposition of isochronal disaccommodation curves, which were constructed according to the formula:

$$\Delta(1/\chi) = 1/\chi_2 - 1/\chi_1 = f(T)$$

where: χ_1 and χ_2 are susceptibilities at times $t_1 = 2$ s and $t_2 = 120$ s after demagnetization.

Using the lognormal distributions of relaxation times, the values of activation energies and pre-exponential factor in Arrhenius law were calculated. Moreover, the analysis of $\Delta(1/\chi) = f(H)$ versus magnetic field amplitude also was accomplished.

This work was partially supported by the grants SK-PL-0013-09, VEGA 1/0286/12, and CZ.1.05/2.1.00/03.0058.

References:

- [1] I. Škorvánek, J. Marcin, J. Turcanová, J. Kovác, P. Švec, FeCo-based soft magnetic nanocrystalline alloys, *Acta Electrotechnica et Informatica*, **10** (3), 14-18 (2010).
- [2] C.F. Conde, J.M. Borego, J.S. Blázquez, A. Conde, P. Švec, D. Janičkovič, Magnetic and structural characterization of Mo-Hitperm alloys with different Fe/Co ratio, *J Alloys and Compounds*, **509** 1994-2000 (2011)
- [3] M.A. Willard, D.E. Laughlin, M.E. McHenry, D. Thoma, K. Sickafus, J.O. Cross, V.G. Harris, Structure and magnetic properties of $(\text{Fe}_{0.5}\text{Co}_{0.5})_{88}\text{Zr}_7\text{B}_4\text{Cu}_1$ nanocrystalline alloys, *Journal of Applied Physics*, **84**, 6773-6777 (1998).

Polycrystalline Fe-Ga Melt-Spun Ribbons for Energy Harvesting Devices

N. Lupu¹, I. Škorvánek², M. Grigoras¹, M. Tibu¹, J. Marcin², and H. Chiriac¹

¹National Institute of Research and Development for Technical Physics, Iasi, Romania

²Institute of Experimental Physics, Slovak Academy of Sciences, Košice, Slovak Republic

The recent studies shown that the subsequent magnetic field annealing can induce anisotropies along the external field direction, influencing the magnetostriction and magnetoelastic coupling values of bcc Fe-Ga alloys [1,2].

In this work, we studied the effect of the longitudinal ($H_{app} = 1.2$ T) (LF) and transversal ($H_{app} = 0.6$ T) (TF) magnetic field annealing ($T_{an} = 500^{\circ}\text{C}$; $t_{an} = 1$ h) on magnetic and magnetoelastic properties (saturation magnetostriction and magnetoelastic coupling coefficient) of polycrystalline $\text{Fe}_{100-x}\text{Ga}_x$ ($x = 19.5$ and 22.5) melt-spun ribbons with thicknesses of $20\ \mu\text{m}$ and width of 2-3 mm prepared by rapid quenching to be used for energy harvesting devices (EHD).

All melt-spun ribbons were found to be polycrystalline in the as-quenched state and their structure consists of a mixture of disordered bcc (A2 phase) and ordered fcc Fe_3Ga (β phase). The magnetic easy axis of the as-quenched ribbons is oriented in-plane and along the ribbons long axis. The anisotropy field decreases from 2.2 T in the as-quenched state to 1.5 T and 1.2 T for magnetic field annealed $\text{Fe}_{80.5}\text{Ga}_{19.5}$ and $\text{Fe}_{77.5}\text{Ga}_{22.5}$ melt-spun ribbons, respectively, almost independent of the applied field direction. However, the MOKE measurements indicate butterfly-shaped hysteresis maps for transversal magnetic field annealing and translated hysteresis loops over y axis with 2 maxima that are approximately equal for longitudinal magnetic field annealed ribbons. Such a specific behavior confirms the presence of A2 and β phases with the easy axis oriented in different directions depending on the direction of the annealing magnetic field.

Magnetostriction increases with the increase of the Ga content, but the most significant increase is obtained for the transversal magnetic field annealed ribbons. Additionally, the increase is even more significant for magnetic field annealed samples containing 22.5 at.% Ga, due to the larger amount of ordered fcc Fe_3Ga phase. The variation of the magnetostriction with the applied stress is significantly diminished after magnetic annealing, as one can see from the slope of the $\lambda(\sigma)$. This behavior is strongly related to the existence of the internal stresses which are the main source of anisotropy, via magnetoelastic coupling, in the as-quenched state, which by magnetic annealing are released. The magnetoelastic coupling coefficient in the as-quenched state is ranging from 0.13 to 0.35, and increases up to 0.75 by applying proper treatments to release the internal stresses. All these aspects will be discussed in connection with the microstructure and magnetic domains structure developed in the melt-spun ribbons before and after magnetic field annealing.

This work was supported by the Bilateral Collaboration Programme Romania-Slovakia (2011-2012).

References

- [1] J.-H. Yoo, J.B. Restorff, M. Wun-Fogle, and A.B. Flatau, J. Appl. Phys. 103 (2008) 07B325.
- [2] J.-H. Yoo, S.-M. Na, J.B. Restorff, M. Wun-Fogle, and A.B. Flatau, IEEE T. Magn. 45 (2009) 4145.

Optical and Magneto-Optical Properties of Ion Implanted $(\text{YBiCa})_3(\text{FeGeSi})_5\text{O}_{12}$ Garnet Films

Kalandadze Lali

Department of Physics, Shota Rustaveli State University, Batumi 6010, Georgia

We have investigated the optical and magneto-optical properties of the ion implanted $(\text{YBiCa})_3(\text{FeGeSi})_5\text{O}_{12}$ garnet films. It has shown that ion implantation influences significantly the magneto-optical properties of the garnet films and practically does not change its optical characteristics. The research of magnetization processes of implanted films showed that implantation leads to a significant inhibition of the growth of anisotropy. The latter is expressed in the decrease of the amount of saturation fields in-plane films. In the proceeding, we have researched the magneto-optical properties of ion implanted $(\text{YBiCa})_3(\text{FeGeSi})_5\text{O}_{12}$ garnet films after it was annealed at 270°C . This kind of the experiment is particularly interesting in the matter of annealing process as it reduces the implantation defects and restores crystalline structure of ferrite garnet [1, 2]. We have also determined the spectral dependences of the component of the tensor of dielectric permittivity for the surface of the ferrite-garnet films before and after implantation process. These calculations let us evaluate the influence of implantation on an electronic energy structure of the surface layer for the sample.

References

- [1] P. Gerard and M. T. Delay: Ion implantation profiles in bubble garnets. *Thin Solid Films*, vol.88, No. 1, (1982), 75-79
- [2] L. Kalandadze: Influence of Implantation on the Magneto-Optical Properties of garnet surface. *IEEE Trans. on Magnetics*, vol. 44, No. 11, (2008), 3293-3295

Magnetic and magneto-volume properties of Co-doped off-stoichiometric Ni₂MnGa

KAŠTIL Jiří¹, Fabbri Simone², Kamarád Jiří¹, Albertini Franca², Arnold Zdeněk¹

¹Institute of Physics ASCR, v.v.i., Prague 8, Czech Republic

²Institute of Materials for Electronics and Magnetism, IMEM-CNR, Parma, Italy

Ni₂MnGa compound belongs to family of ferromagnetic shape memory materials (FSMM). It shows the huge shape memory effect (SME) that is based on the very sharp first order structural transition from the high temperature cubic austenite (A) to the low temperature tetragonal martensite (M). The Co-doped off-stoichiometric (NiCo)₂MnGa Heusler compound exhibit the martensitic transition even to orthorhombic or monoclinic martensite phase. Moreover, the structural martensitic transformation between austenite and martensite is accompanied by a great change of their magnetization. This advantage of FSMM can be used to induce great output strain after application of the magnetic field. By proper doping and stoichiometry of the compounds, the so called metamagnetic shape memory effect (MMSME) can be induced in the off-stoichiometric alloys that are also suggested candidates for application in magnetic cooling technique at room temperature [1-3].

We have studied the polycrystalline Co-doped Mn-rich Ni_{50-x}Co_xMn_{25+y}Ga_{25-y} ($x = 5, 7$ and 9 , $y = 5, 6, 7$ and 8) alloys [1,3]. Positive magnetization jump (ΔM) has been observed at the M-A transitions in all compounds with $x \geq 5$. The ΔM jumps are accompanied by changes of volume ($\Delta V/V$) that increase with increasing content of Co in the compounds [1]. Magnetic field dependence of the magnetization was measured in field up to 14 T and the significant shift of the transition temperature of about -3 K/T was evaluated. With respect to pronounced magneto-volume effects in the studied compounds [2], their magnetization and thermal expansion were measured in pressure range up to 1.2 GPa. The shift of the martensitic transformation temperature of about +30 K/GPa was observed. The isothermal entropy change that accompanies the field induced martensitic transition was calculated from the magnetization measurement and the inverse magnetocaloric effect has been confirmed.

An application potential of the received results will be discussed in the contribution.

References:

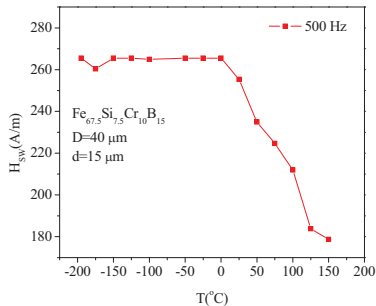
- [1] F. Albertini et al., *Materials Science Forum*, **684** (2011) 151-163
- [2] J. Kamarád et al., *J. Magn. Magn. Mats.* **290-291** (2005) 669-672
- [3] S. Fabbri et al., *Acta Mater.* **59** (2011) 412-419.

Temperature dependence of the switching field in $\text{Fe}_{67.5}\text{Si}_{7.5}\text{B}_{15}\text{Cr}_{10}$ microwire

P. Klein¹, K. Richter¹, R. Varga¹, and M. Vázquez²

¹Institute of Physics, Faculty of Sciences, P. J. Safarik University, Park Angelinum 9, 041 54 Kosice, Slovakia

²Instituto de Ciencia de Materiales de Madrid, CSIC, 28049 Madrid, Spain



Glass-coated microwires are composite materials, which consist of metallic core (100 nm-20 μm) covered by Pyrex-like glass coating (2-20 μm) [1]. They are prepared by modified Taylor-Ulitovsky method by simultaneously quenching and drawing of molten master alloy. The main anisotropies, which determine domain structure of microwire are magnetoelastic and shape anisotropy. The positive magnetostrictive microwire are characterized by a magnetic bistability (only two states of magnetization are allowed in the internal axial monodomain: $+M_S$ and $-M_S$) and magnetization process runs through the single large Barkhausen jump when the external field exceeds the so-called switching field H_{sw} . Such bistability can be used in many applications like magnetic coding, sensors of magnetic field, mechanical stress, temperature [2] etc.

The aim of this paper is to present a study of the temperature dependence of the switching field in amorphous $\text{Fe}_{67.5}\text{Si}_{7.5}\text{B}_{15}\text{Cr}_{10}$ microwire. The chromium has been added to stabilize the amorphous structure and also to reduce Curie temperature [3]. In this way we obtain material in which switching field changes steeply in the working temperature range from 0 °C up to 150 °C.

Support by the project NanoCEXmat Nr. ITMS 26220120019, Slovak grant APVV-0266-10 and VEGA grant No.1/0076/09 is acknowledged.

References

- [1] M. Vázquez, Handbook of Magnetism and Advanced Magnetic Materials: Advanced Magnetic Microwires, Vol. 4, (2007), 2193-2227.
- [2] P. Klein, R. Varga, G. A. Badini-Confalonieri, and M. Vázquez, J. Magn. Magn. Mater. 323 (2011), 3265-3270.
- [3] R. Varga, P. Vojtanik, J. Kovac, P. Agudo, M. Vázquez, and A. Lovas: Influence of Cr on magnetic and structural properties of amorphous $\text{Fe}_{80-x}\text{Cr}_x\text{Si}_6\text{B}_{14}$ ($x=0-14$) alloys, Acta Phys. Slovaca 49 No. 5, (1999), 901-904.

Effect of strontium ferrite on physical-mechanical and magnetic properties of rubber composites

Ján Kruželák¹, Rastislav Dosoudil², Ivan Hudec¹, Denisa Bellušová³

¹ Department of Plastics and Rubber, Faculty of Chemical and Food Technology, Slovak University of Technology, Bratislava, Slovakia

² Department of Electromagnetic Theory, Faculty of Electrical Engineering and Information Technology, Slovak University of Technology, Bratislava, Slovakia

³ Deutsches Institut für Kautschuktechnologie e.V., Hannover, Germany

In the recent years a rapid interest in smart materials consisting of elastomeric matrix and magnetically polarizable particles has been shown [1-2]. The advantage of elastomeric magnetic composites is that their properties can be modified for the requirements of specific applications. Because of their elasticity and easy mouldability there are suitable for additive devices, where elasticity and flexibility are additional and important parameters. Moreover, they have very good magnetic properties. During the vulcanization, magnetic particles in the rubber matrix are oriented to the direction of applied external magnetic field. In dependence on the concentration of magnetic filler or applied magnetic field, the chain-like structure of magnetic particles may vary in wide range. Particles anisotropy affects magnetic as well as mechanical properties of prepared composites.

The aim of the present work was to investigate the influence of strontium ferrite content on the properties of elastomeric composites based on natural and butadiene rubber. The observation of external magnetic field influence on the orientation of ferrite particles inside the rubber matrix was considered. The results demonstrate that the presence of magnetic filler in the rubber matrix leads to the improvement of physical-mechanical properties of prepared composites, especially in case of butadiene rubber based composites. Magnetic characteristics of both types of composites show significant increasing tendency with increasing of magnetic filler content. Magnetization during the vulcanization leads to the formation of the columnar structure of ferrite particles within the rubber matrix.

References

- [1] M. Matsumoto, Y. Miyata: Polymer absorbers containing magnetic particles: effect of polymer permittivity on wave absorption in the quasi-microwave band. *J. Appl. Phys.* 91 No. 12, (2002), 9635.
- [2] G. Diguët, E. Beaugnon, J.Y. Cavaillé: Shape effect in the magnetostriction of ferromagnetic composite. *J. Magn. Magn. Mater.* 322 No. 6, (2010), 3337-3341.

Synthesis and characterization of Co based ferrite nanocomposites

NICA Valentin¹, Gherca Daniel², Brinza Florin¹, Pui Aurel²

¹Department of Physics, Alexandru Ioan Cuza University of Iasi, Iasi, Romania

²Department of Chemistry, Alexandru Ioan Cuza University of Iasi, Iasi, Romania

Spinel-type transition-metal ferrites have attracted an increasing interest because of their wide area of technological applications in energy conversion and storage, magnetic recording, gas sensing, magnetomechanical stress and torque sensors, catalysis, and biotechnology [1,2]. In the present work we reports the synthesis of CoFe_2O_4 and transition-metal substituted ferrite by a co-precipitation method, using metal chlorures as precursors and natural polymer solution as surfactant. The polymer solution used as capping agent provides an alternative process for a nontoxic, simple, environmental and economical synthesis of nanocrystalline ferrites powders.

The annealed samples were characterized by powder X-ray diffraction (XRD), Fourier Transform infrared spectroscopy (FT-IR), scanning electron microscopy (SEM). Thermo-magnetic and sensing measurements were obtained by using a vibrating sample magnetometer (VSM) and lab-made devices, respectively.

Lattice parameters, average crystallite size of particles, microstrain and cation distribution among to the octahedral and tetrahedral sites of the ferrite lattice have been evaluated by Rietveld refinement of the diffraction data. Gas sensitivity and magnetostriction results have been evaluated for the purpose of multifunctional applications.

As the synthesis method plays an important role to the material characteristics, the effects of microstructural modifications on the magnetic and sensing properties of the samples have been investigated for suitable sensor applications.

Acknowledgment

This work was supported by Grant POSDRU/89/1.5/S/49944.

References

[1] J. A. Paulsen, A. P. Ring, C. C. H. Lo, J. E. Snyder, D. C. Jiles, J. Appl. Phys. No. 97 (2005) 44502.

CORE LOSSES AND PERMEABILITY OF THE COMPACTED NiFe AND NiFeMo ALLOYS IN AC AND DC MAGNETIC FIELDS

D. Olekšáková¹, P. Kollár², J. Füzér², S. Roth³

¹ Department of Applied Mathematics and Informatics, Faculty of Mechanical Engineering, Technical University in Kosice, Kosice, Slovakia

² Institute of Physics, Faculty of Science, P. J. Safarik University, Kosice, Slovakia

³ IFW Dresden, Dresden, Germany

NiFe alloys are commonly used as soft magnetic materials, exhibiting high permeability, low coercivity, low magnetostriction and high saturation magnetization. In particular, NiFeMo alloys have very high permeability and relatively low eddy current losses.

The aim of this work was to investigate the ac and dc magnetic properties of bulk soft magnetic materials prepared by the hot compaction:

1. of the small pieces of the NiFe ribbon and powder obtained by the mechanical milling of the ribbon NiFe.
2. of the powder obtained by the mechanical milling of the swarfs NiFeMo.

The samples were consolidated at 800 MPa for 5 min at 500 °C into discs with diameter of 10 mm and height of approx. 2.5 mm.

The dc hysteresis loops and magnetization curves were measured by a fluxmeter based hysteresisgraph. The dc permeability vs. magnetic field was calculated from magnetization curves. The ac hysteresis loops at maximum flux density of 0.2 T in the frequency range 0.5 Hz-50 Hz were measured by a fluxmeter based hysteresisgraph. Complex permeability spectra were measured with an impedance analyzer from 100 Hz to 40 MHz.

From the investigation of magnetic properties of compacted materials we found that:

1. The best value of permeability and hysteresis losses exhibits the samples consisting of the largest particle due to the largest distance mobility of domain walls.
2. The frequency dependence of core losses in frequency range from dc to 50 Hz exhibits the presence of all three components of core losses: the hysteresis losses, eddy current losses and anomalous losses.
3. The resulting magnetic properties strongly depend on the powder particle size, porosity, specific electrical resistivity.

The Laws of Bulk Elasticity in Physical Processes of Effect of Parameters (T-H-P) in Metals, Semiconductors, Magnetodielectrics

Peter I. Polyakov

Inst. For Phys. of Mining Processes, Donetsk, 83114, Ukraine

The work deals with the analysis of results of investigations of combined compositions in physical processes affected by the temperature (T), magnetic field (H) and pressure (P), (P-T-H). The use of three parameters when studying single-crystal magnetodielectrics [1, 2], semicrystal magnetic semiconductors [1], metals [3] established identity of the parameter effect on resistivity, magnetism, resonance properties. This is an evidence of important role of the mechanisms of elastic stresses in physical processes. Those are that form the basis of the structure evolution and, as a consequence, the properties of phase transitions. We should note that at wide variety of models, physical processes and the present mechanisms of elastic stresses have not been analyzed.

Substituting the hypothesis of disturbances with the regularities of elastic stresses, we should take into account that structure formation is determined by atom locations in the lattice at high-temperature physical and chemical reactions. The succeeding experimental analysis of the physical processes under T-H-P effect is connected with the methods of search for the energy of the influence, that controls the mechanisms of inner evolution of the structure as well as phase transitions and properties.

Using ideas about conductivity said by Sommerfeld and Kapitsa [3], where both classical and quantum mechanic interpretations depict the mechanisms of the relation between electron mobility and lattice atoms, the discrepancy between the measurements of conductivity and quantum mechanic model was established. In my opinion, the suggested hypothesis of the introduced parameters of disturbances is the most applicable with respect to additivity of the T-H-P parameter influence on the model of elastic stresses.

The area of the studied structure formed at the rate of stresses of the physical process changes structural stresses and homogeneous character of elasticity due to the total effect of T, H, P. When separating linearity in resistivity, magnetic resistivity, magnetostriction, magnetization, barorestivity, and emphasizing the role of elastic stresses, we should note that compressibility coefficients vary within the range of $10^{-2} - 10^{-8}$. The energy of interactions binding atoms and ions at lattice sites can be presented as [5].

A - Exchange energy – 1-10 eV. **B** - Energy of bond with crystal structure 0,1-1 eV. **C** - Spin-orbital energy $10^{-2}-10^{-1}$ eV. **D** - Magneticspin-spin bonds 10^{-4} eV. **E** - Electron-nuclear interactions $10^{-5}-10^{-6}$ eV. **F** - Energy of elastic deformations within the range of 1-200 GPa or 0,1-20 eV [2]. It should be noted that both pure and bounded structures retain the regularities of linear elasticity.

References

- [1] Polyakov P.I., Kucherenko S.S., 2002 *JMMM*, **248** 396; 2004 *JMMM*, **278** 138.
- [2] Polyakov P.I., Ryumshyna T.A. 2009 *Magnetism and Laws of Bulk Elasticity*. (Kerala. India. TransWorld Research Network.) 196pp.
- [3] Kapitsa P.L., 1988 *Strong magnetic fields, Sci. Works*. (Moscow, Science.)
- [4] D.C. Mattis, 1965 *The Theory of Magnetism* (Harper and Row, New York, Evanston and London) 365pp.

Particulate Fe-Al Thin Films Oxidized Selectively for GHz Frequency Applications

Pyungwoo JANG and Seungchan SHIN

College of Science and Engineering, Cheongju University, Cheongju 360-764, Korea

Iron based alloy films are widely used as thin film inductors and sensors. In order to be used at GHz frequency the films should overcome some problems concerning eddy current. The most effective solutions are thought to be high resistivity and lower dimension of the materials. In this paper new method for reducing the dimension of Fe-Al thin films by selective oxidation was introduced, so that the permeability of the oxidized thin films persisted up to 10 GHz. Results on selective oxidation of Al in bulk Fe-Al alloys were firstly published by Grace [1]. However, no result has been published on the phenomenon of selective oxidation of Al in Fe-Al film. In this study 200 nm Fe-Al thin films were rf-sputtered on 100 nm SiO₂ substrates from Fe-5at.% Al alloy target at room temperature. The films were oxidized at 900°C for 10-200 min in damp hydrogen atmosphere with a dew point of -17°C. The oxidized films were analyzed by SEM, TEM, XPS, XRD, AFM and VSM. In an early stage of the oxidation, the films became cleaved and then changed to particles with increasing time. After oxidation for 200 min, the continuous films were changed to particulates on the SiO₂ substrate as shown in Fig. 1. Disconnected white parts were Fe-Al alloy particles, the Fe content of which became higher than that of as-sputtered film as confirmed by EDS and VSM. The schematic diagram of Fe-Al films oxidized selectively is shown in Fig. 2, in which Fe-Al particles are surrounded by Al₂O₃ films as confirmed by EDS and TEM. Due to becoming particulate, the slope of the VSM magnetization loops of the films became lower with increasing oxidation time due to increased demagnetization of the particles. Thin films with this kind of M-H loop can be used as a thin film inductor at GHz range. Permeability of the oxidized films was measured by CPW method up to 20 GHz as shown in Fig. 3 [2]. Real part of permeability of the 200 nm Fe-Al film after selective oxidation persisted up to 10 GHz. Therefore the selective oxidation of an active element in iron based alloys is very useful and can guide to a new way for manufacturing magnetic sensors and other devices. In conference further discussion will be given concerning the selective oxidation of Fe-Al thin films.

References

- [1] Richard E. Grace and Alan U. Seybolt, *J. Electrochemical Society*, **105**(10), 582, 1958
 [2] S.G.Cho, J.Kim, I.Kim, K.H.Kim, and M.Yamaguchi, *Phys. Stat. Sol.(a)*, **204**, 4133, 2007

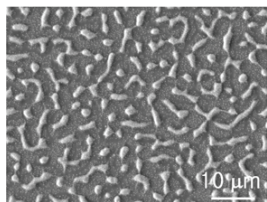


Fig. 1 SEM image of Fe-Al film oxidized at 900°C for 200 min.

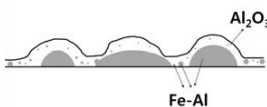


Fig. 2 Schematic diagram of Fe-Al films oxidized selectively.

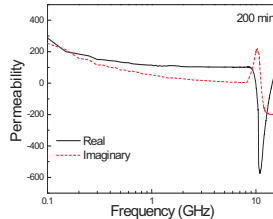


Fig. 3 Frequency vs permeability curves of Fe-Al films oxidized selectively.

Magnetopolymer composites with magnetic soft ferrite filler

Jana Rekošová¹, Rastislav Dosoudil², Ušáková Marianna², Ivan Hudec¹

¹ Department of Plastics and Rubber, Faculty of Chemical and Food Technology, Slovak University of Technology, Bratislava, Slovakia

² Department of Electromagnetic Theory, Faculty of Electrical Engineering and Information Technology, Slovak University of Technology, Bratislava, Slovakia

The properties of magnetopolymer composite materials, where the ferrite powder is dispersed in continuous polymer matrix depend not only on the properties of magnetic filler but polymer matrix too. The magnetopolymer composite materials have advantage that their properties can be adjusted to the requirements of specialty applications [1]. These materials are used on production for resonant circuits, transformers, inductors, cores of electrical rotating machines e.t.c. [2]

The aim of the work was the study of preparation and properties of polymer magnetic composites based on natural rubber SMR 20. As the magnetic filler, soft ferrite of general formula $\text{Ni}_{0,33}\text{Zn}_{0,67}\text{Fe}_2\text{O}_4$ was applied. This type of ferrite was prepared in laboratory conditions by ceramic method.

The influence of ferrite content on physical-mechanical, magnetic and rheological properties of prepared composites was investigated. Structural characteristics of tested materials were evaluated, too. The results revealed that ferrite incorporated in polymer matrix do not substantially influence physical-mechanical properties of prepared polymer systems. By contrast, magnetic characteristic show significant increasing tendency with increasing amount of ferrite. In generally one can say that evaluated composite materials exhibit suitable magnetic and elastic properties.

Acknowledgements:

This work was supported by grant agency VEGA, project No. 1/1163/12

References:

- [1] K. A. Malini, E. M. Mohammed, S. Sindhu, P. Kurian, and M. R. Anantharaman, Rubber and Composites, Vol. 31, No 10, (2002), 449-457
- [2] Van der Zaag, P.J. : Ferrites, Encyclopedia of Materials: Science and Technology, Elsevier Science and Technology, Elsevier Science Ltd, ISBN: 0-008-0431526, (2001), s. 3791-3722

The magnetocaloric effect of Heusler microwires in low and high magnetic fields

T.Ryba¹, R.Varga¹, Z.Vargova², V.Zhukova³, A.Zhukov^{3,4},

¹Inst. Phys., Fac. Sci., P.J. Safarik University, Park Angelinum 9, 041 54 Kosice, Slovakia

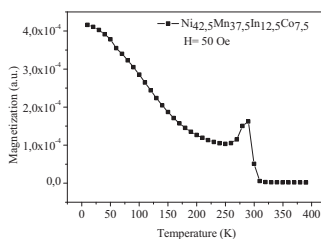
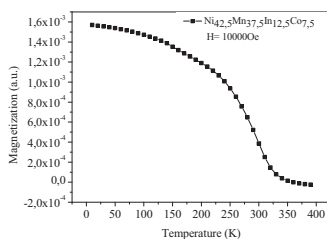
²Dpt. Inorg. Chem., Fac. Sci., UPJS, Moyzesova 11, 041 54 Kosice Slovakia

³Dpt.de Fisica de Materiales, Universidad del Pais Vasco, 20009 San Sebastian, Spain

⁴IKERBASQUE, Basque Foundation for Science, 48011 Bilbao, Spain

Heusler alloys are very perspective group of materials for magnetocaloric applications [1]. The magnetocaloric effect is determined by a large change of entropy in a narrow temperature range under the influence of suitable magnetic field. Usually, high magnetic field is used near the Curie temperature to obtain high magnetocaloric effect. However, the magnetization decreases smoothly at such field in a wide range of temperatures (see fig. below). On the other hand, measuring magnetization at low magnetic field near Curie temperature shows increase of magnetization just below the Curie temperature followed by a steep decrease of magnetization in a narrow temperature range. This effect is known as Hopkinson effect. The Hopkinson effect is result of the different temperature dependence of magnetization and anisotropy [2].

In the given contribution, we are dealing with the influence of Hopkinson effect on magnetocaloric effect. The material used is Heusler alloys with composition of $\text{Ni}_{42,5}\text{Mn}_{37,5}\text{In}_{12,5}\text{Co}_{7,5}$ in the form of glass-coated microwires. The microwires are prepared by Taylor-Ulitovsky method [3] that allows quick and easy preparation of microwires from small amount of materials. Moreover, microwires prepared by Taylor-Ulitovsky method have well-defined direction of easy magnetization [4]. Such microwires are characterized by Hopkinson maximum when exposed to a small magnetic field (50 Oe - see fig. below).



Support by the project NanoCEXmat Nr. ITMS 26220120019, Slovak grant APVV-0266-10 and VEGA grant No.1/0076/09 is acknowledged.

References

- [1] A.Hirohata, et al., Current Opinion in Solid State and Material Science, 10 (2006), 93.
- [2] J.D.Santos, R.Varga, B.Hernando, A.Zhukov, J. Magn. Magn. Materi., 321, (2009), 3875.
- [3] V.S.Larin et al., J. Magn. Magn. Mater., 249 (2002), 39.
- [4] R.Varga, et al., Scripta Materialia 65 (2011), 703.

Properties of Fe-Al Cores Made of Fe-Al Powders Annealed in Damp Hydrogen Atmosphere

Seungchan SHIN and Pyungwoo JANG

College of Science and Engineering, Cheongju University, Cheongju 360-764, Korea

When soft magnetic materials are to be used in magnetic actuators, it seems that high residual magnetization is not recommended because residual force hinders accurate operation of the actuator. If external magnetic field is applied to hard direction, residual magnetization can be reduced. However, there is no magnetic easy or hard axis in general actuators because the materials used in magnetic actuators are polycrystalline. If demagnetization field is applied the residual magnetization can be reduced as in the powder compressed cores. Generally Fe-Si alloys are used in the powder cores because silicon increases the electrical resistivity of the iron alloys. However, Si content in Fe-Si alloys is limited because the formability of the Fe-Si alloy is deteriorated with increasing the Si content. If powders with poor formability are compressed into cores, it gives too high demagnetization field, thus leads to necessity of high applied field. Aluminum is also an element to increase the electrical resistivity of iron alloys. While magnetostriction of Fe-Al alloys is higher than that of Fe-Si alloys, formability of the Fe-Al is much better than that of Fe-Si alloys. It is well known that aluminum is selectively oxidized to Al_2O_3 with high electrical resistivity on the surface of Fe-Al powders when Fe-Al powder is oxidized in damp hydrogen atmosphere [1]. In this study feasibility of Fe-Al powders for the magnetic actuators is tested. Fe-3wt% Al powder was gas-atomized and then mixed with or without alumina and talc powders, which acts as a solid insulator. The powders were annealed in pure hydrogen or in damp hydrogen atmosphere at 800°C for 30 min. The annealed powder was compressed into Fe-Al toroidal cores under a pressure of 1 GPa and then annealed in pure nitrogen atmosphere at 800°C for 30 min. Thus four cores were manufactured from various powders, i.e., selectively oxidized powder with/without solid insulator (core A/core B) and hydrogen-annealed powder with/without solid insulator (core C/core D). After annealing the color of all powder was changed from gray to black, which meant the formation of Fe_3O_4 phase on the surface of powder. The permeabilities of the core A, B, C, and D are 58, 55, 50 and 79, respectively. Core losses of the cores at a frequency of 50 kHz under a condition of 0.1 T were 1449, 5693, 1070 and 1372 mW/cc, respectively. Contrary to our expectation, the loss of the core C is lowest. The reason for the highest loss of the core B is due to the formation of Fe_3O_4 phase, the resistivity of which is much lower than that of Al_2O_3 . In our simulation with STANJAN program, selective oxidation was promoted with increasing oxidation temperature. The reason for the formation of Fe_3O_4 phase is probably due to relatively low oxidation temperature. Iron is oxidized to Fe_3O_4 phase at high temperature in damp atmosphere. Even though hydrogen with 5N purity was used, small amount of water was contained in the gas. Another possibility is dehydration of talc to silicate and water vapor. In the conference the results for the Fe-Al cores made of various powders with higher Al content and oxidized at a temperature higher than 800°C will be presented.

References

- [1] Richard E. Grace and Alan U. Seybolt, *J. Electrochemical Society*, **105**(10), 582, 1958

Alternative route for obtaining NiFe₂O₄ thin films for sensor by pulsed laser deposition

STRATULAT Sergiu¹, URSU Cristian², CALTUN Florin-Ovidiu¹

¹Faculty of Physics, “Alexandru Ioan Cuza” University, Iasi, Romania

²“P. Poni” Institute of Macromolecular Chemistry, Iasi, Romania

Ferrites represent a broad class of materials with high impact in both research and industry. Nickel ferrite is a soft magnetic material with a low conductivity, which is of interest for various applications: magnetoelectric heterostructures, high-frequency microwave devices, spintronics, sensors, etc. One of the most used techniques to obtain thin films of NiFe₂O₄ is pulsed laser deposition (PLD). As with all complex oxides, oxygen atmosphere and high substrate temperature during deposition, or post-annealing in oxygen atmosphere is mandatory for high-quality thin films^[1].

Ferrite thin films have been obtained by excimer laser (KrF, $\lambda=248$ nm) ablation of NiFe₂O₄ sintered target (1250°C). Two types of samples were deposited: with (5×10^{-2} mbar) and without oxygen (5×10^{-6} mbar) atmosphere during the process. The substrate temperature was 550°C, 650°C and 750°C. The characterization of as deposited films was first performed by Raman spectroscopy, method which has been proved to be a very effective for the study of ferrite thin film^[2]. The spectra revealed the formation of nickel ferrite only on the samples prepared in oxygen atmosphere. For the samples obtained in high vacuum, the spectra can be attributed to magnetite^[3]. Energy dispersive X-ray analysis (EDS) revealed presence of Ni in the magnetite samples, in a 1:2 proportion relative to Fe.

We obtained nickel ferrite from the magnetite samples by using a different route than annealing. We irradiated the sample obtained at 750°C with an excimer laser ($\lambda=308$ nm), at various frequencies (10, 25 and 50 Hz), at the lowest energy (0.14 J/cm²), for 45000 and 90000 pulses. Raman spectra revealed the formation of nickel ferrite, as well as the presence of the magnetite phase.

References

- [1] R. Eason: Pulsed Laser Deposition of thin films, Wiley-Interscience, ISBN-13: 978-0-471-44709-2, 2007
- [2] P.R. Graves, C. Johnson, J.J. Campaniello: Raman scattering in spinel structure ferrites, Mat. Res. Bull., 23, (1988), 1651-1660
- [3] Shailja Wiwari, R.J. Choudhary, D.M. Phase: Effect of growth temperature on the structural and transport properties of magnetite thin films prepared by pulsed laser deposition on single crystal Si substrate, Thin Solid Films, 517, (2009), 3253-3256

Local Flux Density and Barkhausen Noise Distribution for Grain-Oriented Electrical Steels

TURNER S.¹, Hall J.P.², Moses A.J.² and Jenkins K³

¹National Physical Laboratory, Hampton Road, TW11 0LW, United Kingdom

²Wolfson Centre for Magnetism, Cardiff University, Cardiff, United Kingdom

³Development and Market Research, Cogent Power Ltd, Newport, United Kingdom

The development of grain-oriented electrical steels signified a step change in performance of core laminations and as a consequence, the efficiency of power distribution transformers also improved. In addition to the development of Goss texture and the exploitation of body-centered cubic iron's easy axis of magnetization, further improvements were achieved through increasing grain size, removing impurities and by laser scribing finished material to optimize the domain structure. Each of these developments made use of the intimate relationship between the magnetic and physical properties of electrical steels and of soft magnetic material in general. However, much of what understand about this relationship is obtained from observations of the bulk magnetic properties and from generalizations about the materials overall microstructure.

In this paper, the samples used are a selection of electrical steels that have been deliberately altered to investigate the effect of microstructural properties, such as grain size and misalignment of Goss texture, on the local magnetic properties. These physical properties have been evaluated using Electron Backscatter Diffraction. To expose the surface of the actual samples measured, HCl acid was used to remove the tensile coating and etch the surface of each strip to reveal the grain structure. However, all samples were also stress-relief annealed prior to measuring, which removed any residual stress imparted during the coating removal process.

To assess these specimens the needle probe technique and a ferrite rod enclose within a coil were used to measure the local magnetic flux density [1] and Barkhausen noise [2] respectively. These two probes were automatically scanned over an area on each strip, using a three-axis positioner. At each point the flux density (along both the rolling and transverse directions) and the Barkhausen noise were measure through an entire magnetization cycle. Although such measurements themselves are not unique, by scanning an area and measuring the entire cycle it is possible to generate an animation. Therefore, the change in distributions of flux density and Barkhausen noise can be compared over time.

References

- [1] H.V. Patel, S. Zurek, T. Meydan, D.C. Jiles and L. Li, Sens. and Act. A: Phys. Vol.129, 112-117 (2006)
- [2] M. De Wulf, L. Dupre', D. Makaveev, and J. Melkebeek: Needle-probe techniques for local magnetic flux measurements, J. App. Phys., Vol 93, Issue 10, pp 8217 – 8273, 2003

Sensor of mechanical Barkhausen noise signal

MACIAKOWSKI P., AUGUSTYNIAK B., CHMIELEWSKI M.

Technical Physics and Applied Mathematics Department, Gdansk University of Technology,
Gdansk, Poland

Mechanical Barkhausen noise effect (MBN) is a quit novel ‘mechanical’ analogue of classical Barkhausen effect. It appears when irreversible movements (jumps) of not 180 deg magnetic domain walls (DW) of ferromagnetic sample with a non-zero magnetostriction are forced to move during mechanical loading. Those jumps can be detected as voltage pulses in a pick-up coil due to Faraday’s law. The induced voltage signal provides information about activity of the 180 deg DW when they are depinned from local stress barriers. This effect allows new type of research of magneto-mechanical hysteresis properties of ferromagnetic materials [1]. However, the most interesting information which can be achieved with MeBN is its residual stress distribution function [2].

We like present in details our newly designed sensor of MBN signal. This sensor is suitable for all types of mechanical loads (torsion, tensile-compression and bending) as well as sample shape (parallelepiped or rod). Our sensor consist of a coil wound over PTFE shell with a ferrite core inside this shell and of electromagnetic shielding wrapped over the coil. The coil consists of 2000 turns of a diameter $d_w = 0.072$ mm copper wire wound on diameter $d_s = 7$ mm shell. Coil is $h = 9$ mm high. A ferrite core of diameter $d_f = 3.5$ mm and length $l = 16$ mm. To achieve stable contact with the examined sample surface the core is pressed to the sample surface by a spring. The sensor is shielded by means of an FeSi thin plates (22 mm x 120 mm x 0.5 mm) with a non-conductive layer between them. Voltage signal from the pick-up coil of this sensor is first amplified by a non-inverting amplifier with a gain of 38 dB. Then it is filtered by a high-pass RC filter with $f_0 = 1$ kHz and again amplified by a non-inverting amplifier with a gain of 18 dB. The next stage of signal processing consists of a second order Butterworth high-pass filter in Sallen-Key topology with $f_0 = 1$ kHz and two inverting amplifiers with a gain of 20 dB. The resulting output voltage signal is of the order of hundreds of mV in amplitude in the case of typical low alloy steels. The signal-to-noise ratio of our signal SNR_{dB} varies within the range 12 dB do 20 dB depending on environment conditions. This is extremely good level when MBN phenomena is detected.

This sensor is now used for research of the MBN signal properties of various steels subjected to tensile-compression or bend like loads. The bending mode of mechanical load applied by means of free vibration of one-end clammed sample is the best way for MBN signal detection because it does not introduces mechanical like noise which is produced by typical MTS like machine. We will show some examples of the MBN signal research. It should be stressed that the as designed sensor allows extremely effective detection of not 180 deg DW activity in ferromagnetic material when mechanical load is applied. This sensor is also very suitable for detection of the classical Barkhausen effect voltage signal which is produced when sample is magnetized be C-core type electromagnet. It means that we are now able to measure both effects simultaneously wusing the same sensor.

- [1] B. Augustyniak , J. Degauque; Microstructure inspection by means of the mechanical Barkhausen effect analysis; *J. de Phys.* vol. 6, (1996) C8_527-C8_530
- [2] B. Augustyniak, P., L. Maciakowski, L. Piotrowski., M Chmielewski ; Assessment with mechanical Barkhausen effect of residual stress in grain oriented polycrystalline 3% Si-Fe sheet; *IEEE Transaction on Magnetics* , vol. 48, no. 4, (2012) 1405-1408

Possibilities of measuring stress and health monitoring in materials using contact-less sensor based on magnetic microwires.

D. Praslicka¹, J. Blazek¹, M. Smelko¹, J. Hudak¹, I. Mikita¹, R. Varga², A. Zhukov³

¹Faculty of Aeronautics, Technical University of Kosice, Slovakia

²Institute of Physics, University of P.J. Safarik, Kosice, Slovakia

³Dpto. Fisica de Materiales, Fac. Quimicas, UPV/EHU, San Sebastian, Spain

Amorphous glass-coated micro-wires are an ideal material for a micro-sensing element for various applications [1]. Magnetic behavior of micro-wires with the high and positive magnetostriction constant is characterized by a rectangular hysteresis loop. Domain structure of micro-wire consists of one axial magnetic domain in the middle of the wire, which cover is formed by radial domains. Closure domains are at the end of the wire. Such a structure shows bistable behavior (e.g. the magnetization can have only two values $+M_s$ and $-M_s$) [1]. The switching between two magnetization values appears at the switching field at which the magnetization process runs through the single Barkhausen jump. As the main anisotropy that determines their magnetic properties is magnetoelastic one [2], the switching field is strongly dependent on the mechanical stress.

In the given contribution, we have studied the stress dependence of the switching field in the glass-coated micro-wires embedded in materials as fiber-laminates and composites. In this case, the microwire is built into the measured structure, the exciting and sensing components of the contact-less sensor must be solved as reading devices attached from outside. We show that for practical application of sensors based on bistable magnetic microwires for measurement of stress in materials, it was, in general, necessary to develop a suitable method of measurement. One from first results of measurement with this method is shown on Fig.1.

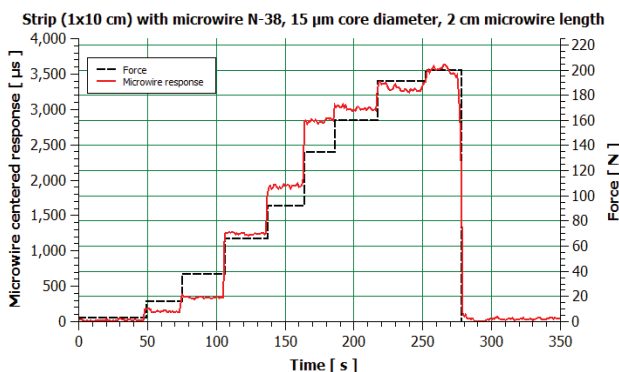


Fig.1: Result of measurement with contact-less sensor, magnetic microwire N38 had 2cm length and was embedded in the tensioned fiber-laminated structures strip (1x10cm).

References

- [1] M. Vázquez, in *Handbook of Magnetism and Advanced Magnetic Materials* edited by H. Kronmüller and S. Parkin, (Wiley, New York, 2007), Vol. 4, p. 2193.
- [2] R. Varga, K. L. Garcia, A. Zhukov, M. Vazquez, P. Vojtanik, *Appl. Phys. Lett.* **83**, 2620 (2003).

Modelling the influence of stress on magnetic characteristics of construction steels

Dorota Jackiewicz¹, Roman Szewczyk², Jacek Salach¹

¹Institute of Metrology and Biomedical Engineering, Warsaw University of Technology, Warsaw, Poland

²Industrial Research Institute for Automation and Measurements, Warsaw, Poland

This paper concerns the possibility of Jiles-Atherton-Sablik extended model usage to describe magnetic characteristics of construction steel ST3 under mechanical stress. Especially important problem is material stress state determination by using non-destructive, magnetic properties based testing techniques.

The frame-shaped sample of construction steel ST3, stretched with tensile stress below the yield point, was examined. Sample with magnetizing and measuring winding was mounted in the material testing machine on presented in figure 1. During the measurements applied stress was changed in the range from 25 to 200 MPa. The experiment results confirms change of hysteresis loop shape under stresses.

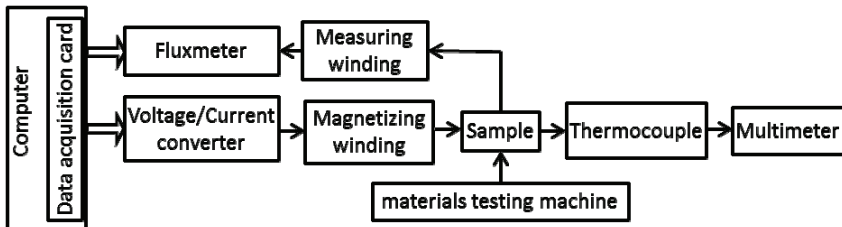


Fig.1. Schematic block diagram of a measuring setup

Next on the base of measurements magnetic hysteresis loops of ST3 steel were modelled with Jiles-Atherton-Sablik extended model. Owing to the fact that in this modified model parameter k changes as a function of magnetization M of the material, the hysteresis loop could be modelled in full range of magnetizing field.

Result of the modelling utilizing extended Jiles-Atherton-Sablik model are consistent with results of experimental measurements which is confirmed by high values of the R^2 determination coefficient. Finally the results show correctness of proposed model for modelling of construction steel ST3 under mechanical stress.

References

- [1] A. Bienkowski: Some problems of measurement of magnetostriction in ferrites under stresses. Journal of magnetism and magnetic materials 112, issue 1-3 (1992), 143-145.
- [2] M. J. Sablik, H. Kwun, G. L. Burkhardt, D. C. Jiles, Model for the effect of tensile and compressive stress on ferromagnetic hysteresis, J. Appl. Phys. 61 (1987) 3799.

Non destructive evaluation of loose assemblies using eddy currents and artificial neural networks

Pierre-Yves Joubert¹, Eric Vourc'h², Guillaume Le Gac², Pascal Larzabal²

¹IEF, Université de Paris-Sud, CNRS, 91 405 Orsay, France

²SATIE, ENS Cachan, CNRS, Universud, 94 235 Cachan Cedex, France

The evaluation of the distance between parts is a major preoccupation in the non destructive evaluation (NDE) of metallic assemblies, which arises in many industrial fields (nuclear, railways, aeronautics...). In this study, we consider the problem of estimating the distance separating two aluminum plates in an assembly representative of an aeronautical structure, with a top plate of unknown thickness. To do so, we consider the eddy current (EC) method since it is easy to use and sensitive for the testing of multilayered structures [1], even in the presence of an air layer [2]. However, the quantitative evaluation of the distance between parts using the EC method requires to elaborate an accurate model of the sensor / structure interactions and secondly to solve an ill-posed inverse problem. In order to bypass these difficulties, as well as to deal with the uncertainties that may be introduced by the experimental set-up (inaccurate knowledge of the features of the assembly, mispositioning of the sensor, possible loss of sensitivity due to the thickness of the top plate, etc...), we chose to implement a "non-model based" approach, elaborated thanks to a statistical learning of the interactions between the sensor and the investigated structure, by the means of an artificial neural network (ANN). Indeed, ANNs are known to be universal approximators [3], and have been proved to be efficient in the resolution of NDE problems starting from experimental data [4]. Here, the ANN is built in a statistical approach starting from the experimental EC data provided by a ferrite cored coil EC sensor used to investigate an assembly mock-up of adjustable configuration. Moreover, in order to build a learning database allowing a robust and accurate ANN to be elaborated, as well as to deal with assemblies of unknown thicknesses, we consider EC data obtained at different frequencies chosen in an optimal bandwidth. The implementation of the proposed approach on assembly mockups featuring air layers ranging from 0 to 300 μm , did give estimation root means square errors (RMSE) in the order of 1% to 20% (for top plates ranging from 1 mm to 8 mm respectively) as well as an estimation of the top plate thickness featuring RMSE lower than 10%. These promising results enable further works focusing on the evaluation of more realistic assemblies by means of tailor-designed EC sensors and ANN to be envisaged.

References

- [1] Renakos I.T., Theodoulidis T.P., Panas S.M., Tsiboukis T.D., Impedance inversion in eddy current testing of layered planar structures via neural networks, *NDT&E international*, 30 (1997), pp. 69-74.
- [2] T.L. Cung, P.Y. Joubert, E. Vourc'h, P. Larzabal, On the interactions of an eddy current sensor and a multilayered structure, *Electronics Letters* 46(23) (2010), pp.1550–1551.
- [3] Hornik K, Stinchcombe M, White H., Multilayer feedforward networks are universal approximators, *Neural Networks* 2 (1989), pp.359-366.
- [4] Yusaa N., Chengb W., Chena Z, Miyaa K., Generalized neural network approach to eddy current inversion for real cracks, *NDT&E International* 35 (2002), pp.609–614.

Identification of Plastic Deformation in Steel Samples Using Two-Axial Transducer with Rotational Excitation Field

PSUJ Grzegorz

Department of Electrical and Computer Engineering, Faculty of Electrical Engineering, West Pomeranian University of Technology, al. Piastow 17, 70-310 Szczecin, Poland

Steel influenced by a repeating or alternating stresses gradually degrades. Taking into account the fact that most of the constructions are subjected to repeated loading or vibration, it becomes necessary to carry out a study to determine the status of their structure and to estimate the degradation of the material. Fatigue and stress changes affect the electric and magnetic properties of ferromagnetic materials depending on the loading direction. Therefore measurements of magnetic properties find widespread application in industry to test ferromagnetic materials [1]. However utilization of a method which allows evaluation of the material only in one direction can be insufficient to achieve satisfying estimation of its state. Real constructions are subjected to multi-axial loading forces which results in damage occurring at different angle to the selected scanning direction. Therefore, a transducer with two sensitivity axes and rotational excitation field was introduced [2]. In this paper the transducer (Figure 1) was utilized to identify plastic deformations which arise in the material during the degradation process at different angle. First, numerical simulations are carried out in order to introduce the data processing algorithm allowing the identification of defects alignment in the tested samples. Then, preliminary experiments utilizing plate with artificial notches are performed to verify the performance of the proposed procedures based on real measurements. Finally, the experiments using steel samples loaded to different stress value are carried out in order to validate the discrimination ability of the whole system. All details of the experiments will be presented in the final version of the paper.

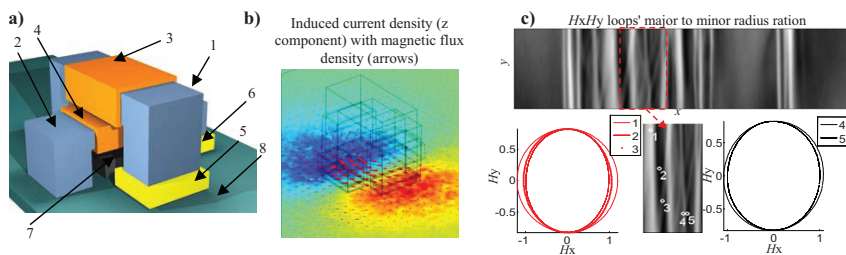


Figure 1. 3D view of the transducer and selected results of the carried out numerical simulations and measurements; 1,2 - core of Y- and X-directions, 3,4 - excitation coil of Y- and X-directions, 5,6 - pick-up coil of Y- and X-directions, 7 - magnetic sensor, 8 - sample

References

- [1] J. Sievert, „Two-dimensional magnetic measurements – history and achievements of the workshop“, *Electrical Review*, R. 87, No 9b, 2011, pp. 2-9
- [2] T. Chady, G.Psuj, „Electromagnetic transducer with rotational excitation field for evaluation of fatigue and stress loaded steel samples“, *IEEE Transaction on Magnetics*, Volume 45, Issue 10, October 2009, pp. 3897-3900

A Formal Presentation of Differential Sensor Pairs With Common and Crossed Feedback

ROBBES Didier, ALLEGRE Gilles, FLAMENT Stéphane

GREYC – UMR 6072, University of Caen USBN and ENSICAEN, Caen, France

We propose a general framework to deal with various sensing devices equipped with actuators and arranged in balanced pairs. The concept includes magnetic sensor devices as well. That formal modeling make good use of high gain, fully differential, instrumentation amplifier, to describe in a unified way various physical quantities at the sensing and actuating ports of the sensor pair. The approach is shown very efficient for gradiometric sensing of scalar physical quantities such voltage or temperature and it is applied to derive a two outputs sensing device giving both electrical voltage and its associated electric field. Because many sensing applications, in industrial, noisy, environments require highly linear sensing systems, having large measuring range and bandwidth together with very low noise, the concept is used to provide such very large dynamic range. Such a case is typically found in non destructive evaluation (NDE) using eddy currents [1]. The case of aircraft wheels is a good reference, where the searched defects signature is very small with respect to the superimposed ones, both from environmental noise and strong magnetic bars in the wheel. The former perturbation can be reduced using a conventional sensor/reference pair [2], but the latter require a gradiometric configuration, to remove large common mode signals, due to the scanning process in NDE technics. Such configurations are addressed in our contribution : given an input physical quantity (X) to be measured in any point of a given volume (containing gas or liquids), a balanced pair of sensors coupled to a high gain, fully differential, instrumentation amplifier (GIA) is used to provide feedback on the actuating inputs of the sensors. That multi-sources/multi-loops feedback is shown to be conveniently managed, under some realistic restrictions, in some way generalizing those introduced many years ago for the practical use of the famous operational amplifiers (OPA).

The paper is arranged as follows : part II, starting from the state of the art, gives the GIA concepts. Part III reports on the general framework of balanced differential pair of sensors with feedback. Results of an implementation, leading to a composite voltmeter – electrometer, validates the approach [3]. Part IV then discusses the implementation for magnetic sensors, especially those based on miniature search coils, to get “over the top” bandwidth and dynamic range. Finally, the simultaneous measure of components of both electric field and magnetic field in a single pair of conductors is addressed.

References

- [1] J. Clarke and A.I. Braginski, *The SQUID Handbook*, Ed. J. Clarke and A.J. Braginsky, Wiley – VCH, 2006
- [2] O. Paul, *MEMS a practical guide to design, analysis and applications*, Norwich (NY USA) : William Andrew Publishing, Ed. J. G. Korvink and O. Paul, 2006, p. 29 and p. 33.
- [3] Didier Robbes, *Physical Quantity Measuring Unit and Device for Measuring a Voltage and an Electric Field* European Patent Application No. 09290213.9 , date 20.3.2009

Minimalistic devices and sensors for micromagnetic materials characterization

SZIELASKO, Klaus¹, MIRONENKO, Ivan², ALTPETER, Iris¹, HERRMANN, Hans-Georg¹, BOLLER, Christian^{1,2}

Fraunhofer Institute for Non-Destructive Testing (IZFP), Saarbrücken, Germany
Saarland University, Saarbrücken, Germany

Micromagnetic materials characterization requires sensors which essentially consist of two critical elements: an electromagnet which introduces a well-defined magnetic field to the material, and a sensor assembly which detects the material's response to the applied magnetic field. The devices developed at Fraunhofer IZFP obtain a multi-parametric "magnetic fingerprint" with these sensors by evaluating magnetic Barkhausen noise, harmonics of the magnetic tangential field strength, eddy current impedance and incremental permeability. The magnetic fingerprints of calibration samples are used as input for pattern recognition or regression analysis, this way allowing the prediction of mechanical-technological material characteristics (hardness, yield strength, etc.) or residual stress. This approach is called 3MA (Micromagnetic Multi-Parameter Microstructure and Stress Analysis).

The long-term stability and reproducibility of the sensor and device characteristics are crucial to the reliability of the measured results. Therefore, the measuring hardware should follow a minimalistic approach. In this paper, we propose ways of simplifying the measuring hardware by making multiple use of sensor elements, reducing the analog signal processing chain and transferring most signal processing tasks to the PC. We present devices designed according to these rules, outline the fields of application and discuss the results obtained so far.

References

- [1] K. Szielasko: Development of metrological modules for electromagnetic multiparameter materials characterization and testing. Doctoral dissertation, Saarland University, Saarbrücken (2009).
- [2] K. Szielasko: Umsetzung und Weiterentwicklung des 3MA-Prüfverfahrens mit innovativer Miniatur-Prüfgerätetechnik, *ZfP-Zeitung der DGZfP*, 122 (2010), S. 33-36.
- [3] I. Mironenko, K. Szielasko, I. Kiselmann, H. Kopp, M. Kopp, I. Altpeter, G. Dobmann, C. Boller: Wideband Micromagnetic Multi-Parameter Materials Characterization with 3MA. Proc. of the 9th ICBM (2009).

Determination of the Magnetic Losses in Laminated Cores under PWM Voltage Supply

N. Vidal, K. Gandarias, G. Almandoz, J. Poza

Faculty of Engineering, University of Mondragon, Mondragon, Spain

In the laminated ferromagnetic cores employed in transformers and electrical machines energy losses occur resulting in a warming effect and efficiency decrease. Having a tool to obtain the most accurate estimation of the magnetic losses is of great interest in addressing the design of the machine as the excessive heat can lead to a deterioration of thermal performance that adversely affect to the magnetic properties of the magnets and magnetic cores, and reduce the performance. Normally, the manufacturers only provide iron losses data when a sinusoidal voltage supply is applied, and often only up to 50 Hz or 60 Hz, but the actual operating characteristics of electrical machines include non-sinusoidal supply, in particular pulse width modulation (PWM). Only measuring systems that have function generators with arbitrarily programmable waveforms allow measurements in presence of higher harmonics. It is of great interest, therefore, the validation of the analytical models available in the literature for the prediction of iron losses.

In this paper, first, the influence of the modulation amplitude and the switching frequency of the PWM signal in the magnetic losses of soft magnetic materials is studied. Then, a procedure based on the analytical expressions presented in [1]-[3] for the estimation of losses in laminated cores that delivers results with acceptable accuracy under all operating conditions and, more specifically, for feeding PWM, is described and validated. For this purpose, non-oriented fully processed electrical steels have been measured in a single sheet yoke with a commercial AC permeameter.

References

- [1] A. Boglietti, A. Cavagnino, M. Lazzari, M. Pastorelli: Predicting Iron Losses in Soft Magnetic Materials with Arbitrary Voltage Supply: an Engineering Approach. *IEEE Trans. on Magnetics* 39 No. 2, (2003), 981-989.
- [2] M. Popescu, T. Miller, D.M. Ionel, S. J. Dellinger, R. Heidemann: On the Physical Basis of Power Losses Laminated Steel and Minimum-Effort Modeling in an Industrial Design Environment. *Proc. 42nd IAS Annual Meeting Industry Applications Conf. Record of the 2007 IEEE*, (2007), 60-66.
- [3] D.M. Ionel, M. Popescu, C. Cossar, M.I. McGilp, A. Boglietti, A. Cavagnino: A General Model for Estimating the Laminated Steel Losses under PWM Voltage Supply. *IEEE Trans. On Industry Applications* 46 No. 4, (2010), 1389-1396.

New RF EMAT for complex fluid characterization

Y. Wang¹, N. Wilkie-Chancellor¹, S. Serfaty¹, L. Martinez¹, B. Roucaries¹, J.-Y. Le Huérou¹

¹Laboratoire Systèmes et Applications des Technologies de l'Information et de l'Energie (SATIE), Université de Cergy-Pontoise, UMR CNRS 8029, Cergy-Pontoise, France

Instantaneous direct measurements are of the utmost importance for developing industrial “on line” effective monitoring techniques for the elaboration of new soft materials. In order to characterize the micro-rheological evolution of nanostructures, various nondestructive techniques have been developed in our lab using ultrasounds and Thickness Shear Mode resonators. These techniques are suitable for industrial application monitoring thanks to their simplicity, their low cost, their high-resolution mass sensing and their capability to monitor the viscoelastic characteristics. This work presents a new RF EMAT design and technique for remotely sensing the micro-rheological properties of complex fluids in hidden places.

The new sensor consists in a single electrode loop deposited on the surfaces of an AT cut quartz substrate magnetically coupled with a high quality RF antenna (multiturn transmission line resonator, $Q \sim 120$). Using this design, the magnetic resonant frequency can be calculated in a relatively simple manner: number of coil turns, the coil width, the substrate thickness, and dielectric constant. The shape of this EMAT is then optimized to generate ultrasonic shear waves at 9 MHz.

The wireless excitation of this sensor is based on an original RF technique designed to inductively monitor the electrical impedance of the EMAT. This sensor is inductively excited by a loosely coupling with a T/R circular probe. The impedance of the EMAT is extracted by studying the variation of the probe response near the resonance frequency between the unloaded and loaded transducer.

In the case of weak coupling between the probe and the sensor, we can show that the variation of mechanical boundary conditions of the EMAT modify the electrical impedance in agreement with mechanical and electrical properties of the fluid. A suitable electrical model of the probe/loaded EMAT is proposed in order to extract the mechanical and electrical properties of a complex fluid in contact. First, it is shown that the resonant frequency shift and the damping linked to the viscoelastic properties of the loaded material can be represented by additional induced equivalent inductance (L_i) and resistance (R_i) in a R - L - C series equivalent electrical resonant circuit. According to the mechanical boundary interactions, we show that the parameters R_i and L_i can be related to the complex elastic modulus.

For Newtonian liquids, the power dissipation and energy storage components are equivalent, and both are proportional to the square root of the product viscosity - density of the liquid. Various tabulated Newtonian liquids (made from water-glycerol mixtures) are then studied to validate the capability of this technique to monitor their viscosity. These preliminary results show that this technique allows the online monitoring of hidden complex fluids.

Sensor of Magnetic Flux Density Waveform Distortion

ZEMÁNEK Ivan¹, Havlíček Václav¹, Havránek Aleš¹

¹Department of Circuit Theory, Czech Technical University, Prague, Czech Republic

The distortion of required magnetic flux density waveform $B(t)$ caused by the magnetic flux dispersion and non-zero resistance of the magnetizing winding MW is an unwanted effect occurring in AC SST measurements of soft magnetic materials parameters at high magnetic field intensities. The main part of the improved compensation SST KF9a [1] is the corrector of the $B(t)$ waveform completed by the sensor of the $B(t)$ waveform distortion (Fig.1).

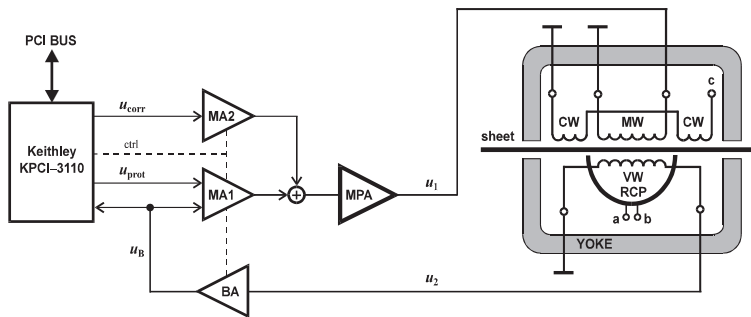


Fig.1 Magnetizing and correcting system with sensor of the $B(t)$ distortion

The sensor of the $B(t)$ waveform distortion consists of the measuring voltage winding VW of the magnetizing equipment (yoke), measuring amplifier BA, DAQ PC plug-in board Keithley KPCI-3110 and digital signal processing algorithms. The actual magnetic flux density $B(t)$ is indicated by the induced voltage $u_2(t)$ represented by the digital signal $y[n]$:

$$y[n] = K_{ADC} H_{BA} u_2(t) \Big|_{t=nT_S} = K_{ADC} H_{BA} N_2 S \frac{dB}{dt} \Big|_{t=nT_S} .$$

The $B(t)$ waveform distortion is expressed by the difference between the spectrum \mathbf{Y} of the $y[n]$ and the spectrum \mathbf{X} of the digital exciting signal prototype $x[n]$ generating the voltage prototype $u_{prot}(t)$ and theoretically the required magnetic flux density waveform $B(t)$.

$$\mathbf{Y}(k) = \mathbf{FFT}[y[n]] \quad \mathbf{X}(k) = \mathbf{FFT}[x[n]] \quad \mathbf{D}(k) = \mathbf{Y}(k) - \mathbf{X}(k)$$

The spectrum difference \mathbf{D} indicated by the sensor is used for the digital-analogue generation of the correction signal $u_{corr}(t)$, increasing the correction efficiency of the analogue correction feedback loop (magnetizing pre-amplifier MA1 – magnetizing power amplifier MPA – magnetizing winding MW – voltage winding VW – measuring amplifier BA):

$$u_{corr}(nT_S) = K_{DAC} H_{MA2} \mathbf{IFFT}[\mathbf{D}(k)].$$

References

- [1] I. Zemánek: Single sheet and on-line testing based on MMF compensation method. Przeglad Elektrotechniczny, 85 (2009), No 1/2009, 79-83.

Dynamic Hysteresis Loops Modelling by Means of Extended Hyperbolic Model

NOVÁ Ivana¹, HAVLÍČEK Václav², ZEMÁNEK Ivan²

¹Dept. of Electric Drives and Traction, Czech Technical University, Prague, Czech Republic

²Department of Circuit Theory, Czech Technical University, Prague, Czech Republic

Dynamic hysteresis loops of soft magnetic materials were simulated by means of analytical functions. Proposed approach is based on the hyperbolic model [1] – [2], which was extended for purpose of simulating sufficiently the loop shape. Two hyperbolic components ($n = 2$) of the original model were used to construct the elementary “sigmoid” part of the loop:

$$B_{+n} = \sum_{i=1}^n (A_i f_{+i} + b_i) - A_0 f_0, \quad B_{-n} = \sum_{i=1}^n (A_i f_{-i} - b_i) + A_0 f_0,$$

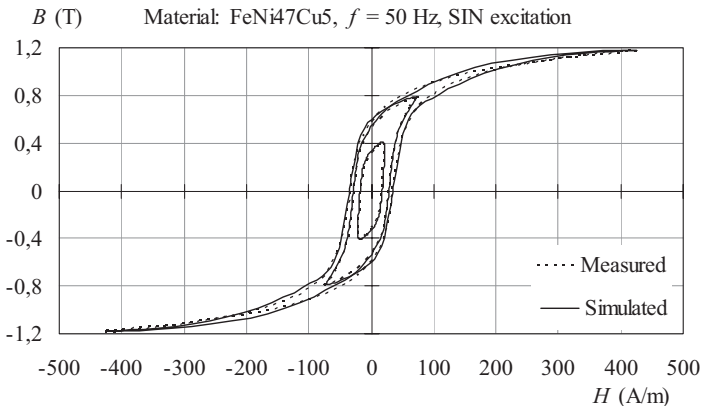
$$f_{+i} = \tanh(\alpha_i (H - a_{0i})), \quad f_{-i} = \tanh(\alpha_i (H + a_{0i})), \quad b_i = \frac{A_i}{2} [f_{-i}(H_{\max}) - f_{+i}(H_{\max})].$$

The extension consists in addition of new f_0 component [3], which features the rounded as far as elliptical shapes of dynamic loops at smaller excitation levels:

$$f_0 = \left| 1 - \left(\frac{H}{H_{\max}} \right)^2 \right|^k.$$

Presented components together are able to simulate varied shapes of dynamic hysteresis loops. The model contains at most eight parameters that depend on the excitation level. Their analytical expressions were found, using rational functions.

Material samples were measured by means of the compensation ferrometer KF9a [4]. Experiments show quite good similarity between measured and simulated dynamic loops.



References

- [1] J. Takács: Mathematics of Hysteretic Phenomena, Wiley-VCH, Berlin 2003.
- [2] L. K. Varga, Gy. Kovács, J. Takács: J. Magn. Magn. Mater. 320 (2008), L26-29.
- [3] I. Nová, I. Zemánek: J. Electrical Engineering. 61 (7/s) (2010), 46-49.
- [4] I. Zemánek, I. Nová: Proceedings of WMM'08, Ghent 2008, 413-429.

Anisotropic Magneto-Resistance in Ni₈₀Fe₂₀ Antidot Arrays Prepared by Bottom-up and Top-down Nanolithography

Marco Coïsson¹, Gabriele Barrera¹, Luca Boarino¹, Federica Celegato¹, Emanuele Enrico¹, Paola Tiberto¹, Franco Vinai¹

¹INRIM, Electromagnetism Division, Torino, Italy

Antidot arrays, consisting of a magnetic thin film patterned with regularly spaced holes, have recently been studied for their potential application as sensing elements of magnetic fields, because of their anisotropic magneto-resistance (AMR) properties. AMR is a variation of the electrical resistance of a magnetic conductor that depends on the relative orientation of the local magnetization and the local current density vectors. Antidot arrays enhance the AMR effect because of their nanostructure: in fact, the magnetization is submitted to local magnetic anisotropies which vary on the scale of the lattice parameter of the holes, thus favouring a fine control of its orientation with respect to the electrical current by means of an applied magnetic field.

In this paper, two different nanolithography techniques are exploited to prepare Ni₈₀Fe₂₀ antidot arrays. A top-down process involves electron beam lithography to pattern regular arrays of holes in the continuous thin film, with extremely well controlled diameter and centre-to-centre spacing. Samples prepared with this methodology are characterized by a very high quality but are limited in size; additionally, the preparation process is time consuming and expensive. An alternative bottom-up process involves the self-assembling of polystyrene nanospheres, which spontaneously arrange in a close-packed hexagonal monolayer on top of the Si-oxide substrate. By means of a reactive ion etching process the nanospheres diameter can be controlled, while preserving their centre-to-centre distance. A subsequent sputtering of the magnetic material on top of the nanospheres fills the gaps between them, covering the substrate only in the interstices. Finally, nanospheres removal by sonication reveals the magnetic antidot array [1]. Samples prepared with this methodology are characterized by a regular antidot configuration on a scale of a few micrometers, but can cover extremely large surface areas (several mm² or cm²); additionally, the preparation process is much quicker and cheaper.

AMR measurements have been performed on samples prepared with both techniques, as a function of the magnetic field and of temperature, from 4.2 K through 300 K, with the 4-contacts technique. The role of holes diameter and spacing is discussed. The comparison between samples prepared with the two different methodologies allows to investigate the effect of the disorder of the antidot geometry in the AMR properties.

References

[1] P. Tiberto, L. Boarino, F. Celegato, M. Coïsson, N. De Leo, F. Vinai, P. Allia: Magnetic and magnetotransport properties of arrays of nanostructured antidots obtained by self-assembling polystyrene nanosphere lithography. *J. Appl. Phys.* 107 (2010), 09B502.

Temperature drift of offset and sensitivity in full-bridge magnetoresistive sensors

MICHAL VOPÁLENSKÝ¹, Antonín Platil²

¹Department of Electrical Engineering and Informatics, College of Polytechnics Jihlava, Jihlava, Czech Republic

²Department of Measurement, Czech Technical University in Prague, Prague, Czech Republic

A typical commercially available magnetoresistive sensor, and particularly an anisotropic magnetoresistive sensor, employs a full bridge of the Wheatstone type formed by two complementary magnetoresistive elements in each branch [1-2]. This configuration provides linearized response and enlarged sensitivity compared to any other configuration made up of the same elements [3-4]. Since in a large scale production it would be expensive to adjust the zero-field resistances of all the four elements to an exactly identical value, there is always some zero-field offset present at the bridge output diagonal even when the sensor is placed in the zero magnetic field.

The sensitivity of the sensor, i.e., the ratio of the output voltage change to the change of the measured field H , is associated with the sensitivity of the individual elements. The sensor sensitivity S is usually expressed and indicated in relation to one volt of the bridge supplying voltage [1-2]. Then the sensitivity is $(\Delta V_{\text{out}}/V_{\text{ss}})/\Delta H$, where ΔV_{out} is a change in the output voltage of the sensor supplied with $V_{\text{ss}} = 1\text{V}$, related to a change of 1A/m in the acting field H . The change of the output voltage is determined by the change of the resistance of the individual elements, and for an ideal voltage-supplied bridge it can be derived that $V_{\text{out}} = V_{\text{ss}} \Delta R/R_0$, where R_0 is the zero-field resistance of each element.

It can be seen that both the offset and the sensitivity is dependent on the zero-field resistances R_0 of the elements. However, as in every metallic material, the resistance of a magnetoresistive element increases with increasing temperature. Hence, both the offset and the sensitivity of a real magnetoresistive sensor is temperature dependent.

It can be shown that, theoretically speaking, the offset is temperature independent when the bridge is supplied with a constant voltage (but the sensitivity in that case is temperature dependent), and the sensitivity is temperature independent when the bridge is supplied with a constant current (but the offset in that case is temperature dependent). The situation gets more complicated when the sensor is flipped periodically and when it works in a compensated mode.

This work deals with a mathematical model of the offset and sensitivity of a current- and voltage driven full-bridge magnetoresistive sensor, taking into account the effects of flipping and feedback compensation mode. A comparison with experimental data is presented.

References

- [1] KMZ 51 datasheet. Available online at http://www.datasheetcatalog.org/datasheet/philips/KMZ51_3.pdf
- [2] HMC1001 datasheet. Available online at http://www51.honeywell.com/aero/common/documents/myaerospacecatalog-documents/Missiles-Munitions/HMC_1001-1002-1021-1022_Data_Sheet.pdf
- [3] Tumanski, S: Thin film magnetoresistive sensors. Institute of Physics Publishing, 2001, ISBN 0 7503 0702 1
- [4] Ripka, P. (ed.): Magnetic sensors and magnetometers. Artech House Publishers, 2001, ISBN 1-58053-057-5

Wednesday, July 4

ORAL SESSION

NANOPARTICLES, PERMANENT MAGNETS

Magnetic nanoparticles for therapy and diagnostics

E. Pollert¹, P. Kašpar², K. Závěta¹, V. Herynek³, M. Burian³ and P. Jendelová⁴.

¹Institute of Physics, ASCR, v.v.i. Prague, Czech Republic

²Czech Technical University, Faculty of Electrical Engineering, Prague, Czech Republic

³Institute for Clinical and Experimental Medicine, Prague, Czech Republic

⁴Institute of Experimental Medicine, ASCR, v.v.i., Prague Czech republic

An enormous increase of the interest about a possible application of magnetic nanoparticles in biology and medicine brought together to a close collaboration chemists, physical scientists, biologists and physicians in order to solve this multidisciplinary problem aimed on a concrete solution of the people's health.

For the present the research and utilization of the magnetic nanoparticles are preferentially oriented on magnetite Fe_3O_4 and maghemite $\gamma\text{-Fe}_2\text{O}_3$. The control of their magnetic properties in a desirable way is, however, rather difficult which limits their applications. A possibility to solve this problem is the use of complex oxides allowing an appropriate adjustment of the properties of the magnetic cores. This approach is now demonstrated on an example of the $\text{La}_{1-x}\text{Sr}_x\text{MnO}_3$ perovskites selected as possible materials for magnetic fluid hyperthermia and magnetic resonance imaging. The preparation of the final product, i.e. stable suspensions of the magnetic nanoparticles, consists of two steps. The first is the synthesis of the magnetic cores effectuated by the sol-gel method supplemented by the thermal and mechanical treatment. Further it is the formation of a protective layer preferentially of a hydrated silica oxide on the surface of cores ensuring stability of their suspensions in the water medium. The protective layer simultaneously forms a biologically inert barrier, protecting the surrounding environment from the chemical effects of the core. Solution of the outlined task is considerably complex and its success requires a qualified feedback based on a number of the characterization methods. It includes X-ray analysis, TEM, magnetic studies, magnetic heating experiments measurements of the relaxivities and biological tests of the viability. This long and uneasy way was now successfully accomplished by *in vitro* and *in vivo* experiments. Nevertheless in spite of the promising results the real clinical applications require a cautious approach and an considerable effort in the near future.

Selected literature.

E. Pollert, O. Kaman, P. Veverka, M. Veverka, M. Maryško, K. Závěta, M. Kačenka, I. Lukeš, P. Jendelová, P. Kašpar, M. Burian, V. Herynek:

Core-shell $\text{La}_{1-x}\text{Sr}_x\text{MnO}_3$ nanoparticles as colloidal mediators for magnetic fluid hyperthermia.

Phil. Trans. R. Soc. A 2010 368, 4389-4405

E. Pollert and K. Závěta

Nanocrystalline Oxides in Magnetic Fluid Hyperthermia

Chapter in Magnetic Nanoparticles, From Fabrication to Clinical Applications

Editor Nguyen Thi Kim Thanh, London UK CRC Press/Francis & Taylor Group,

Magnetic and crystalline structure in ordered arrays of Co nanopillars

Vivas L.G., Trabada D.G., Ivanov Y., Chubykalo-Fesenko O., Del Real R.P. and Vázquez M.

Institute of Materials Science of Madrid, CSIC, 28049 Madrid, Spain

Patterned arrays of single-domain nanomagnets are attracting much attention due to their applications in spintronics, logic devices, MRAM and microwave materials. Thus, a deep understanding of the magnetic properties of individual nanomagnets and of their interactions has been the goal of recent experimental and micromagnetic studies [1]. Opposite to most studied case of Permalloy, the magnetic behavior of ordered arrays of Co nanopillars is determined not only by shape but also by crystalline anisotropy. In these systems a strong dependence is expected on the crystalline structure (*hcp* or *fcc* phase) and texture.

Anodic alumina membranes have been used for template-assisted electroplating growth of hexagonally ordered arrays of Co nanowires under different synthesis conditions (i.e., pH and nanopore diameter). Scanning Electron Microscopy allowed us to determine the pillar diameter D (tailored from 35 to 80 nm), the interpillar distance (fixed at 105 nm) and their length L (fixed at ~ 120 nm). X-ray diffraction spectrum show that for $D \sim 35$ nm, one obtains the *fcc* crystal Co-phase, in agreement with recent results [2]. However, when D increases the *hcp* phase is the only detected in the X-ray diffraction spectrum and the orientation of the crystal hexagonal *c*-axis has been found to change from parallel ($D \sim 44$ nm) to perpendicular to the wire axis ($44 \text{ nm} < D \sim 75$ nm). That suggests a reorientation of the magnetocrystalline easy axis above a critical diameter of around 50 nm.

The arrays magnetic characterization has been performed in a Vibrating Sample Magnetometer, and the analysis of magnetization curves reveals that the magnetic properties (i.e., coercivity) depend on nanopillar diameter, crystal structure and on the magnetostatic interactions.

Parallel micromagnetic simulations have been performed using the Magpar package [2,3] with finite element discretization. The dynamics of the demagnetization process has been studied in individual Co nanopillars as a function of diameter for vanishing (*fcc*-phase) and strong *hcp*-phase Co magnetocrystalline anisotropy. In addition, the influence of magnetostatic interactions has been simulated in a model of seven nanopillars hexagonally arranged.

Through the combined analysis of experimental and micromagnetic data, we conclude that: i) crystallite size and structure depend on the nanopillar diameter; ii) the magnetic behavior is in most cases governed by the magnetostatic interactions among nanopillars, and iii) a strong longitudinal magnetic anisotropy is achieved for nanopillars with *c* axis (*hcp* phase) parallel to their axis.

References

- [1] K.R. Pirota, M. Knobel, M. Hernandez-Velez, K. Nielsch, and M. Vazquez, "Magnetic nanowires" in: "Handbook of Nanoscience and Nanotechnology", ed. A.V. Narlikar and Y.Y. Fu (Oxford Un. Press, USA, 2010) Chapt. XXII.
- [2] L.G. Vivas, R. Yanes, O. Chubykalo-Fesenko, and M. Vazquez, Appl. Phys. Letters 98 (2011) 232507.
- [3] W. Scholz, J. Fidler, T. Schrefl, D. Suess, R. Dittrich, H. Forster, and V. Tsiantos, Comput. Mater. Sci. 28 (2003) 366.

Sensors magnetization technique overview

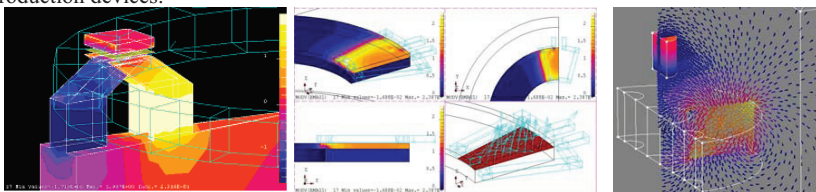
Dr. Stefano Tizianel

Laboratorio Elettrofisico Engineering S.r.l. Nerviano (MI) Italy

In a wide range of applications, hall sensors read magnetic field from permanent magnet supports. These PM supports are built and assembled with industrial production lines. One of the most delicate process is the MAGNETIZATION.

One may think that charging a capacitor bench of the electric energy $1/2CV^2$, and abruptly discharging it into a solenoid obtaining magnetic energy $1/LI^2$, is a boring task, not worthy dealing with from a scientific point of view. Indeed the matter conceals a big source of application performance improvements and exciting theoretical understanding.

Design and construction of magnetizing fixtures starts from prototypes, based on analytical and FEM calculations, and fast moves to robust construction for high duty cycle industrial production devices.



FEA simulations: transverse flux coil, single pole coil, 4 poles sensor

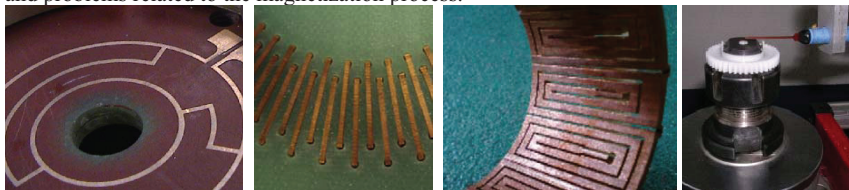
The very first step consists of defining what type of support we want to magnetize, such as what kind of PM material, which orientation, how many pole pairs, how many traces on the same support, how regular must be the polarities distribution.

Then the accuracy of the magnetic footprint must be defined, such as saturation level, pole single or total pitch errors accepted.

A more practical task is to understand what other stuff is around the support, such as metallic magnetic parts, bearings, field PM of electric motor inductors, over-moulding, what productivity is required in terms of magnetizations per hour.

The design procedure starts from deciding which kind of magnetizing fixture is required, in a wide range of typologies, direct or indirect fixtures, iron or iron-less cored, solenoids or multi-polar fixtures....; next steps are calculation and simulations, design, construction and test.

The aims of this work are to introduce the argument of the industrial magnetization and to focus on the calculation and design of those fixtures that required us years and years of R&D, in order to show how the application designer could take profit being aware of potentiality and problems related to the magnetization process.



magnetization fixtures details and test device

Analytical Calculation of Magnet Systems for Sensor and Actuator Applications

Jean-Paul YONNET¹ and Hicham ALLAG²

¹ Laboratoire de Génie Electrique de Grenoble, G2E Lab (UMR 5269 CNRS / INPG-UJF),
Institut Polytechnique de Grenoble, ENSE3, 38402 St Martin d'Hères cedex, France

² Laboratoire d'Electrotechnique de Constantine, LEC, Université Mentouri, Constantine,
25000 Algérie

The development of the 3D analytical calculation of the interactions between two magnets started in the 1980 years. The first publications have been made on long shaped magnets in interaction for magnetic bearings. These long magnets can be treated as a 2D problem. The 3D fully analytical expressions of the energy and force exerted between two cuboidal magnets were calculated by Akoun [1] and published in 1984. The forces and interaction energy were analytically calculated for parallel magnetization directions, which are parallel to one of the magnet edges. Other positions can also be calculated, for example when the two magnets are in angled position. The magnets are supposed to be perfect, with their polarizations J and J' rigid and uniform, and a relative permeability of 1. They can be replaced by distributions of magnetic charges on the poles. It is the coulombian representation of the magnetization. The analytical calculation is made by integration of the force distribution. The first integral is easy to do, but the last ones are very difficult.

Recently a new step has been made by the analytical calculation of energy and force when the magnetization directions of the two magnets are perpendicular. By combination with the parallel case, the force for any magnetization direction and for any magnet position can be calculated by analytical expression. The torque calculation is another recent and innovative step [2]. The three torque components between two magnets can be fully written with analytical expressions, for a rotation around any point.

Now, all the interactions between two elementary magnets represented by the 6 components (Force F_x , F_y , F_z and Torque τ_x , τ_y and τ_z) can be calculated by simple analytical expressions. The analytical expressions are a very powerful calculation method, giving a very fast answer to magnetic interaction determination. It is why the analytical expressions of all the interactions, energy, forces and torques between two cuboidal magnets are very important results.

Many calculations of sensor and actuator systems can be solved with these analytical expressions. The simplest shape of elementary volume is the parallelepiped, with its cuboidal volume. By the superposition of 3D interactions between elementary magnets, many 3D calculations can be made. The first application is the analytical calculation of interaction between two magnets of any shape. Moreover the analytical calculation is not limited to magnets only. If iron yokes are used, they can be taken into account by using image effects. And interaction between coils and magnets can also be obtained: a coil is equivalent to the amperian currents around a magnet; it can be considered like a magnet.

[1] G. AKOUN and J-P. YONNET, IEEE Trans. Magn., MAG 20, n° 5, Sept. 1984, p. 1962 - 1964.

[2] J.-P. YONNET and H. ALLAG, IEEE Trans. Magn., Vol. 47, n° 8, Aug 2011, p. 2050 - 2055.

Wednesday, July 4

ORAL SESSION

NDE, SQUID, , MAGNETOELASTIC, CALIBRATION

Resonance parameters of a magnetoelastic viscosity sensor and their dependence with temperature

I. Bravo-Imaz¹, A. García-Arribas², E. Gorritategi³, A. Arnaiz¹, J.M. Barandiaran²

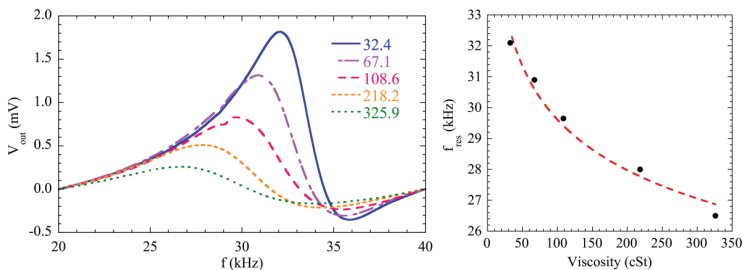
¹Intelligent Information Systems, IK4 - TEKNIKER, Eibar, Spain

²Departamento de Electricidad y Electrónica, Universidad del País Vasco, Bilbao, Spain

³Technical Office, atten2 – Advanced monitoring technologies, Ermau, Spain

The actual trend in the field of maintenance in mechanical and electrical machinery, points towards the implementation of the so-called proactive maintenance. In this framework, different parameters of the system are monitored so that the current health state of the machinery can be precisely known. The health state of the lubricating oil is within the set of parameters that are to be monitored. Nearly 40 % of the total reported malfunctions in heavy machinery are due to failures in lubrication [1]. Among the different parameters that define the state of lubricant oil, viscosity is one of the most important. Lubricant oil prevents moving parts to get into direct contact so, inadequate viscosity may cause malfunctioning and even a fatal breakdown. Besides, the monitoring of the viscosity can help establishing the state of degradation of the lubricating oil.

Magnetoelastic sensors based on the magnetoelastic resonance phenomena have been shown to be useful in the determination of viscosity [2]. In this work we describe an experimental prototype to determine the viscosity of lubricant oils using the magnetoelastic resonance. The measurements are done using different commercial oils with viscosities ranging from 32 to 326 cSt. A least squares fit to a theoretical resonance curve allows to extract a correlation between selected parameters of the fit and the viscosity of the oil. For instance, the dependence of the resonance frequency with the viscosity is shown in the figure. Finally, the effect of temperature on the results – will be discussed.



Left: Magnetoelastic resonance curves measured for oils with different viscosities.
Right: Dependence of the resonance frequency with the viscosity of the lubricant oil.

References

- [1] R. Smith, R. Keith Mobley: Rules of thumb for maintenance and reliability engineers. ISBN: 978-0-7506-7862-9.
- [2] I. Bravo-Imaz, A. Garcia-Arribas, E. Gorritategi, M. Hernaiz, A. Arnaiz, J. Terradillos, and J. M. Barandiaran: Magnetoelastic viscosity sensor for lubricant oil condition monitoring. Key Engineering Materials Vol. 495 (2012), 71-74.

Non-destructive measurement of permeability and magnetostriction in ribbons and wires

KTENA Aphrodite¹, Hristoforou Evangelos²

¹Department of Electrical Engineering, TEI of Chalkida, Evia, Greece

²Laboratory of Metallurgy, NTUA, Zografos, Greece

The magnetostrictive delay line principle of operation is used to evaluate the magnetic and magnetostrictive response of materials with magnetostriction constant higher than 1ppm and in a waveguide-like shape, which practically includes all ferromagnetic ribbons or wires. The arrangement uses the under test material as the magnetostrictive delay line on which the following fields are applied: a pulsed field along with a dc bias field at the excitation point and a dc bias field at the receiving end. The peak and the shape of the output pulse depend on both the excitation and bias fields, acting as controls. Varying one of the two bias fields while keeping the other constant, allows the decoupling between the magnetic and the magnetostrictive parameters. More specifically, it is shown, that varying the dc bias field at the receiving end results in the permeability measurement as a function of the dc field, $\mu(H)$, the integral of which yields the dc hysteresis loop of the material; on the other hand, the response obtained upon varying the dc bias field in the excitation point is related to the dc magnetoelasticity loop, $\lambda(H)$. The experimental arrangement is such that it allows for the evaluation of the spatial variation of the measured macroscopic parameters suggesting that the method may also prove to be a valuable tool in the quality control of the production of amorphous ribbons and wires used in sensing applications.

Separability of multiple deep crack defects with a NDE Eddy Current System

R. Hamia, C. Cordier, C. Dolabdjian

GREYC, CNRS UMR 6072 - Université de Caen Basse-Normandie and ENSICAEN, France.

We propose in this paper to study the spatial resolution of a NDE Eddy Current system and the ability to separate a network of deep crack defects. A high sensitive Improved Giant Magneto-Resistance Magnetometer was used in the NDE system and its performances will be rapidly presented as they were previously studied and analyzed in detail [1].

We show in this work that the spatial resolution of EC system depends not only of the sensitive element dimensions [2] but also of different parameters of the system, such as the sensor lift-off, the excitation frequency and also the cracks depth. Finite Element simulations were done on an aluminum plate with two parallel deep crack defects separated by a distance d_0 (figure 1.a). We find the existence of an optimal frequency for each plate thickness, which can provide a minimal spatial resolution for the NDE system but which is not necessary compatible with the highest defect magnetic signature.

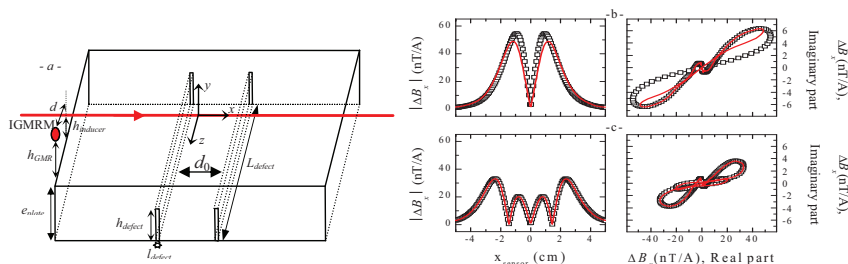


Figure 1: a) The plate sample with two deep crack defects, b-c) comparison of the Magnetic response of two buried defects (symbol line) and the superposition of the response of each crack (solid line), for $d_0 = 5$ and 30 mm, respectively.

Furthermore, we have studied the interactions between the magnetic responses of multiple buried defects. The detected magnetic response of two buried defects is compared to the magnetic response obtained by the superposition of each defect response (figures 1.b and 1.c). The results show that when the distance between the two defects is lower than a limit distance, the superposition principle is no longer valid. This important aspect will be useful for defect reconstruction in the inverse problem.

References

- [1] R. Hamia, C. Cordier, S. Saez, C. Dolabdjian, "Eddy Current Non Destructive Testing using an Improved Giant MagnetoResistance Magnetometer and a single wire as inducer: A FEM Performance Analysis", IEEE Trans On Magnetics, vol.46, No.10, pp: 3731-3737, October 2010.
- [2] R. Hamia, C. Cordier, S. Saez, C. Dolabdjian, "Giant Magneto Impedance Sensor for Non Destructive Evaluation Eddy Current System," Sensor Letter, vol. 7, No. 3, (2009), 437-441.

NANOSENSORS BASED ON SUPERCONDUCTING QUANTUM INTERFERENCE DEVICE FOR NANOMAGNETISM

C. Granata¹, E. Esposito¹, B. Ruggiero¹, R. Russo¹, M. Russo¹, P. Silvestrini², A. Vettoliere¹.

¹Istituto di Cibernetica del CNR, 80078, Pozzuoli (Napoli), Italy

²Dipartimento di Ingegneria dell'Informazione-SUN, 80131, Aversa (Caserta), Italy

Nanosized Superconducting Quantum Interference Devices (nano-SQUIDs) offer the possibility to investigate small spin populations and the magnetization of nanoparticles opening new horizons in the interesting word of nanomagnetism[1]. Furthermore, the nanoSQUIDs can be employed in stimulating applications such as the spintronics, the single photon detection, the readout in quantum computing, the nanoelectronics including memory, the quantum metrology and the scanning SQUID microscopy with a very high spatial resolution [2]. We will report our recent results about the design, the fabrication and the characterization of Dayem bridges based nano-SQUIDs having a loop area ranging from $4 \mu\text{m}^2$ to $0.04 \mu\text{m}^2$. The devices have been patterned by Electron Beam Lithography in a 20-25 nm thick Nb layer [3,4]. The smallest sensor has shown a spectral density of the magnetic flux noise of $1.5 \mu\Phi_0/\text{Hz}^{1/2}$ corresponding to a spin sensitivity of about 60 spin/Hz^{1/2} (in units of Bohr magneton). Preliminary measurements on Fe₃O₄ nanoparticles having a size between 4 and 8 nm will be discussed [4]. We also report the main results about a new magnetic flux noise theory which we have recently developed taking into account the non-sinusoidal current-phase relationship [5].

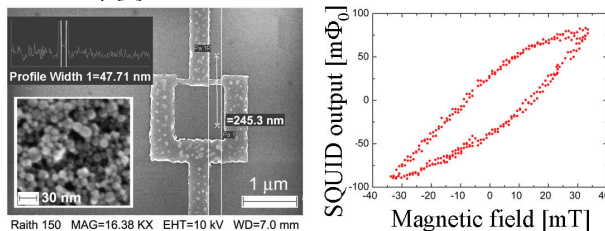


Figure 1: *left*) Scanning electron micrograph of a nanoSQUID having a hole side length of $0.75 \mu\text{m}$. The lower inset shows the nanoparticles on the sensor. *right*) Magnetic field dependence of the magnetization for a small cluster of (Fe₃O₄-SiO₂) core/shell nanoparticles at $T = 4.2 \text{ K}$ [5].

References

- [1] C.Granata, E.Esposito, A. Vettoliere, L.Petti, M.Russo, Nanotechnology 19, 275501 (2008); A.G.P. Troeman, H. Derking, B. Boerger, J. Pleikies, D. Veldhuis, H. Hilgenkamp, Nano Lett. 7, 2152 (2007).
- [2] C. P. Foley and H. Hilgenkamp, Supercond. Sci. Technol. 22, 064001(2009).
- [3] C. Granata, A. Vettoliere, R. Russo, E. Esposito, M. Russo and B. Ruggiero, Appl. Phys. Lett. 94, 062503 (2009).
- [4] R. Russo, C. Granata, P. Walke, A. Vettoliere, E. Esposito and M. Russo, J. Nanopart. Res., DOI: 10.1007/s11051-011-0330-2 (2011); E. Esposito, C. Granata, A. Vettoliere, R. Russo, D. Peddis and M. Russo, J. Nanosci. Nanotechno, (in press).
- [5] C. Granata, A. Vettoliere, M. Russo and B. Ruggiero, Phys. Rev. B 84, 224516 (2011)

Digital magnetometers calibration method with 3D coils

Kaveh MOHAMADABADI^{1,2}, Alexis JEANDET¹, Mathieu HILLION², Christophe COILLOT¹

1-LPP Laboratory of Plasmas Physics, Ecole Polytechnique, Palaiseau, France.

2- SYSSNAV, Vernon, France

Today low cost magnetic sensors are used in several applications, these kinds of sensors has substantial source errors while they used as IMUs or AHRS like Hard and Soft Iron effects, Scale factor, Non-orthogonality and etc. Due to this, several calibration methods have been proposed to compensate the sensor reading and improve the performance for high accuracy measurement. In addition, the data set of sensor measurement in 3D free outdoor rotation is needed in order to use the least squares method (LSQ) for the calibration. According to the constant Earth magnetic field the norm of magnetic field measurement by 3D sensors should be constant and equal to the earth magnetic field. But this is not the case in indoor measurement by the reason of magnetic field perturbation which comes from annoying urban electromagnetic field.

In this paper we propose an indoor calibration method for three axes magnetometers, by simulating the sensor rotation in earth magnetic field in 3D coil. For providing constant magnetic field in 3D coil, currents injected to the cubic Helmholtz coils which are controlled by the electronic circuitry based on DAC monitored by a microcontroller. According to this method the non-orthogonality error of the 3D coil also calibrated digitally by the MATLAB processed data and microcontroller which is used to transfer the digital values to the desire currents.

References

- [1] Caruso, M.J, Applications of magnetic sensors for low cost compass systems, Position Location and Navigation Symposium, IEEE 2000.
- [2] Renaudin, V. and Afzal, M.H. and Lachapelle, G. Complete triaxis magnetometer calibration in the magnetic domain, Journal of Sensors, 2010.
- [3] Hotra, Z. and Holyaka, R. and Bolshakova, I. and Yurchak, I. and Marusenkova, T. Arbitrary rotation method for 3D magnetic sensors calibration IEEE 2011.

Wednesday, July 4

ORAL SESSION

METROLOGY

Towards wafer scale inductive determination of magnetostatic and dynamic parameters of MTJ stacks

S. SERRANO-GUISAN¹, N. LIEBING¹, S. SIEVERS¹, P. NASS¹, K. ROTT², G. REISS², M. PASQUALE³, J. LANGER⁴, B. OCKER⁴, H.W. SCHUMACHER¹

¹Physikalisch-Technische Bundesanstalt, Bundesallee 100, D-38116 Braunschweig, Germany

²Dep. of Physics, University of Bielefeld, Universitätsstr. 25, 33615 Bielefeld, Germany

³Instituto Nazionale di Ricerca Metrologica, Strada della Cacce 91, 10135 Torino, Italy

⁴Singulus AG, Hanauer Landstrasse 103, D-63796 Kahl am Main, Germany

Determination of magnetic parameters in magnetic tunnel junction (MTJ) systems is essential to optimize MTJ nanodevices for spin torque (ST) and sensor applications. While some critical parameters like the resistance area product (RA) can be determined by wafer probe measurements [1] others like the ST critical current density j_C require a time consuming nano patterning and elaborated magneto transport measurements [2].

Here we present time- and frequency domain inductive measurements of CoFeB/MgO/CoFeB based MTJ stacks with different MgO thicknesses (t_{MgO}) [3]. They deliver the ferromagnetic

resonance (FMR) frequency f_{FMR} and linewidth of the precession of the MTJ free layer. Analysis of the field dependence of f_{FMR} allows the determination of magnetostatic parameters such as saturation magnetization, anisotropy, and exchange coupling. Furthermore the Gilbert damping α is derived. In the Sloncewski ST model α is proportional to j_C and thus to the key ST device parameter. The dependence of the various device MTJ parameters on t_{MgO} will be discussed. With respect to α we find a critical value of t_{MgO} below which an asymmetric increase of α is observed [4]. Note that for this thickness range also an asymmetric increase of j_C has been found in MTJ nanodevices [2]. In combination with wafer probe RA measurements this in principle allows a lithography free metrology of the optimum t_{MgO} of ST MTJ stacks.

We further present a first prototype of an inductive probe head suitable for wafer scale

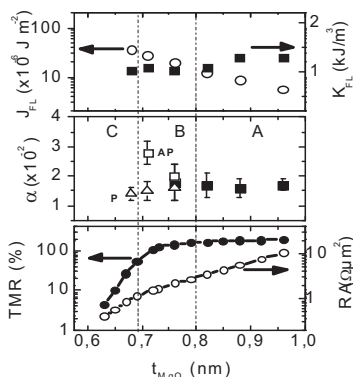


Fig. 1: MgO thickness dependence of MTJ parameters: a) exchange coupling J_{FL} and uniaxial anisotropy K_{FL} of the free layer. b) effective damping α . c) TMR and RA from wafer probe measurements. In b) below $t_{\text{MgO}} < 0.8$ nm α is increased for antiparallel (AP, open square) but not for parallel P configurations (triangles).

inductive measurements. First measurements will be presented and compared to data obtained by a conventional probe. Based on this the prospects of fast inductive wafer scale metrology for MTJ key parameters will be discussed.

The work has been co-funded by EMRP IND 08 and the EMRP participating countries.

[1] D. C. Worledge et al., Appl. Phys. Lett. 83, 84 (2003)

[2] W. Skowronski et al., J. Appl. Phys. 107, 093917 (2010)

[3] MTJ stacks are sputter deposited in a Singulus NDT Timaris cluster tool.

[4] S. Serrano-Guisan et al., J. Appl. Phys. 110, 023906 (2011)

Modeling and characterization of graphene Hall sensors

A. Manzin¹, R.K Rajkumar^{2,3}, O. Kazakova², D.C. Cox^{2,3}, S.R.P. Silva³ and A. Tzalenchuk²

¹Istituto Nazionale di Ricerca Metrologica (INRIM), Torino, Italy

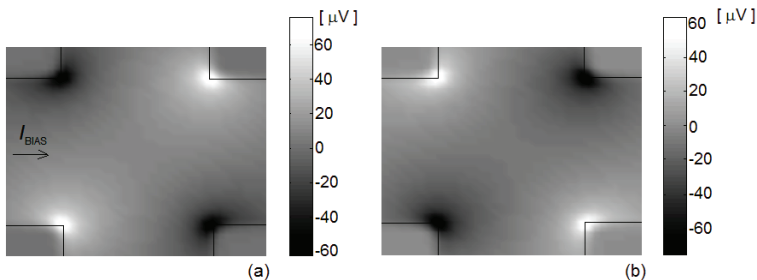
²National Physical Laboratory (NPL), Teddington, UK

³University of Surrey, Guildford, UK

The response to local magnetic and electric fields of epitaxially grown graphene based devices has been characterized by means of a scanning probe microscopy technique [1]. The field contributions include the stray magnetic field produced by a magnetic tip as well as the electric field originating from electrostatic charging of the tip surface due to parasitic effects. As a result, the extrapolation of the device magnetic sensitivity from transverse voltage measurement becomes critical, requiring a clear separation of the different field terms.

To support experimental result interpretation, we have developed a finite element model able to provide the spatial distribution of the electric potential inside Hall plates, in the presence of a magnetic tip that locally applies magnetic and electric fields [2]. This model, based on the assumption of diffusive transport regime, has been employed to compute the transverse voltage for different positions of the tip above the junction area. The tip stray field is included representing the magnetic coating as a 3D distribution of magnetic dipoles, while the electric field effects are introduced defining a region with modified charge density under the tip.

The numerical results have been compared to experimental data demonstrating a good agreement in different working conditions, obtained varying the bias current versus, the orientation of the tip magnetization and the distance of the tip apex from the sensor surface. The transverse voltage exhibits peak values at the device corners with diagonally opposing corners having the same sign (see figure). These effects are mainly due to the electric field contribution and to the corresponding deviation of the local current path. At the center of the device, the signal is different from zero and its sign depends on the bias current versus and on the orientation of the tip magnetization, as a response to the Lorentz force resulting from the tip stray field.



Computed maps of the response of a graphene Hall cross when scanned by a magnetic tip, considering a tip – sample separation of 25 nm, a tip magnetization oriented "down" and a positive (a) and negative (b) bias current.

References

- [1] V. Panchal et al.: Small epitaxial graphene devices for magnetosensing applications. *J. Appl. Phys.* 111, 07E509, (2012).
- [2] L. Folks et al.: Near-surface nanoscale InAs Hall cross sensitivity to localized magnetic and electric fields. *J. Phys.:* *Condens. Matter* 21, 25 5802, (2009).

Triaxial magnetic compensation system for well-defined metrological calibrations of magnetometers

JANOŠEK M.^{1,2}, Ulvr M.², Petrucha V.¹, Kupec J.²

¹Dept. of Measurement, Faculty of Elec. Eng., Czech Tech. Univ., Praha, Czech Republic

²Dept. of Electromagnetic quantities, Czech Metrology Institute, Praha, Czech Republic

Metrologically correct calibrations of triaxial magnetometers are challenging. The calibrations may be performed by utilizing a scalar magnetometer, Earth's field vector and an iterative algorithm, but the metrological parameters are in this case of "scalar calibration" [1] complicated by estimating the accuracy of proton or Overhauser magnetometer and by the iterative algorithm. Another method for calibrations is building a complete two or three-coil compensating/calibration system, driven by quantum He-Cs magnetometers, which might achieve pT resolution in Earth's field range [2]. However from metrological point of view, the instruments are often depending on a commonly agreed gyromagnetic ratio constant, rather than on standards of units. High cost and complexity of such setup is another disadvantage.

Our method represents a mixture of a classical approach using a magnetic flux density standard and a dual calibration coil system with Earth's field compensation. The coil standard of magnetic flux density has been calibrated and its uncertainty is 30 ppm. The wooden-frame coil system at Průhonice ex-observatory site of Geophysical Institute, CAS, consists of triaxial, 2-m Braunbeck coils, which serve for Earth's field compensation, and of a triaxial 1-m Helmholtz coil system of Billingsley Aerospace & Defense. The Earth's field compensation relies on remotely located fluxgate sensor with vector compensation and high stability [3] in an open-loop servo system – the long-term drifts of offset/position and sensitivity/coil factor are corrected by a custom compensation electronics unit driven by an algorithm in LabView before each calibration campaign. The X,Y,Z coils of Braunbeck type are driven with high-voltage amplifiers with more than 1 kHz bandwidth, allowing to compensate also 50-Hz magnetic fields and their harmonics including industrial and urban noise, which is coming from nearby traffic and DC electric railway. The stable 1-m Helmholtz coils, which are located inside of the compensating Braunbeck coils, are calibrated by direct comparison with the magnetic flux density standard and a fluxgate probe for zero-field detection. The combined uncertainty of coil constant in each axis using a 5.5-ppm shunt and 6.5 digits DMM is better than 50 ppm. With this approach, also a scalar magnetometer may be calibrated using a correct metrological chain with accuracy better than 50 ppm (1 nT in Earth's field range), although its manufacturer-stated precision may be 2-orders better.

As for every compensating system, magnetic field gradients and mainly gradient of magnetic noise are an issue. Gradient of magnetic noise has been measured and special precautions were taken to minimize the residual field and noise in the compensating coils, which is allowed by the developed LabView algorithm.

References:

- [1] J. M. G. Merayo, P. Brauer, F. Primdahl, J.R. Petersen, O.V. Nielsen: Scalar calibration of vector magnetometers. *Meas. Sci. Technol.*, vol. 11, 120 (2000), 120-132
- [2] V. Ya. Shifrin, V. N. Khorev, A. E. Shilov, P. G. Park: Magnetoresistive Sensors for Nondestructive Evaluation. *IEE Trans. Instr. and Meas.*, vol. 54, 2 (2005), 727-729
- [3] V. Petrucha, P. Kaspar: Compact Fluxgate Sensor with a Vector Compensation of a Measured Magnetic Field. *IEEE Sensors 2010 conference, IEEE (2010), 1795-1798*

Magnetization Dynamics of Nanostructured Antidot Arrays

PASQUALE MASSIMO¹; KUEPFERLING, MICHAELA¹; AMBRA CAPRILE¹;
CELEGATO, FEDERICA¹; BOARINO, LUCA¹; DELEO, NATASCIA¹; COISSON,
MARCO¹; MAGNI, ALESSANDRO¹; SCHUMACHER, HANS WERNER²

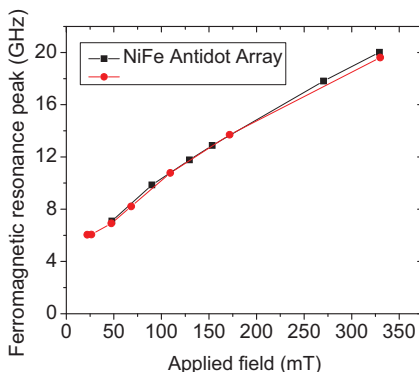
INRIM, Divisione Elettromagnetismo, Torino Italy

²Physikalisch-Technische Bundesanstalt, Bundesalle 100, D-38116 Braunschweig, Germany

Planar magnetic films with regular submicron features are currently under close scrutiny due to their unique properties associated to the spatial confinement and nonuniform distribution of the magnetization which can be exploited for microwave and spintronic applications, as filters or selective sensors in specific frequency ranges.

In this work we have investigated the dynamic behavior of NiFe and Co films of 20-60 nm thickness patterned with hexagonal antidot patterns with ~ 250 nm dimension and ~ 500 nm center to center. The patterns were generated by self assembly of polystyrene spheres. The arrays were characterized using a ground-signal-ground coplanar waveguides applying electromagnetic radiation at frequencies starting from a few MHz up to 40 GHz range, under an applied magnetic field H_a up to 0.3 T in-plane/1.3 T out-of-plane. Structural and magnetic characterization was performed by scanning electron microscopy, atomic/magnetic force microscopy, alternating gradient force microscopy and Kerr microscopy. Electromagnetic characterization was either performed with a Vector Network Analyzer or analyzing the transmitted power through or near the sample using a detector diode and a lock-in amplifier. This setup allows a wideband characterization allowing a direct comparison of sample performance at different frequencies (i.e. 1-40 GHz) and applied field values (-1.3 T- 1.3 T).

Besides the expected ferromagnetic resonance behavior (shown in the figure for a NiFe antidot array $3 \times 3 \text{ mm}^2$), where the anisotropy is influenced by the presence of the holes, we observed the emergence of large variations in signal absorption [1,2] during a magnetization cycle. These variations can be connected to the collective behavior of strongly pinned domain walls and to the field evolution of macroscopic domain structures encompassing large portions of the sample.



References:

- [1] A. Barman et al., J. Phys. D: Appl. Phys. 43 (2010) 195002
- [2] E. Mengotti JAP 103, 07D509 (2008)

Magnetic Environment and Measurement Systems with Improved Field Stability using the Single-Volume Approach

TURNER S., HALL M.J and Harmon S.A.C

National Physical Laboratory, Hampton Road, TW11 0LW, United Kingdom

The continued advancement of magnetic sensors (such as fluxgate gradiometers) for applications such as geomagnetic exploration of mineral deposits, magnetic decontamination of spacecraft and aircraft navigation, is only achievable with the support of the underpinning metrology that can accurately characterise essential performance criteria. Measurements of properties such as linearity, noise, gain and resolution, are key to determining the success of any new development [1]. However, fluctuations in the ambient magnetic field due to changes in the geomagnetic field, solar activity or from local man-made contributions make such measurements difficult to realise. Ambient field cancellation and stabilisation systems based on coils that provide stable magnetic environments are therefore essential for characterising and calibrating such devices. However, as manufacturers continue to improve the performance of magnetic sensors, it is essential to mirror each advance with a similar development in the magnetic environment capabilities.

The National Physical Laboratory have developed such a system using 3 m diameter tri-axial Helmholtz coils, controlled through a 3-axis reference magnetometer located 60 m from the main coil system. This reference magnetometer detects fluctuations in the ambient field and, after suitable gain and offset corrections are applied, the inverted outputs from each axis are fed into the corresponding Helmholtz coils. These generate fields that cancel fluctuations in ambient field and reduce noise to below 20 pT/ $\sqrt{\text{Hz}}$ at 1 Hz. Unfortunately, the open loop control provided by the reference magnetometer cannot compensate for changes in the ambient field over an extended time period (i.e. 20000 s) and the approach is limited by the local gradient in magnetic field. Therefore an alternative approach has been employed, in which the reference magnetometer is replaced by an atomic resonance magnetometer located within the cancellation volume. It is suggested that with this single-volume approach [2] it is possible to lower the noise floor within the cancelled volume towards 1 pT/ $\sqrt{\text{Hz}}$ at 1Hz.

This paper will introduce both approaches and will demonstrate the advantages and limitations associated with each. In addition to this, finite element modeling and experimentation will be used to describe the development of each component within the resulting single-volume system.

References

- [1] P. Ripka: Sensors based on bulk soft magnetic materials: Advances and challenges, *J. Magn. and Magn. Mater.*, Vol. 320, pp. 2466-2473, 2008
- [2] V. Y. Shifrin, E.B. Alexandrov, T.I. Chikvadze, V.N. Kalabin, N.N. Yakobson, V.N. Khorev and P.G. Park: Magnetic flux density standard for geomagnetometers, *Metrologia*, Vol. 37, pp. 219-227, 2000
- [3] D. Platzek, H. Nowak, F. Giessler, J. Rother and M. Eiselt: Active shielding to reduce low frequency disturbances in direct current near biomagnetic measurements, *Review of scientific instruments*, vol. 70, No. 5, pp. 2465-2470, 1999

Author's index

Abdallah M.	100	Cordier C.	149
Adenot-Engelvin A. L.	93	Corodeanu S.	66
Aissaoui M.	45	Couderette A.	43
Albertini F.	116	Cox D.C.	154
Allag H.	145	Čverha A.	49
Allegre G.	133	Daniel L.	90
Almandoz G.	135	Dascalu G.	104, 105
Alnassar M.	111	Dehbaoui M.	28
Altpeter I.	134	Del Real R.P.	143
Alves F.	55	Deleo N.	156
Ambra A.	156	Denoual M.	36
Arai K.I.	31	Derebasi N.	52
Arnaiz A.	147	Devasahayam A. J.	106
Arnold Z.	116	Diraison Y. L.	41
Asfour A.	51	Dobrotă C. I.	107
Augustyniak B.	128	Dolabdjian C.	33, 35, 36, 65, 149
Badini-Confalonieri G.A.	67, 95	Dosoudil R.	118, 123
Baltag O.	76, 77	Draxler K.	46, 85
Bansropun S.	59	Dufay B.	33, 35
Barandiaran J. M.	64, 147	Dumas R.	28
Barrera G.	139	Đuran I.	57
Bartok A.	90	Ekonomov N.A.	88
Baudin T.	90	El Kammaoui R.	95
Bellušová D.	118	Enrico E.	139
Beran P.	60	Esposito E.	150
Bieńkowski A.	68	Fabbrici S.	116
Blažek J.	49, 129	Faktorová D.	108
Blyzniuk M.	21	Farine P. A.	27
Boariano L.	139, 156	Fernández E.	34
Boda M.	61	Fetisov L.Y.	89
Boller Ch.	134	Fetisov Y.K.	88
Bolshakova I.	57	Fisher B.	53
Bourdelle P. F.	27	Flament S.	133
Bravo-Imaz I.	147	Flores A. G.	109, 110
Brinza F.	119	Focsa C.	104
Burdin D.A.	88	Fodil K.	36
Burian M.	142	Fry N.	53
Butta M.	83	Frydrych P.	47, 48
Butvin P.	84	Fryml K.	46
Butvinová B.	84	Fujiwara N.	75
Caltun O. F.	104, 105, 126	Füzer J.	120
Caylak O.	52	Gac G. L.	131
Celegato F.	139, 156	Gamcova P.	94
Cerio F.	106	Gandariás K.	135
Cima L.	43	García A.	44, 72, 101
Coillot Ch.	24, 54, 61, 87, 151	García-Arribas A.	34, 147
Coisson M.	156	Gherca D.	119
Coisson M.	139	Giouroudi I.	111

Gonzalez J.	74	Jendelová P.	142
Gorritxategi E.	147	Jenkins K.	127
Granata C.	150	Joubert P. Y.	41, 43, 131
Griesmar P.	41	Jun J.	29
Grigoras M.	114	Jung I. S.	97
Grimberg R.	108	Jung I.S.	99
Grössinger R.	111	Kalandadze L.	115
Gutiérrez J.	64	Kaleta J.	112, 113
Haddab Y.	25	Kamara S.	28
Hall J.P.	127	Kamarád J.	116
Hall M.J.	157	Kanazawa T.	75
Hamia R.	149	Kanetaka H.	73
Han F.	82	Kašpar P.	79, 142
Harada S.	82	Kaštil J.	116
Harmon S.A.C.	157	Kato K.	31
Harnois M.	36	Kazakova O.	22, 154
Hashi S.	73	Kejik P.	27
Hasiak M.	112, 113	Khodakova J.A.	42
Hattori Y.	75	Kim J.	29
Havlíček V.	137, 138	Kim K.	28
Havránek A.	137	Kim Y. K.	97, 99
Hernández M.	67	Kitamura Y.	73
Herrmann H. G.	134	Klein P.	94, 117
Herynek V.	142	Kobayashi N.	31
Hillion M.	151	Kollár D.	120
Hlavacek J.	46	Konczykowski M.	59
Hlenschi C.	66	Kosel J.	111
Hohe H. P.	60	Kost Y.	57
Hosaka T.	75	Kovalyova N.	57
Hristoforou E.	40, 148	Kovarik K.	57
Hudak J.	129	Kruželák J.	118
Hudák J.	49	Ktena A.	148
Hudec I.	118, 123	Kuboki T.	73
Chang Ch. R.	58	Kuepferling M.	156
Chanteur G.	54	Kupec J.	155
Charar S.	28	Kurlyandskaya G. V.	34
Chashin D.V.	88	Kurlyandskaya G.V.	56
Chen S. P.	58, 78	Lahrech H.	100
CheolGi K.	28	Lai M.F.	98
Chiriac H.	66, 92, 114	Lam Chok Sing M.	65
Chmielewski M.	128	Langer J.	153
Cho Ch.	29	Larzabal P.	131
Chromčíková M.	84	Lasheras A.	64
Chubykalo-Fesenko O.	143	Le Huérou J. Y.	136
Iñiguez J.	109, 110	Le-Bihan Y.	55
Ipatov M.	74	Lee Ch. P.	98
Ishiyama K.	73	Lee J.	29
Ito D.	75	Lee J. J.	97, 99
Itoh Y.	73	León L. M.	64
Ivanov Y.	143	Lepalovskiy V.N.	56
Jackiewicz D.	68, 130	Leroy P.	87
Jang P.	122, 125	Liebing N.	153
Janošek M.	39, 84, 155	Lipovský P.	49
Jeandet A.	151	López M. J.	72

Łukiewski M.....	112, 113	Platil A.	140
Lupu N.	114	Polik Z.	63
Maciakowski P.	128	Pollert E.	142
Magnes W.	81	Polyakov P. I.	121
Magni A.	156	Poza J.	135
Makido O.	57	Praslicka D.	129
Mansour M.	24	Praslička D.	49
Manzin A.	154	Prochazka R.	46
Mapps D.	53	Psuj G.	132
Marcin J.	114	Pui A.	119
Marčić T.	102	Rajkumar R.K.	154
Martinez L.	136	Ramirez P.	72, 101
Masilamany G.	41	Rao B. P.	105
Medvedev A.V.	89	Rao G. S. N.	105
Menard D.	33, 35	Rao K. H.	105
Miglierini M.	112, 113	Raposo V.	109, 110
Mikita I.	129	Rau M.	77
Mironenko I.	134	Rau M.C.	76
Mlejnek P.	79	Razek A.	90
Mohamadabadi K.	151	Redondo C.	109, 110
Mohellebi H.	100	Reiss G.	153
Morales R.	44	Rekošová J.	123
Morón C.	44, 72, 101	Reymond S.	27
Moses A.J.	127	Rhouni A.	87
<u>Mosser V.</u>	23, 25, 59	Rhyu S. H.	99
Moucha V.	49	Richter K.	117
Moulin J.	55	Ripka P.	39, 62, 69, 84, 85
Moussaoui D.	45	Robbes D.	133
Moutoussamy J.	61	Roháč J.	62
Moutoussamy J.	54	Rook K.	106
Nakano H.	31	Roth S.	120
Nass P.	153	Rott K.	153
Navas D.	109, 110	Roucaries B.	136
Nguyen Van Dau F.	24	Roux A.	24
Nica V.	119	Ruggiero B.	150
Nikitin M.P.	42	Russo M.	150
Nikitin P.I.	42, 70	Russo R.	150
Nikitina I.L.	70	Ryba T.	124
Nová I.	138	Sabol R.	49
Nováček P.	62	Saez S.	33, 35
Ocker B.	153	Safronov A.P.	56
Olekšáková D.	120	Salach J.	47, 48, 68, 130
Olivera J.	67	Salvi F.	27
Orlov A.V.	42	San S. M.	64
Oudina A.	45	Sasada I.	82
Ozawa T.	31, 73	Sasasa I.	83
Panchal V.	22	Savin A.	108
Panina L.	53	Senéz V.	36
Pasquale M.	153, 156	Sentkerestiová J.	57
Peng T.	55	Serfaty S.	41, 136
Perov N.S.	89	Seron D.	25, 59
Peters V.	60	Serrano-Guisan S.	153
Petrucha V.	50, 155	Shin S.	122, 125
Pišek P.	102	Shtabalyuk A.	57

Shurygin F.	57	Ursu C.	126
Schott Ch.	21	Ušáková M.	123
Schumacher H.W.	153, 156	Varga R.	67, 94, 117, 124, 129
Sievers S.	153	Vargova Z.	124
Silva S.R.P.	154	Vas'kovskiy V.O.	56
Silvestrini P.	150	Vazquez M.	93, 94
Skidanov V.	71	Vázquez M.	67, 95, 117, 143
Smelko M.	129	Vetoshko P.	71
Somolinos J. A.	44	Vetoshko P.M.	70
Somolinos J.A.	101	Vettoliere A.	150
Sou G.	87	Vidal N.	135
Srinivasan G.	89	Viererbl I.	57
Srinivasulu G.	89	Vilas J. L.	64
Stancu A.	107	Virtič P.	102
Steigmann R.	108	Vivas L.G.	143
Stempkovskiy A.	71	Volchkov S.O.	56
Stratulat M. S.	104	Vopálenský M.	38, 140
Stratulat S.	126	Vourch E.	43, 131
Styblíková R.	85	Vyhnánek J.	39
Sunjong O.	28	Wakiwaka H.	75
Svalov A. V.	34	Wang Y.	43, 136
Szewczyk R.	47, 48, 68, 130	Wei Z. H.	98
Szielasko K.	134	Wilkie-Chancellor N.	136
Škorvánek I.	114	Xu Y.	103
Štumberger B.	102	Yabukami S.	31, 73
Švec P.	84	Yajima H.	75
Takashima K.	73	Yelon A.	33, 35
Tang Y.	103	Yonnet J. P.	51, 145
Tashiro K.	75	Yuriev M.V.	70
Terki F.	28	Yuvchenko A.A.	56
Thiaville A.	93	Zaragoza V.	25
Tibu M.	114	Závěta K.	142
Tizianel S.	144	Zazo M.	109, 110
Torrejón J.	93	Zbroszczyk J.	113
Trabada D.G.	143	Zemánek I.	137, 138
Tran Q. H.	28	Zhuang X.	65
Tremps E.	72, 101	Zhukov A.	74, 94, 124, 129
Trzcinka K.	47, 48	Zhukova V.	74, 124
Tsai S. Y.	98	Zidi M.	51
Turner S.	127, 157	Zikmund A.	69
Tzalenchuk A.	154	Zou J.	103
Ulvr M.	155		